

Electronic Supplementary Information

Maleimide-based metal-free ligation with dienes: a comparative study

Alexis Lossouarn,^a Dr. Kévin Renault,^a Lætitia Bailly,^a Axel Frisby,^a Patricia Le Nahenec-Martel,^a Pr. Pierre-Yves Renard^a and Dr. Cyrille Sabot*^a

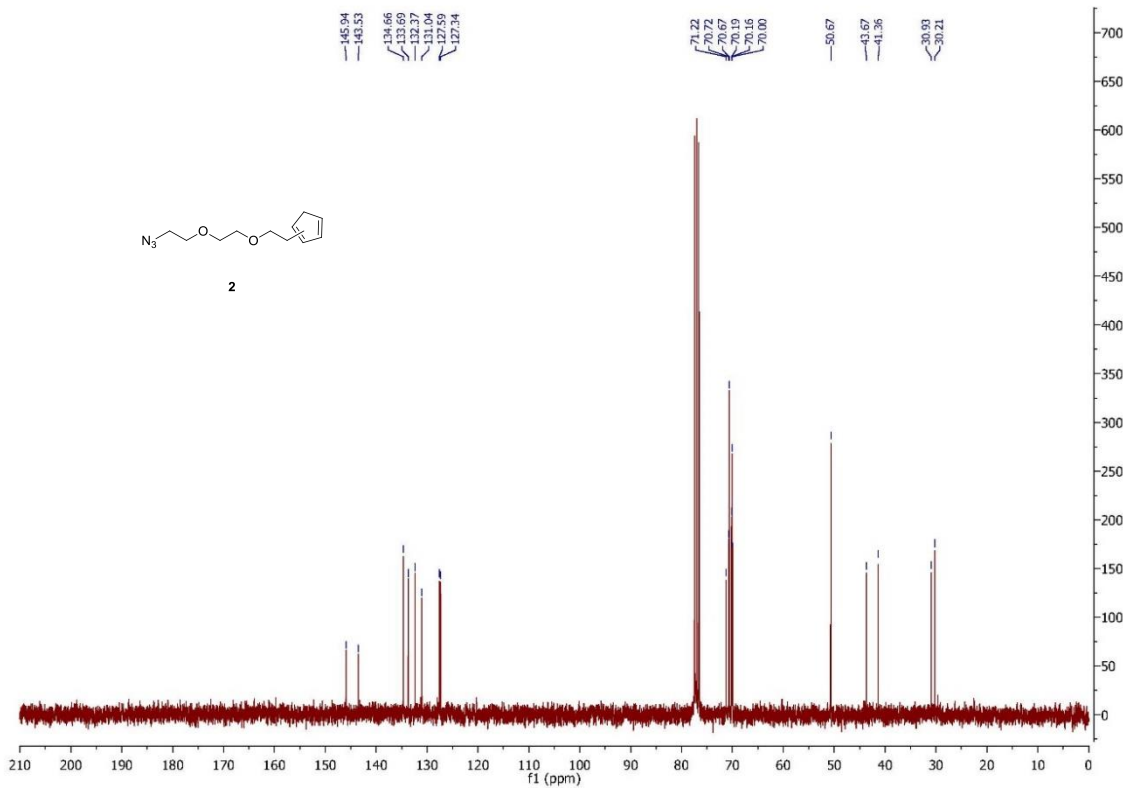
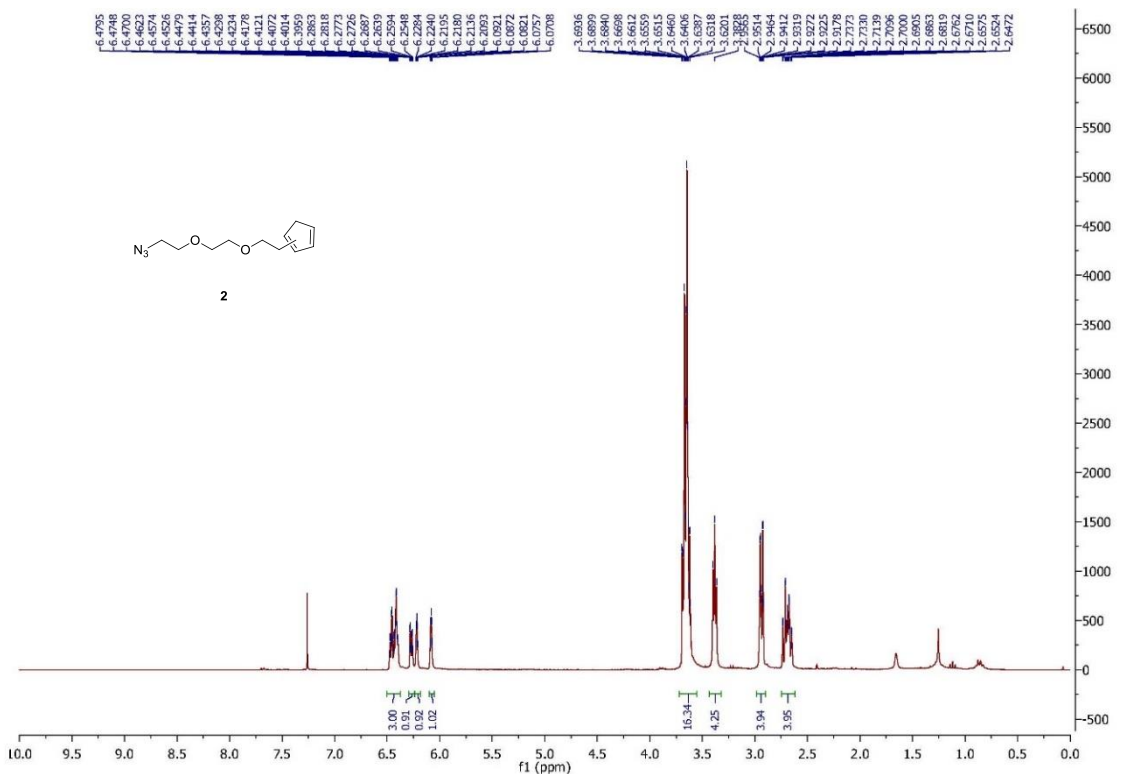
^aNormandie Univ, COBRA, UMR 6014 & FR 3038; Univ Rouen; INSA Rouen; CNRS, 1 rue Tesnière 76821 Mont-Saint-Aignan, Cedex (France).
E-mail : cyrille.sabot@univ-rouen.fr

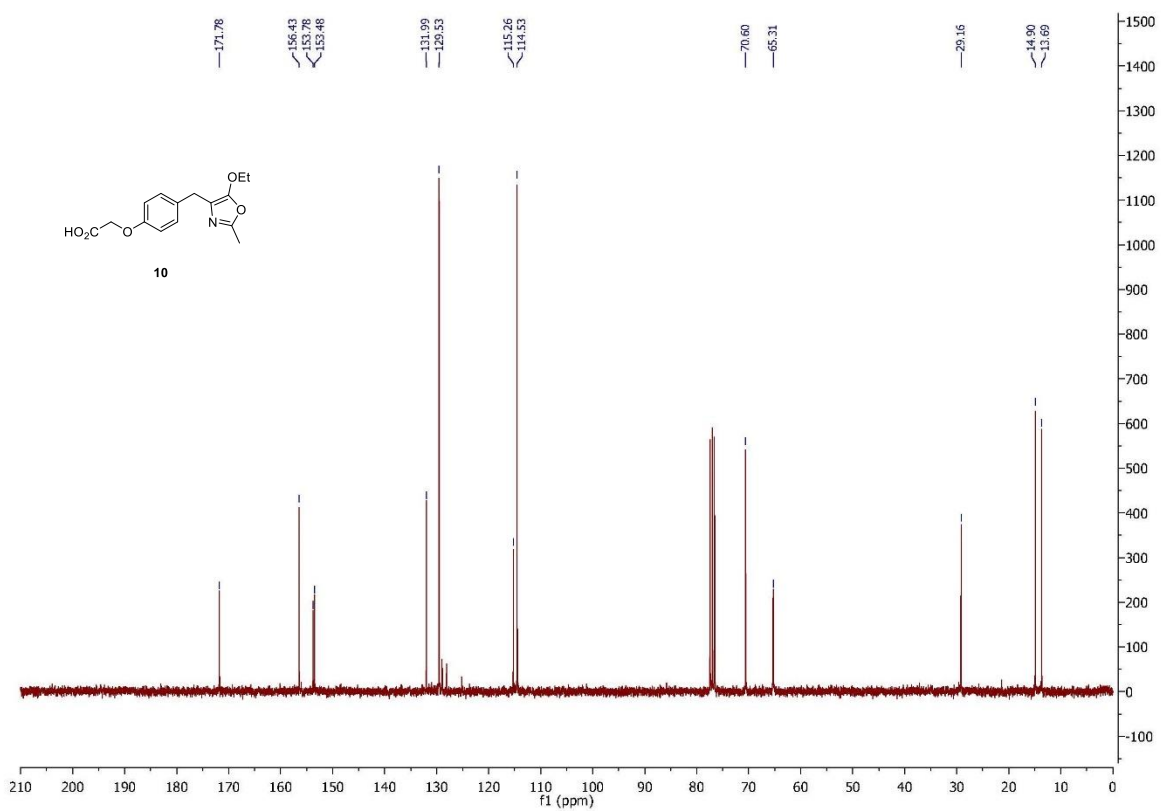
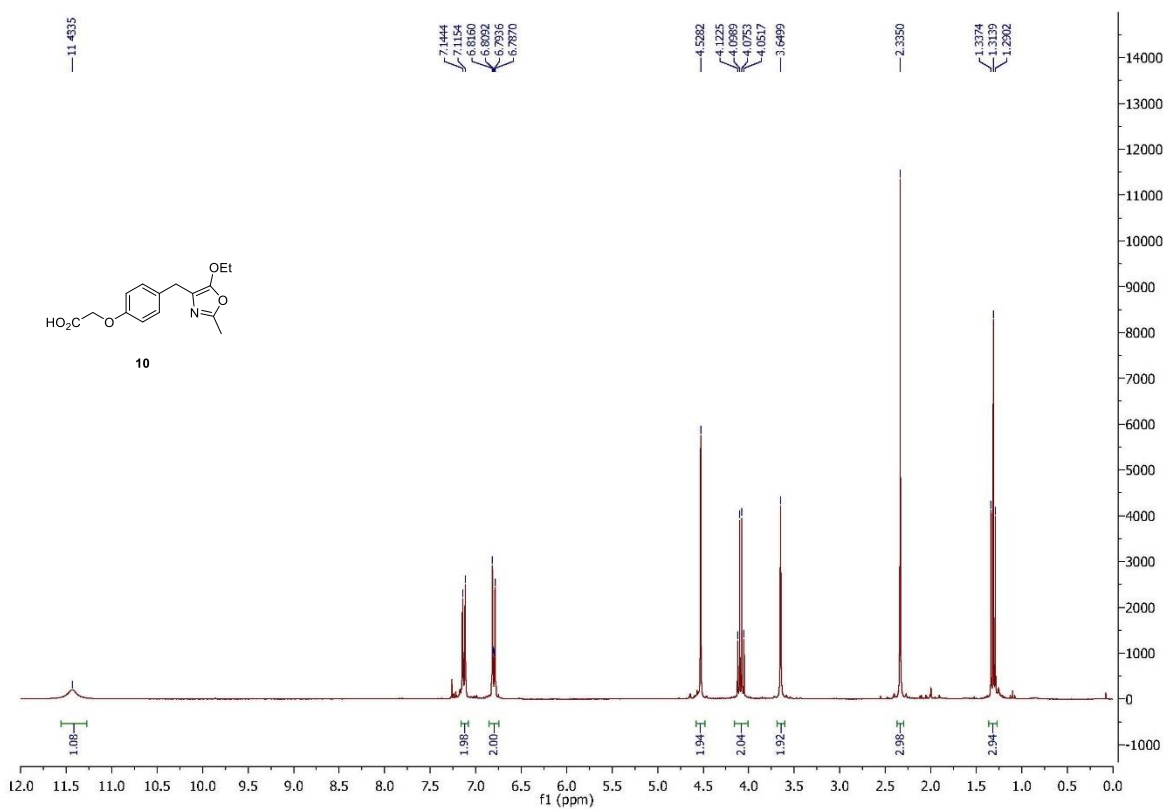
Table of contents

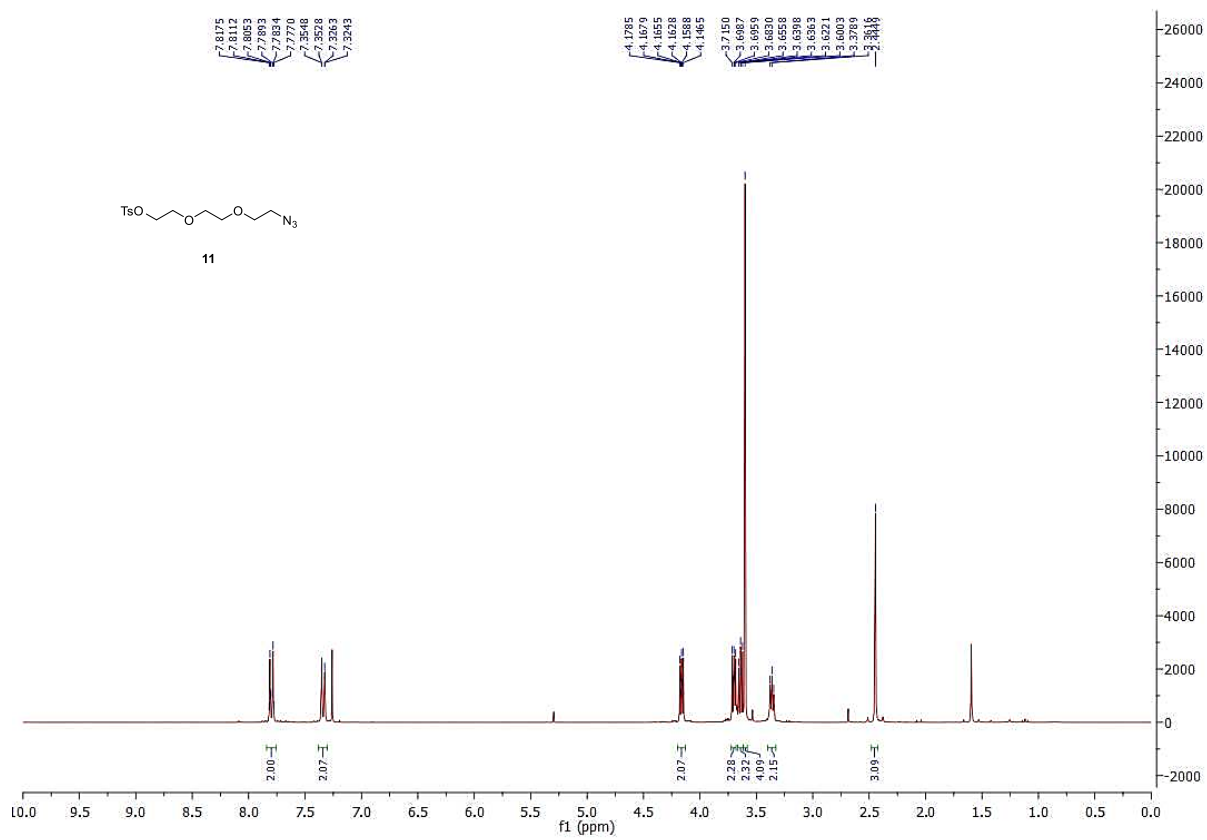
I. Copies of ¹ H and ¹³ C NMR spectra and RP-HPLC chromatograms.....	2
I.1. Copies of ¹ H and ¹³ C NMR spectra.....	2
I.2. RP-HPLC chromatograms.....	22
I.3. Photophysical data for compounds 3 and 26	29
II. Kinetic experiments.....	30
II.1. Monitoring of fluorescence intensity change of Diels-Alder reactions.....	30
II.2. RP-HPLC monitoring of cycloadducts formation	32
II.3. Reaction rate determination of cycloaddition of probe 16 with dienes 1-3 , 6 , and 8-9	40
II.4. One-pot double labeling strategy with dienes 2 and 8	50
III. Study of stability of dienes 2, 3, 8, 9 and conjugates 19-24.....	55
III.1 Study of stability of dienes 2 , 3 , 8 , and 9	55
III.2. Study of stability of conjugates 20-26	64

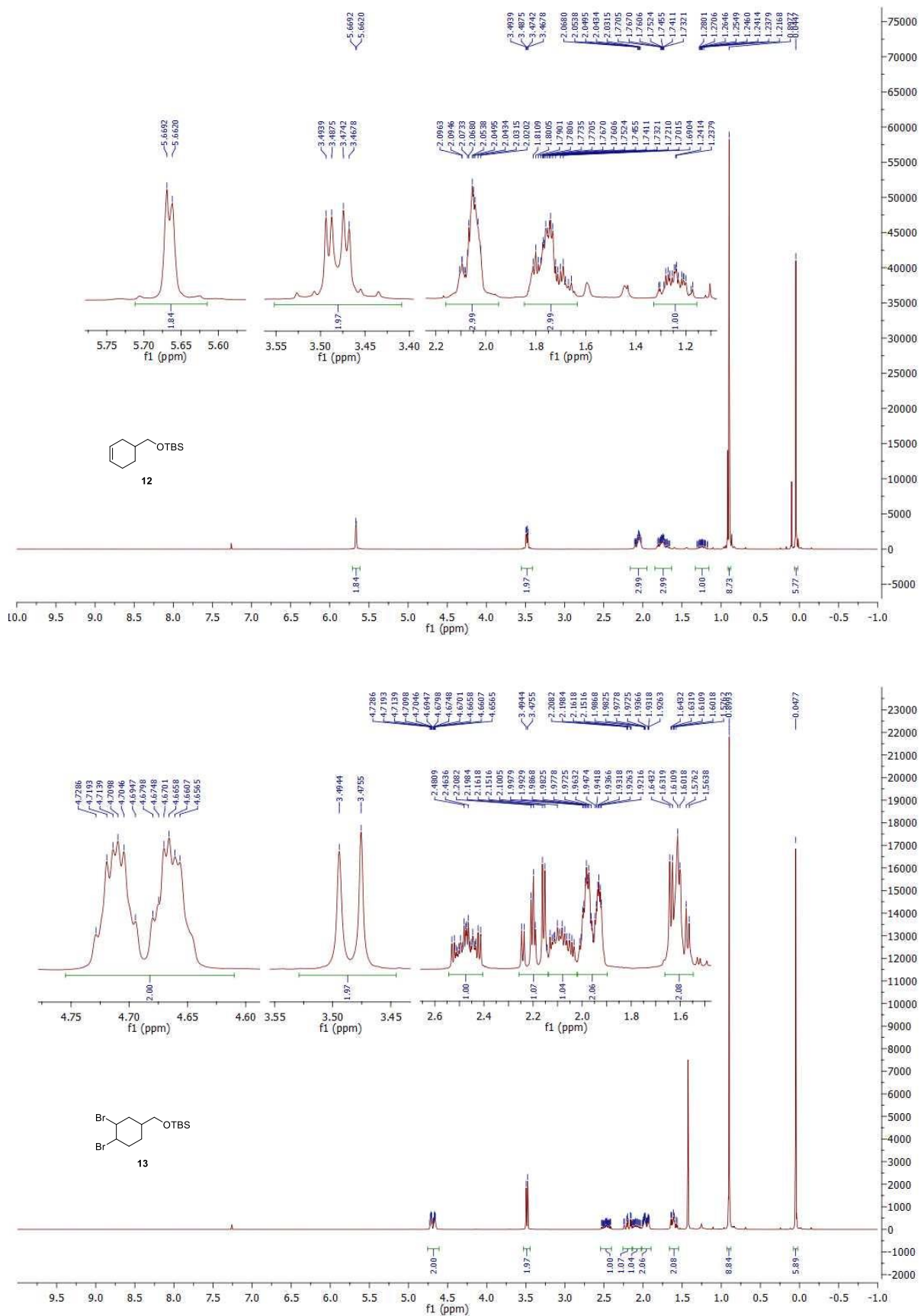
I. Copies of ^1H and ^{13}C NMR spectra and RP-HPLC chromatograms

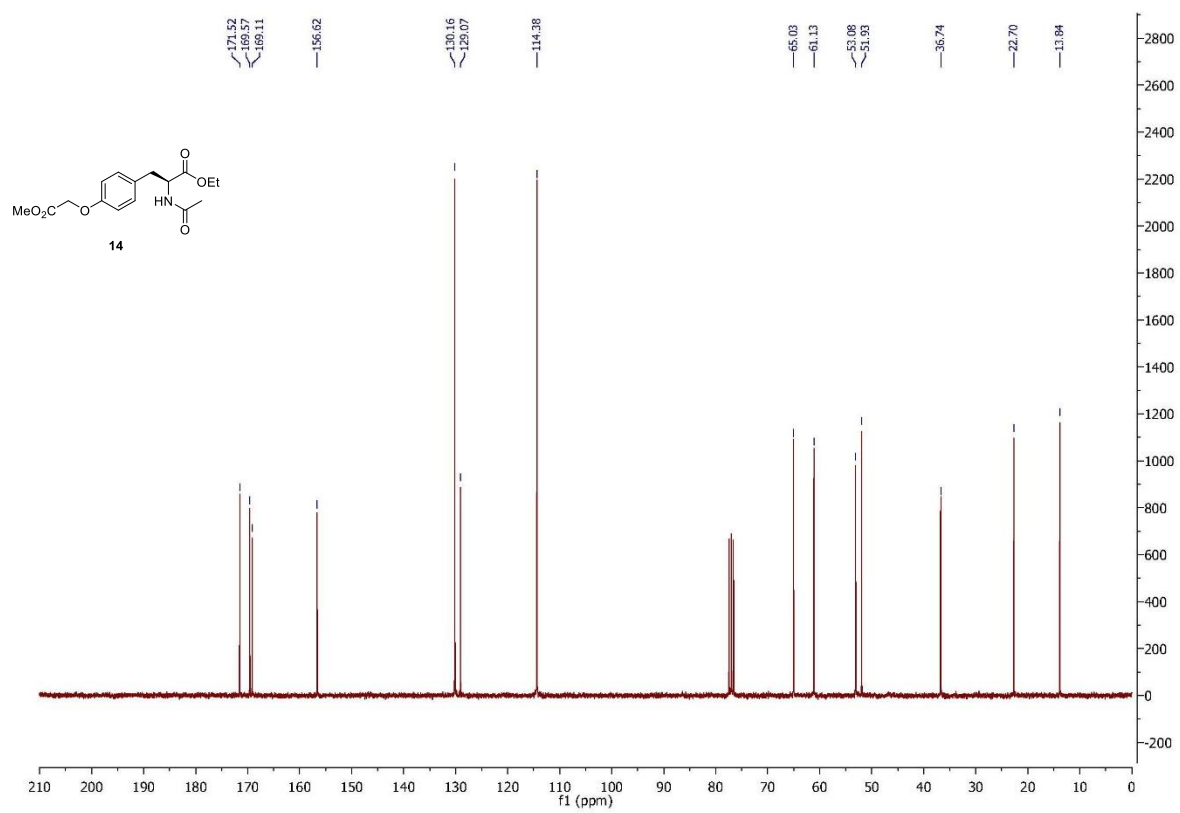
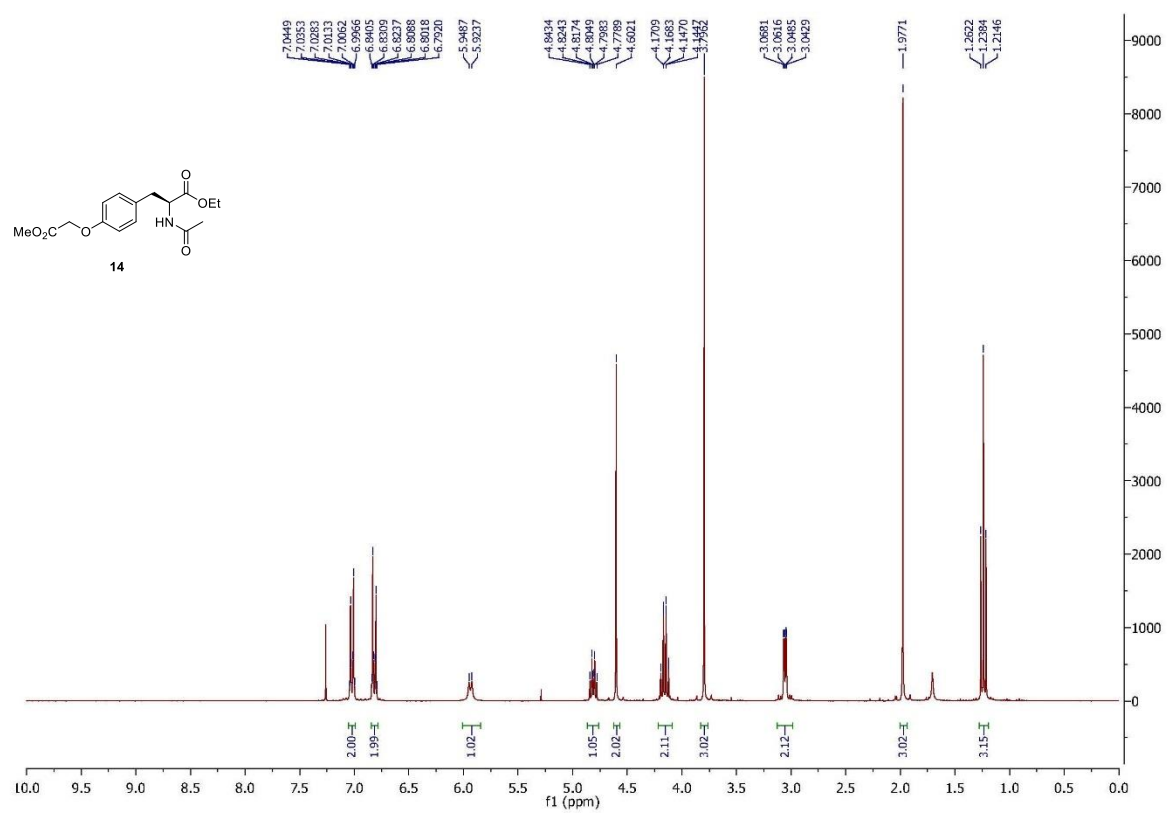
I.1. Copies of ^1H and ^{13}C NMR spectra

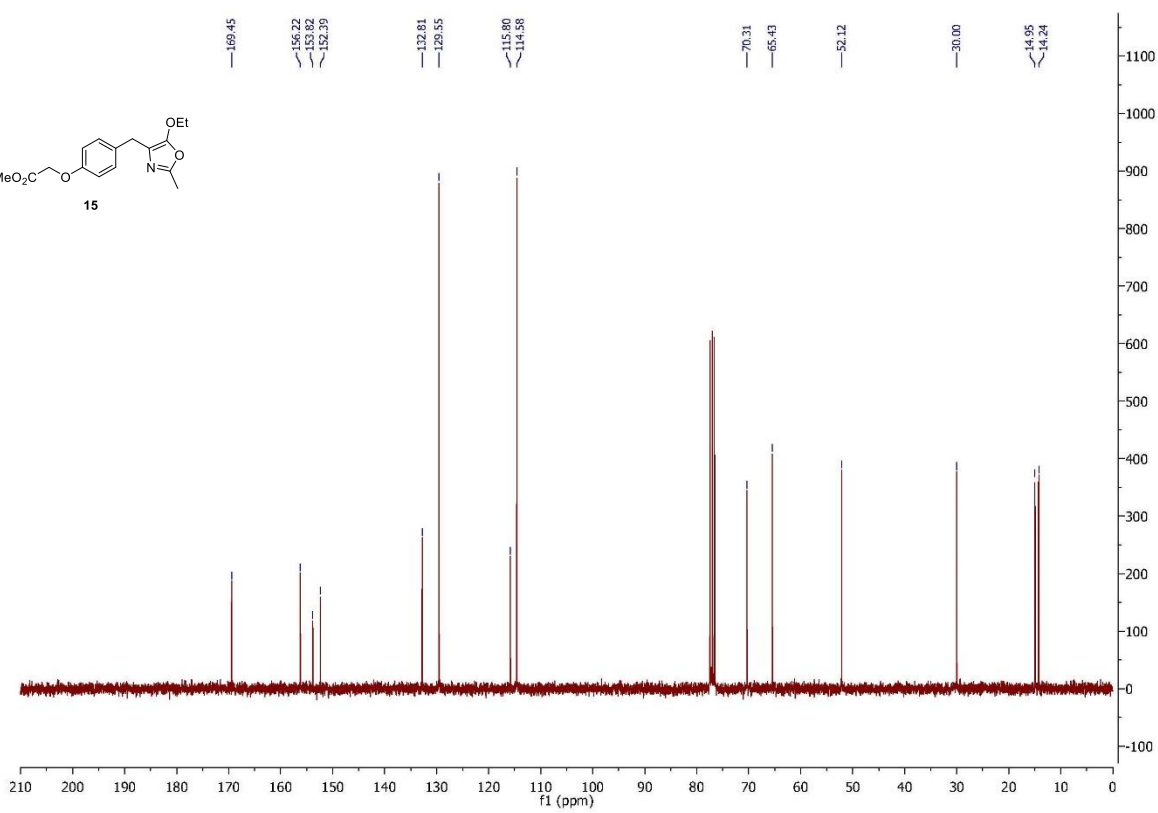
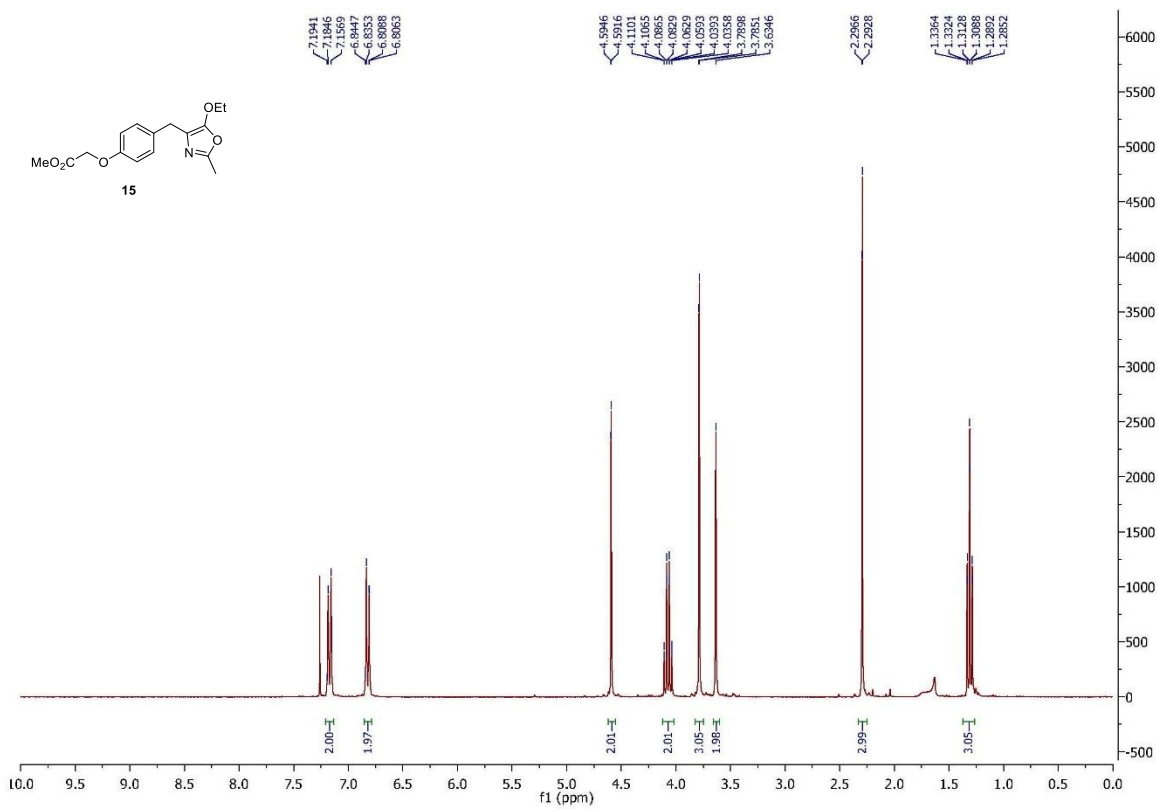


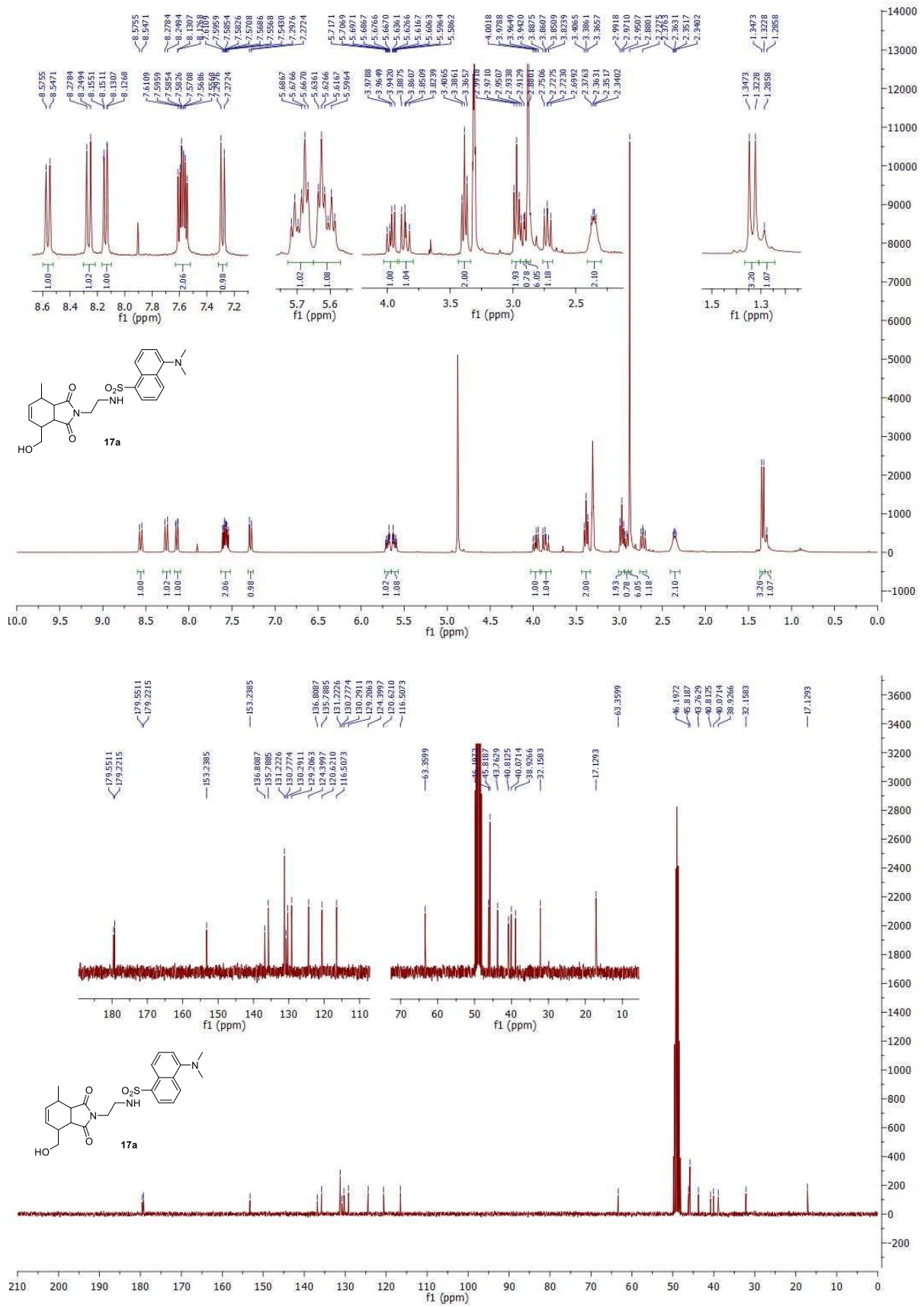


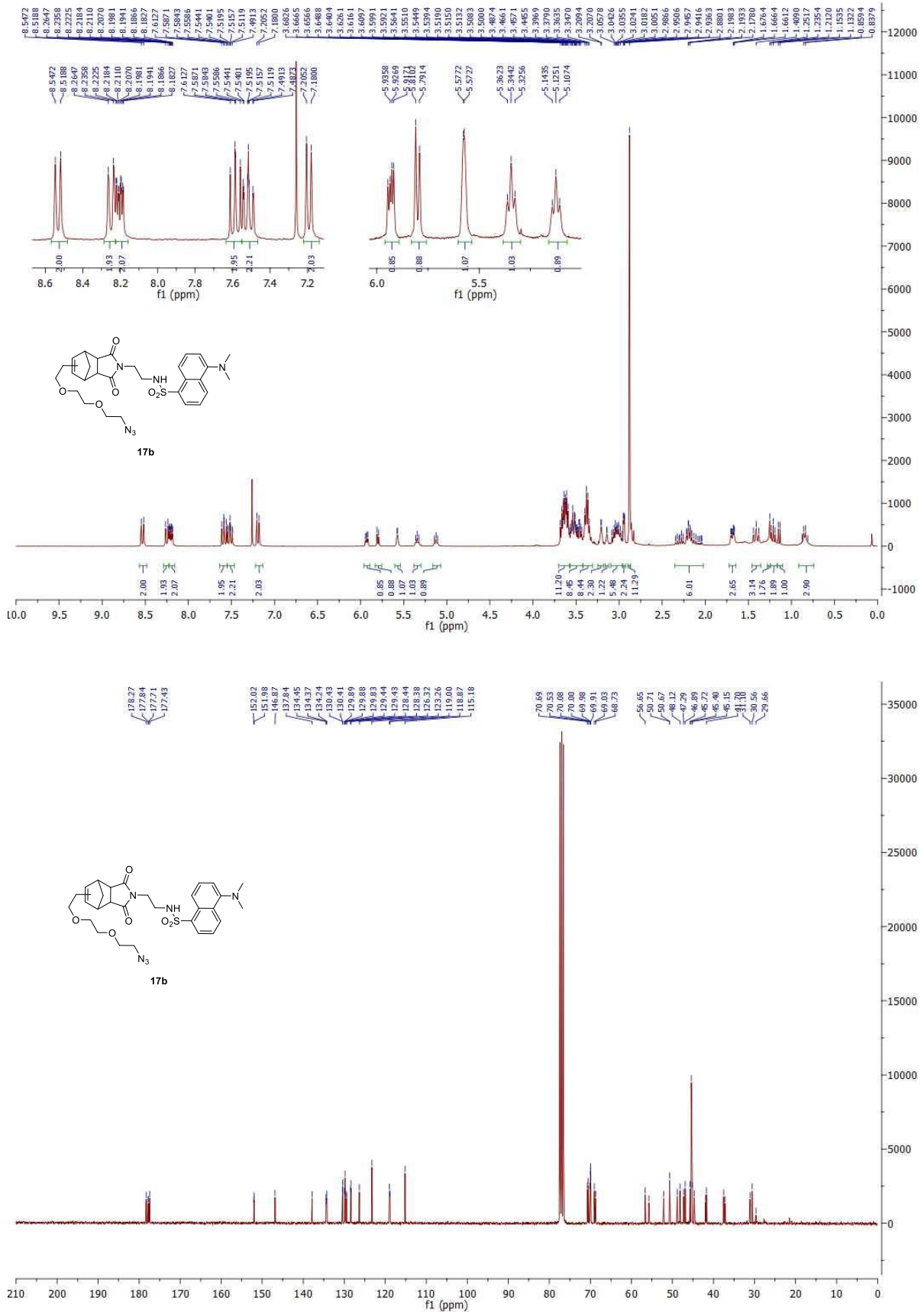


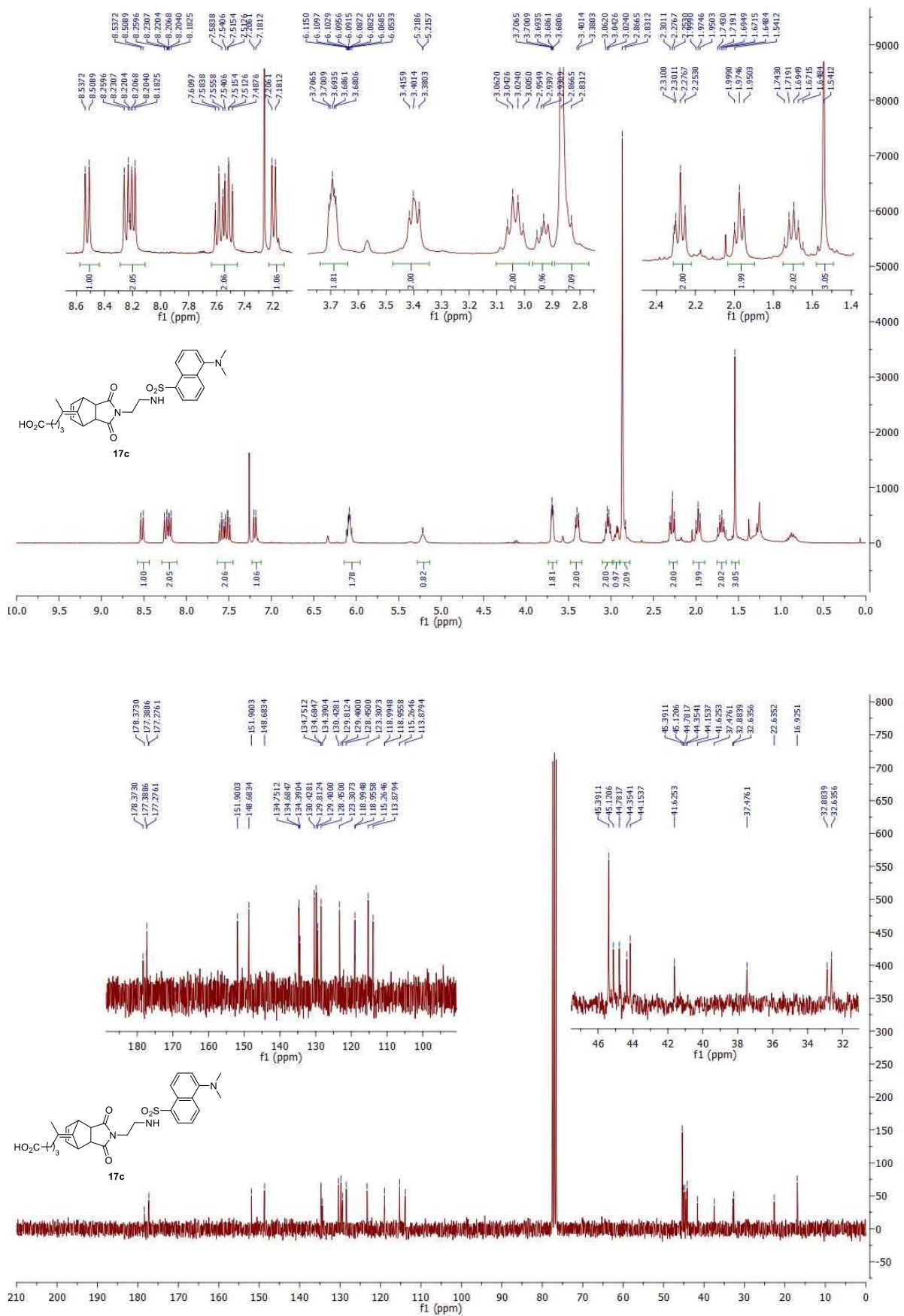


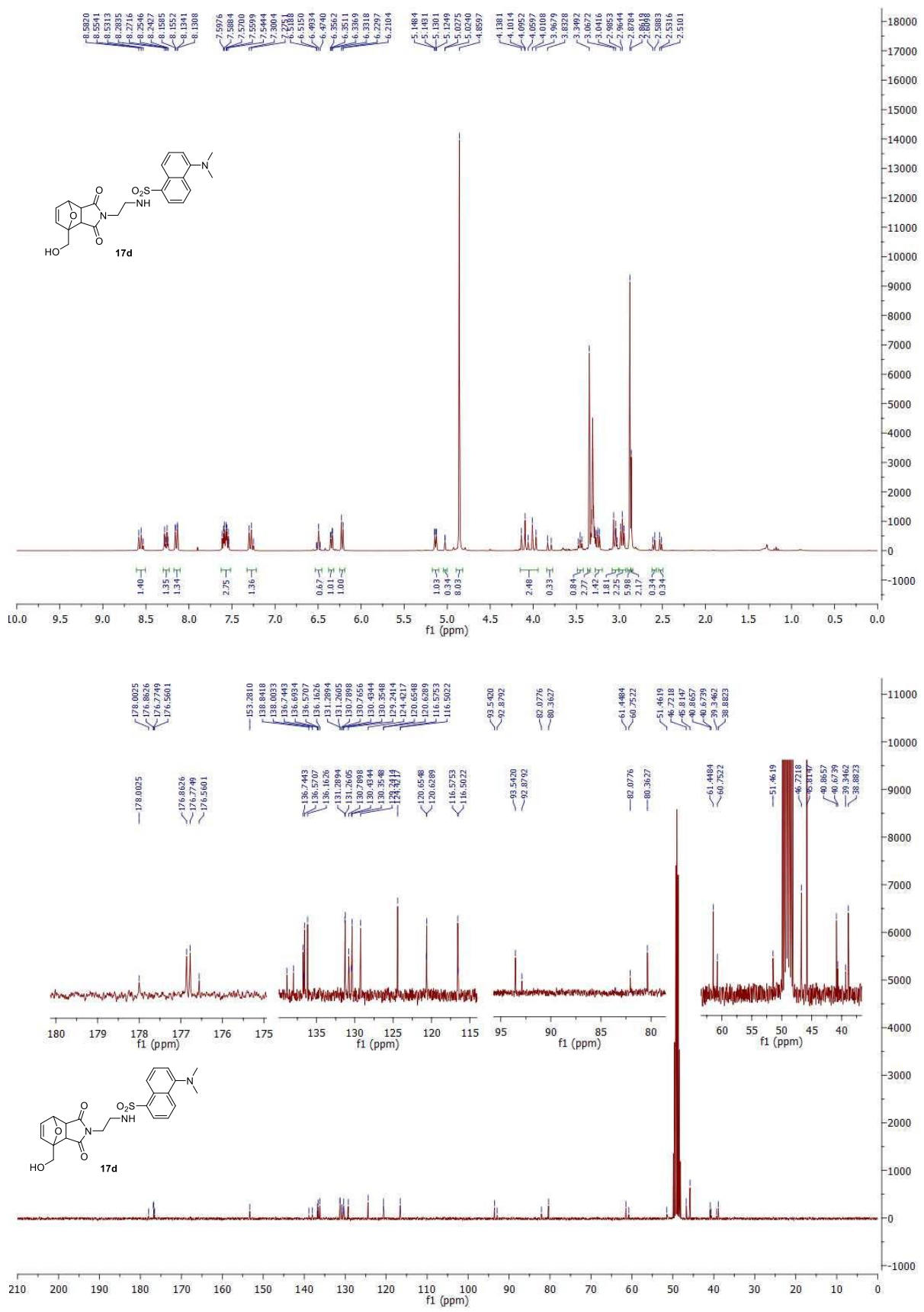


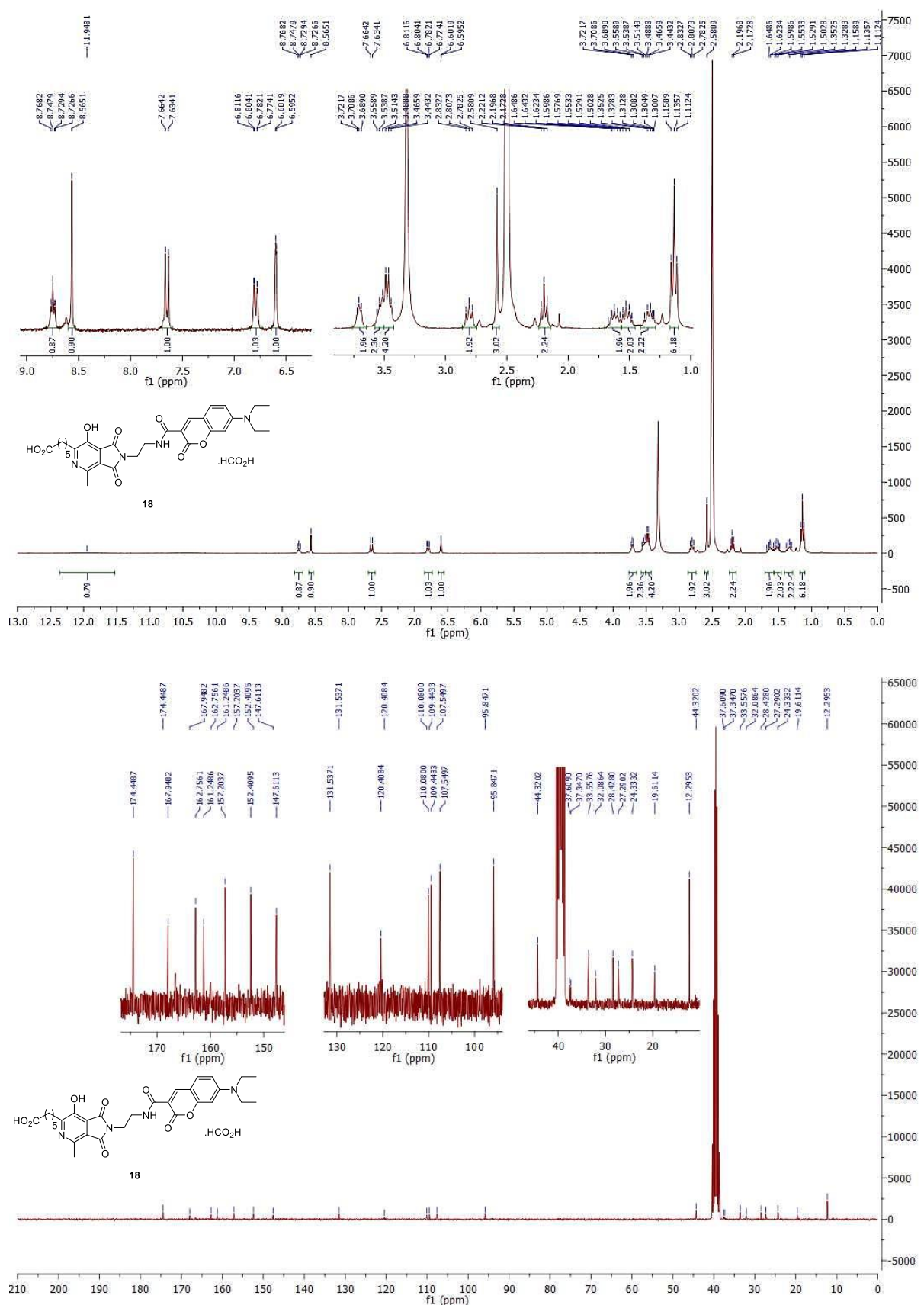


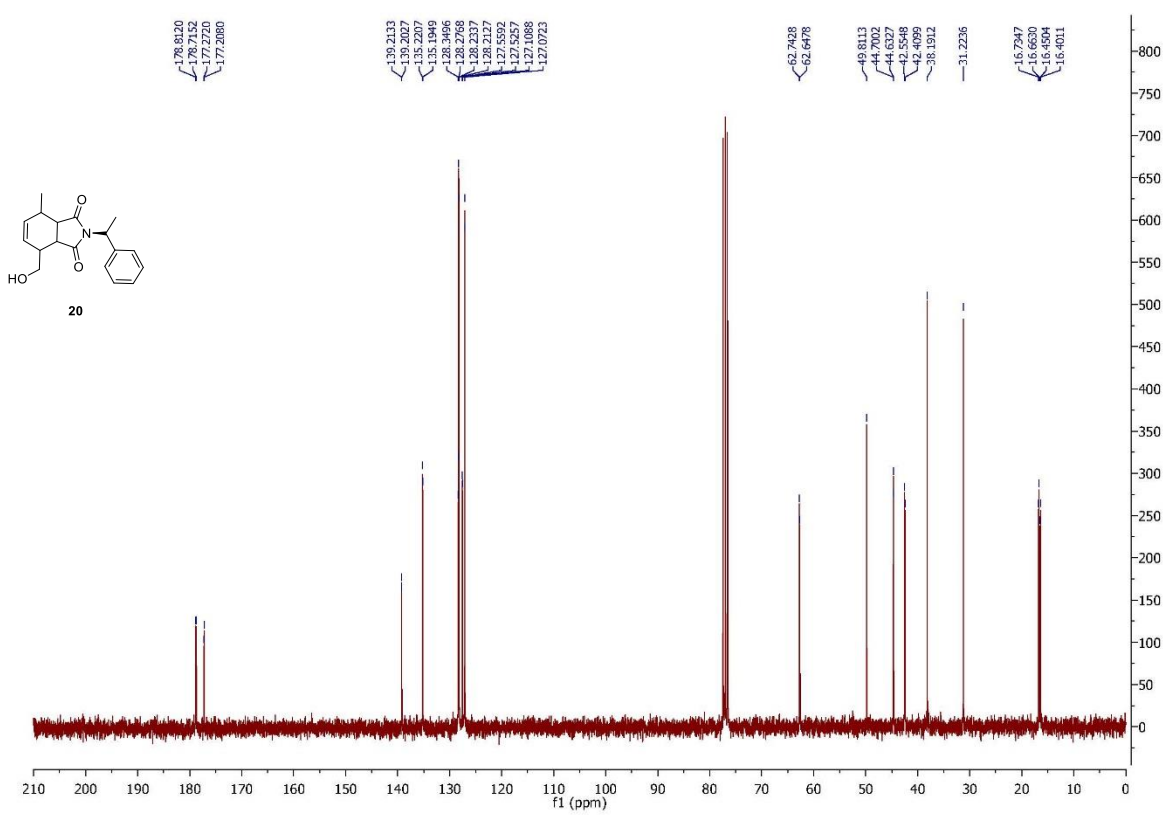
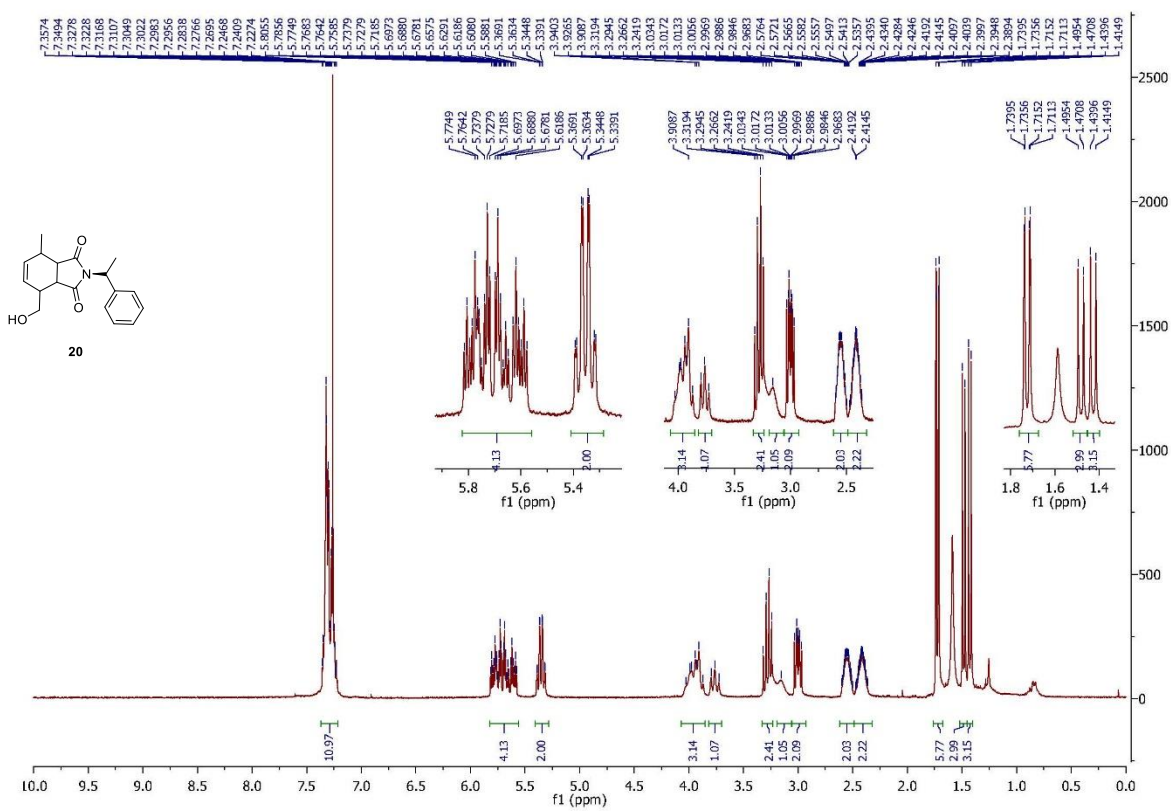


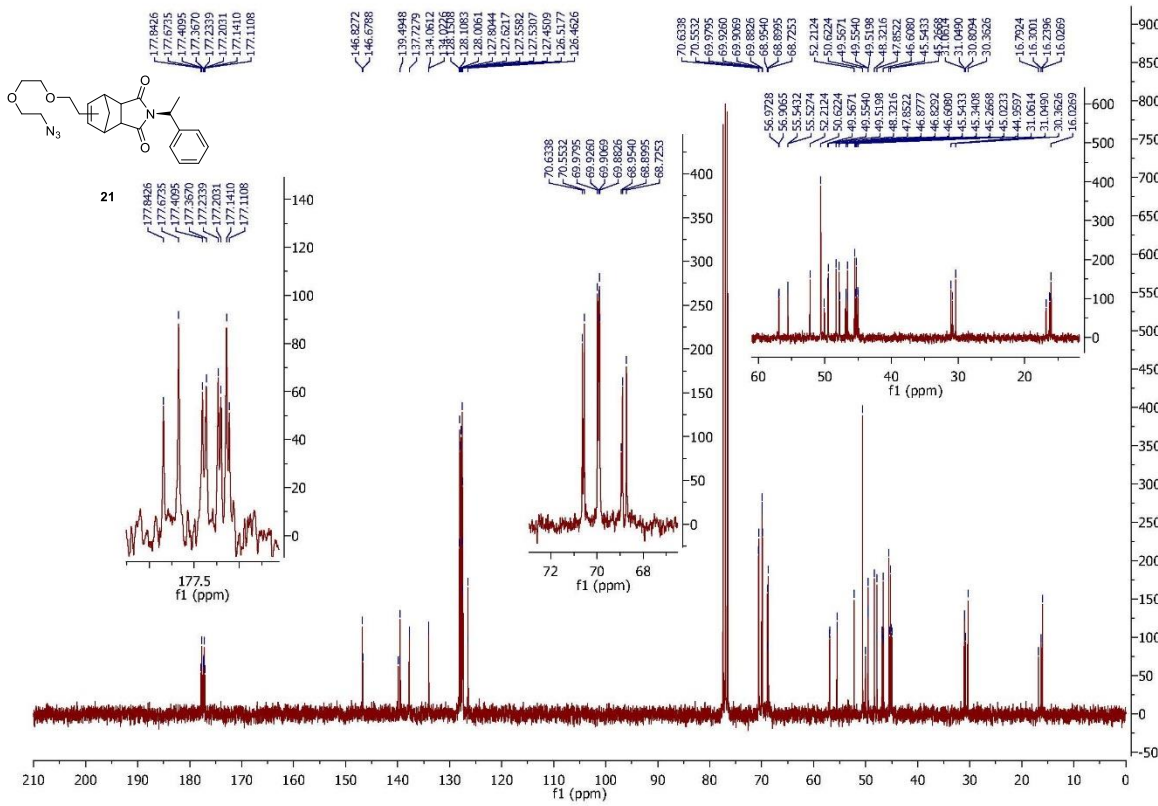
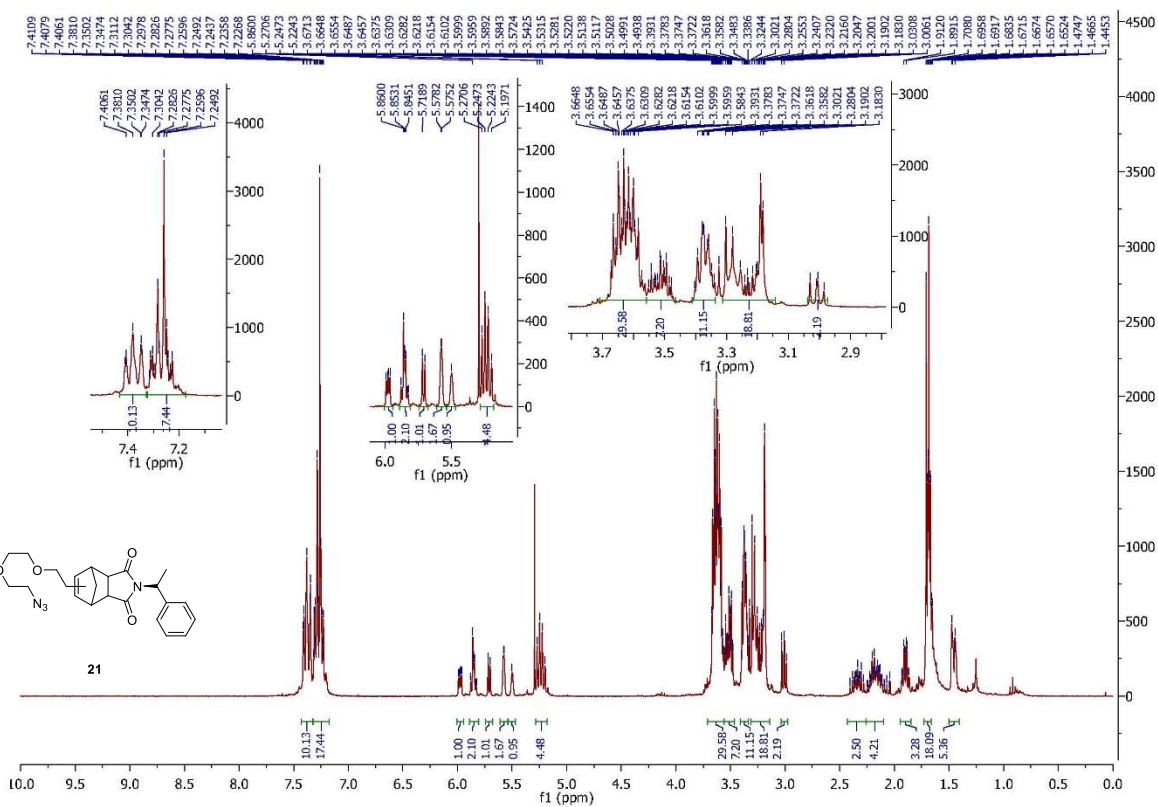


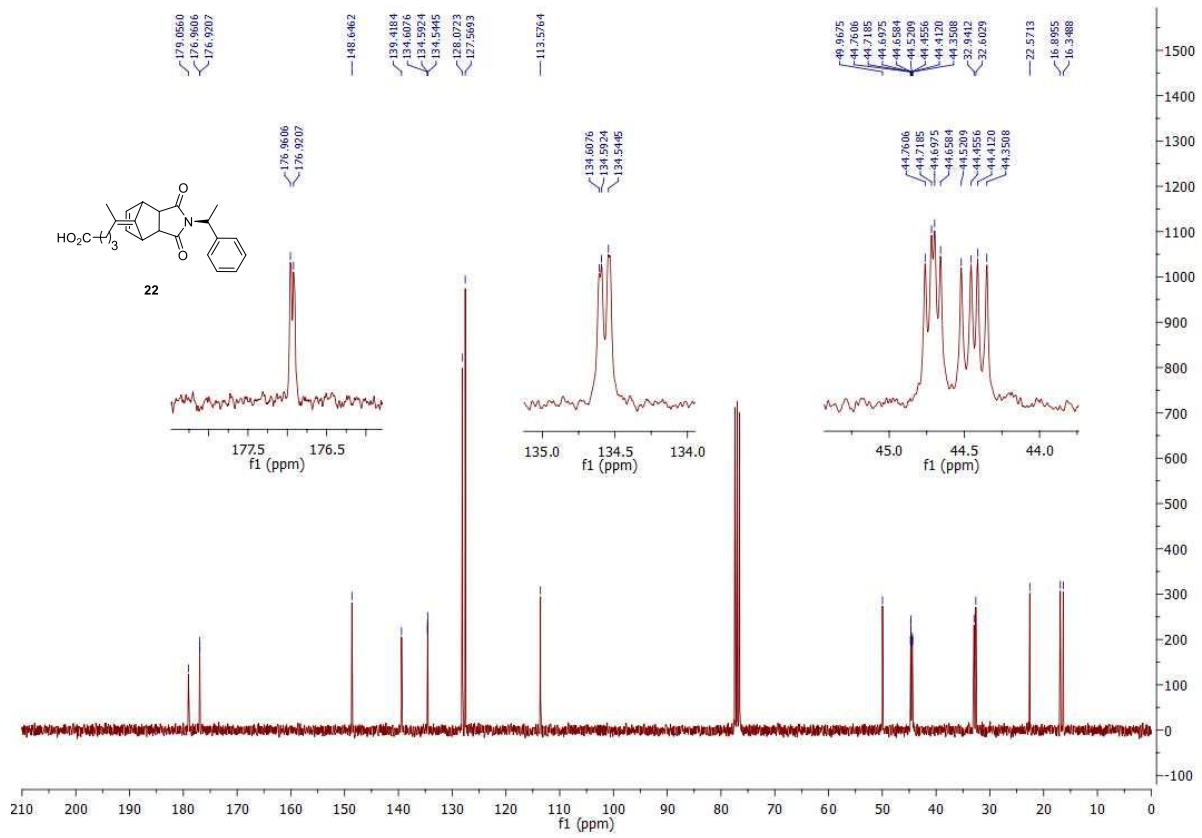
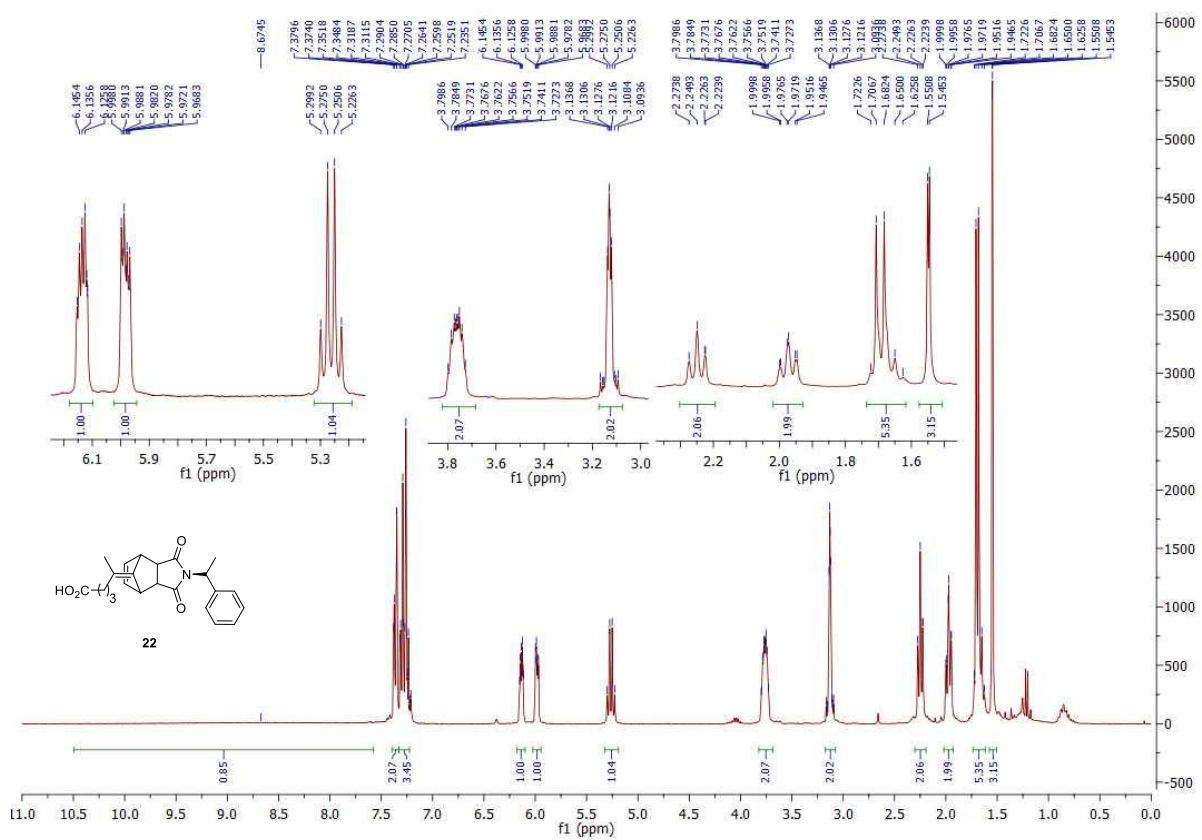


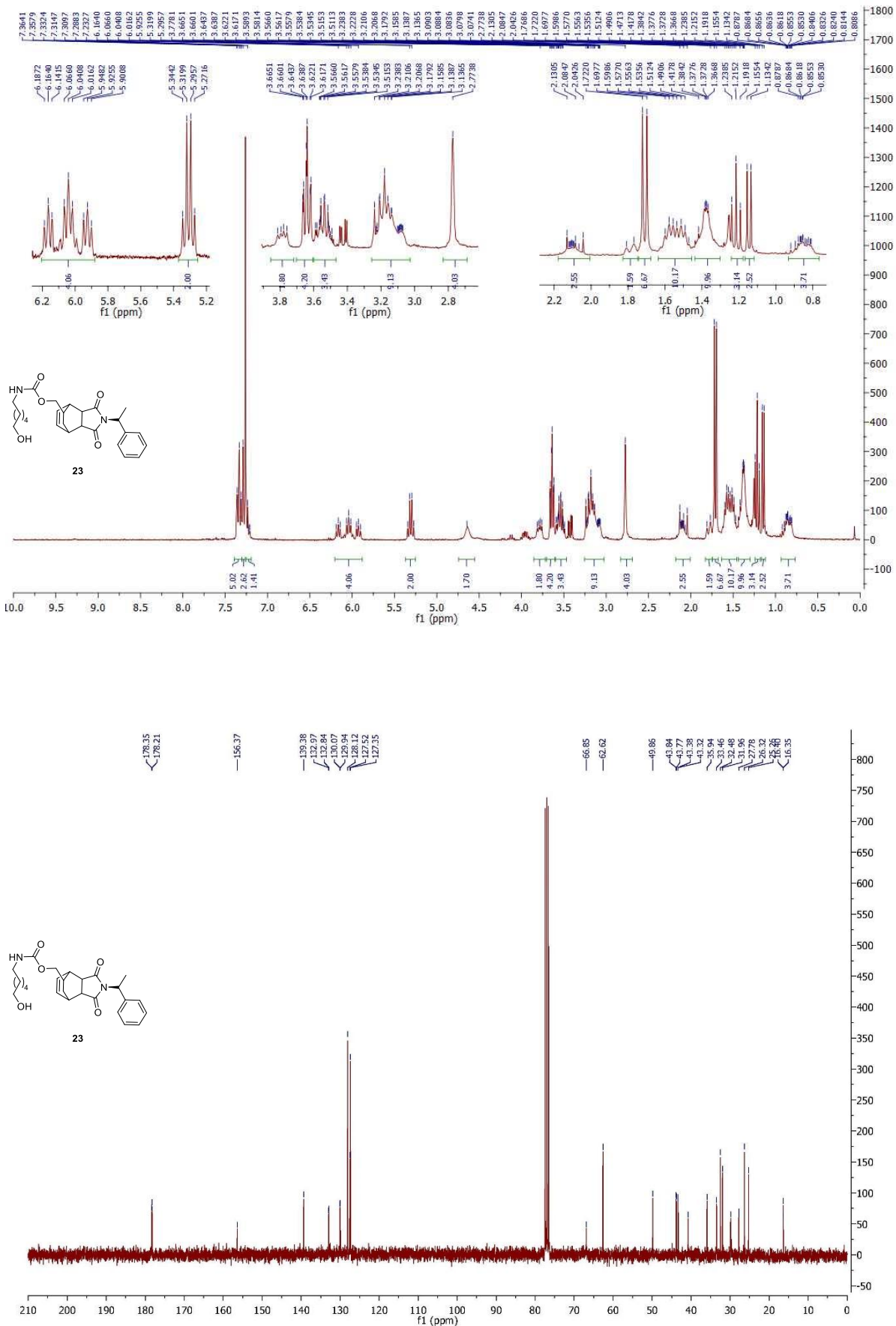


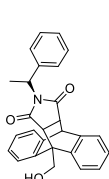
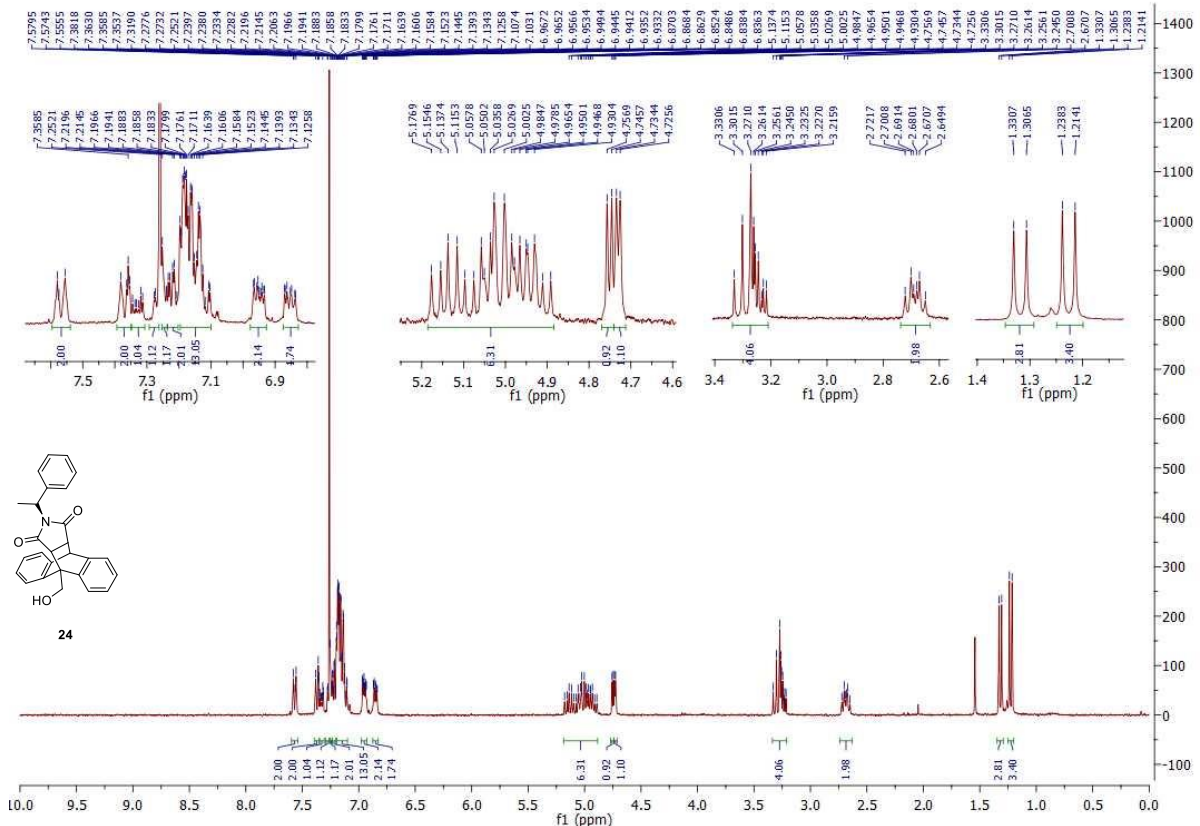




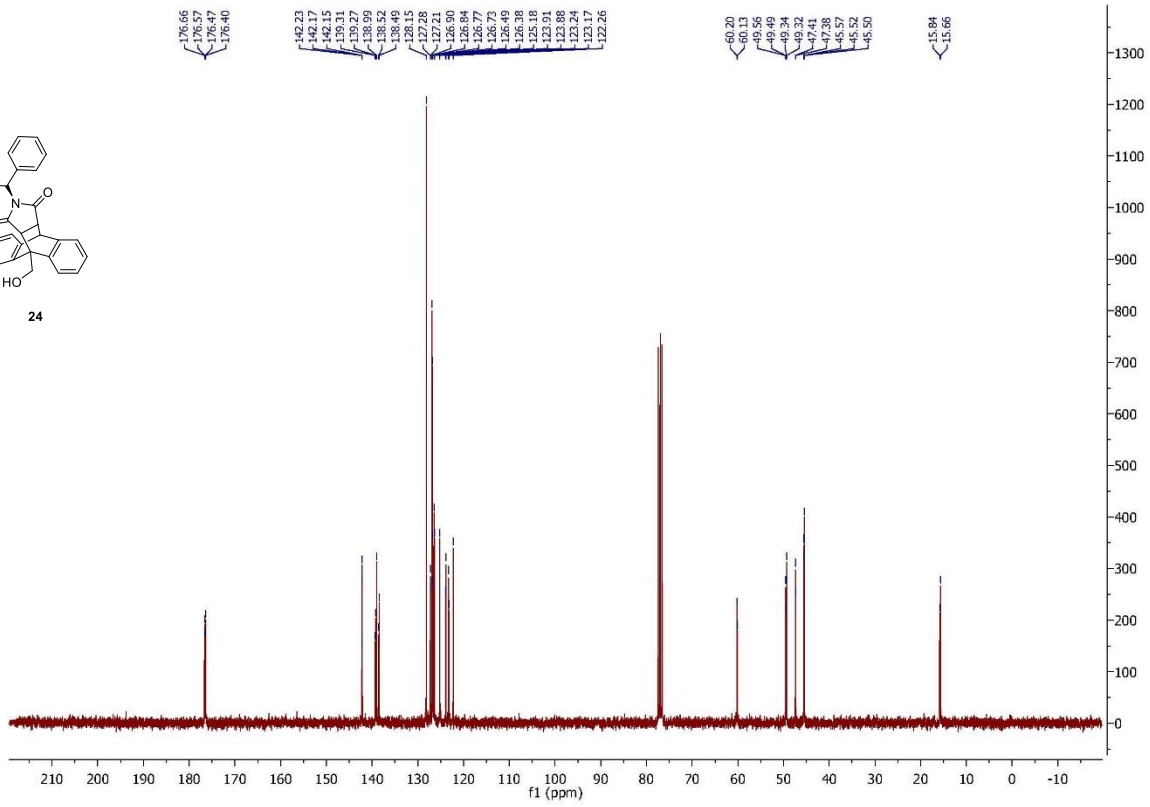


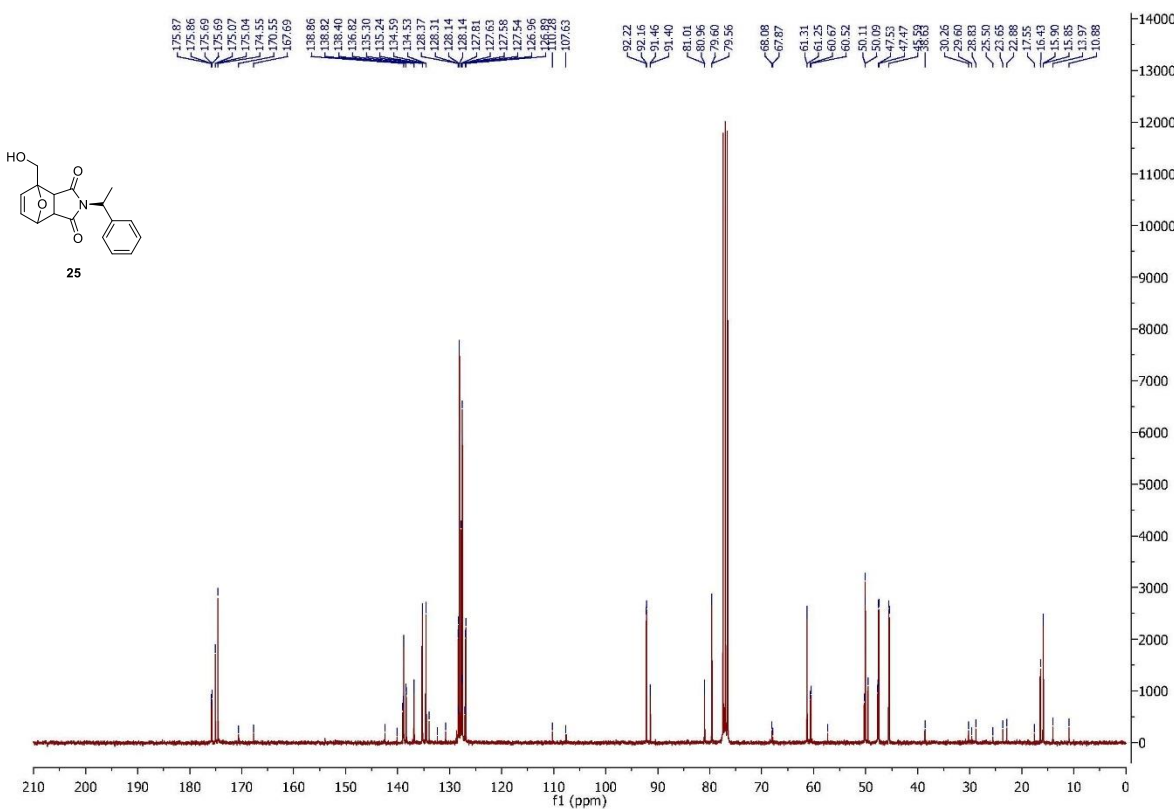
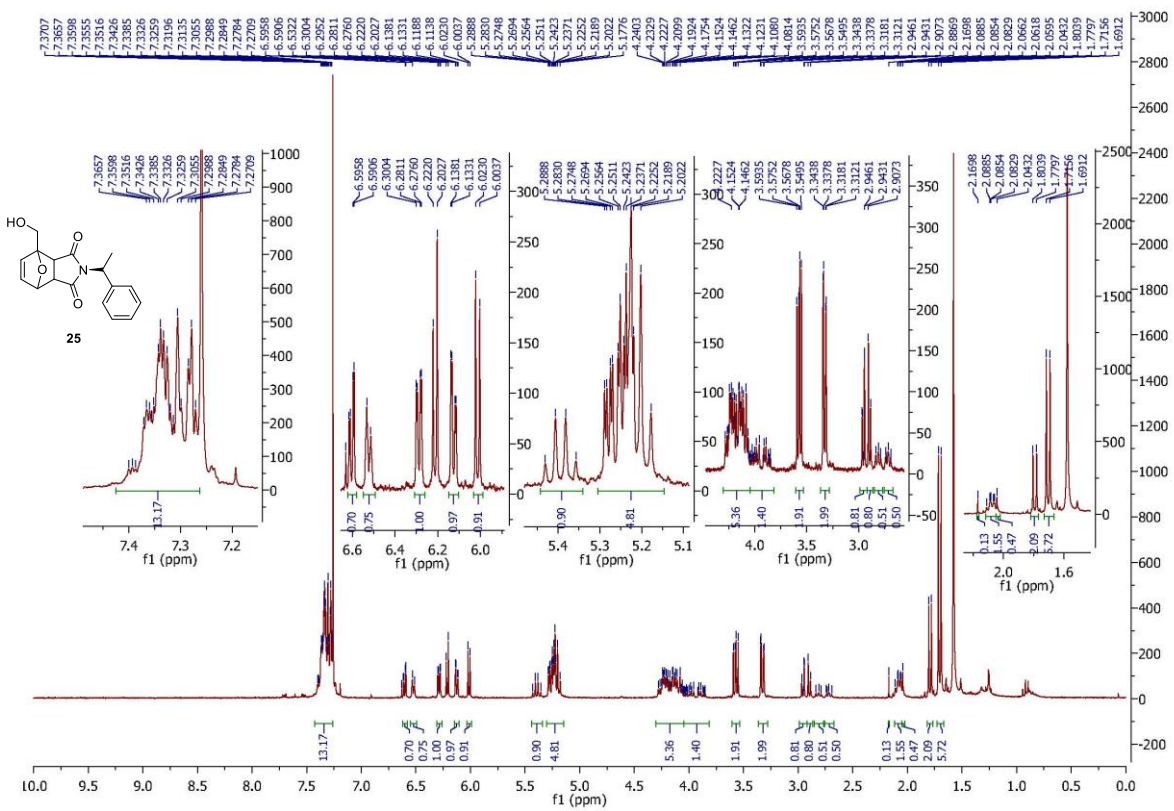


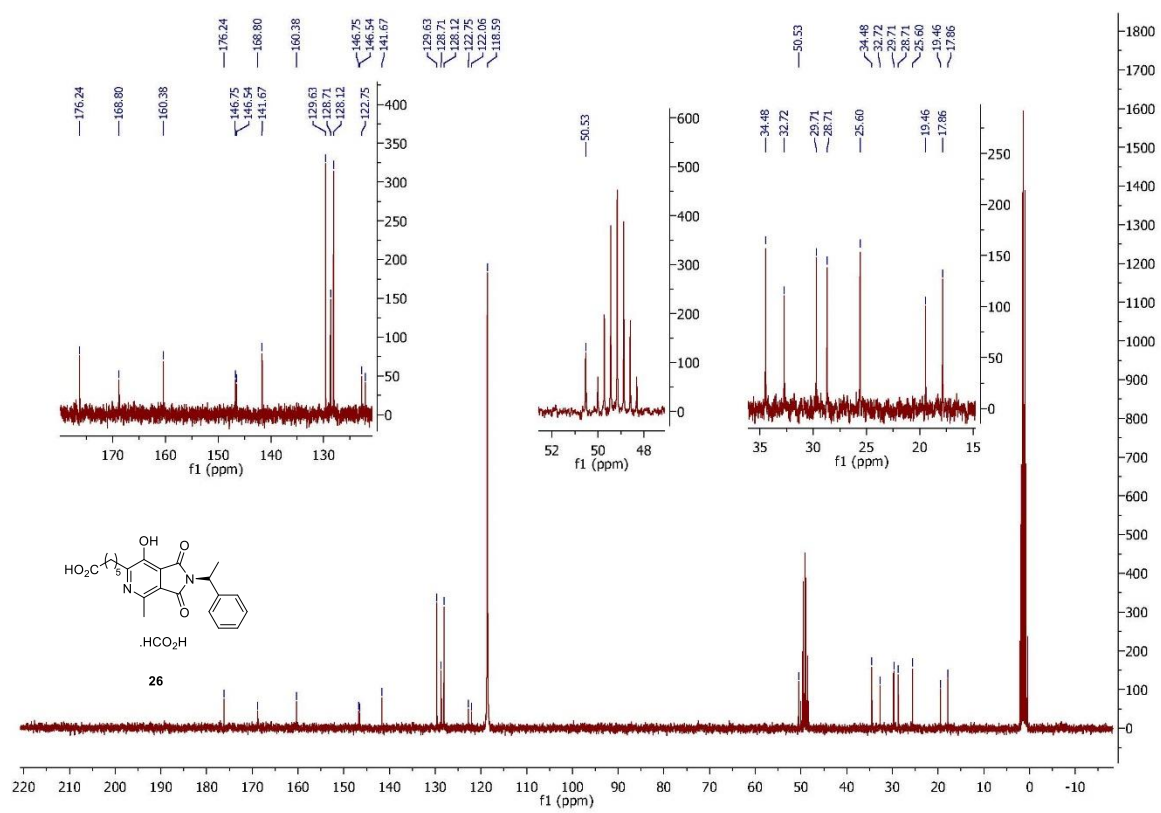
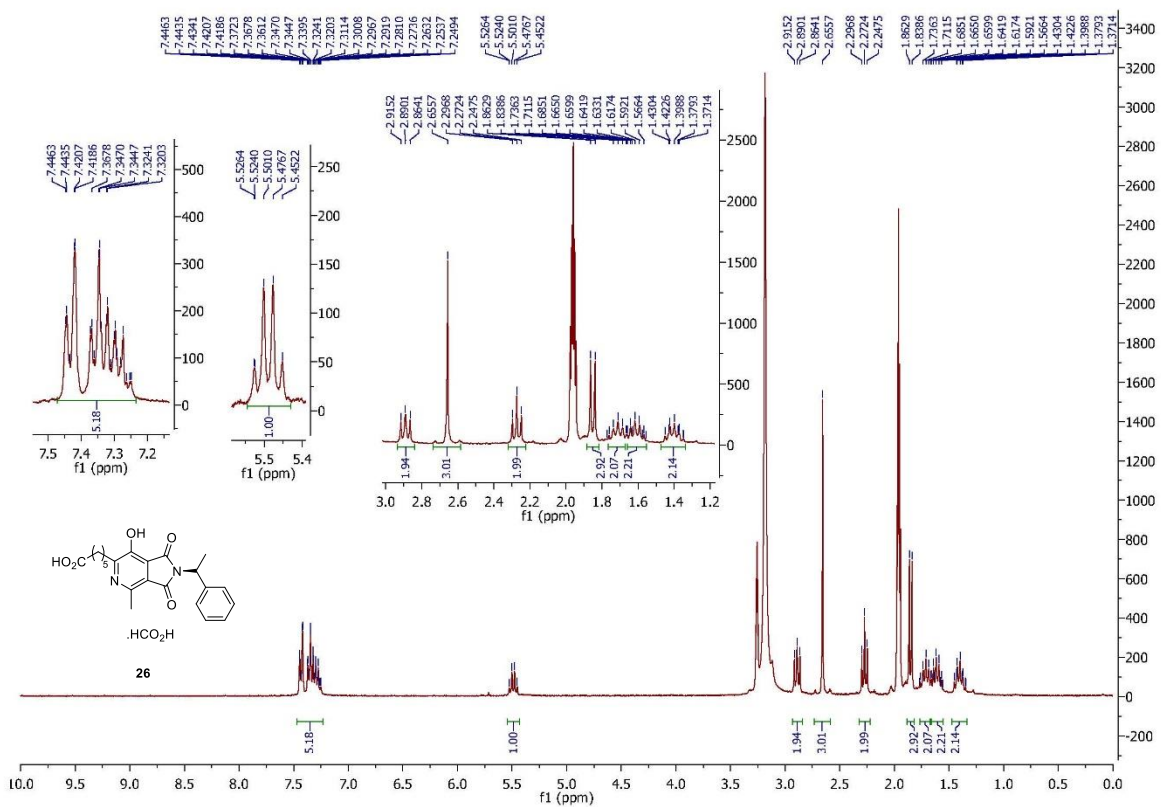


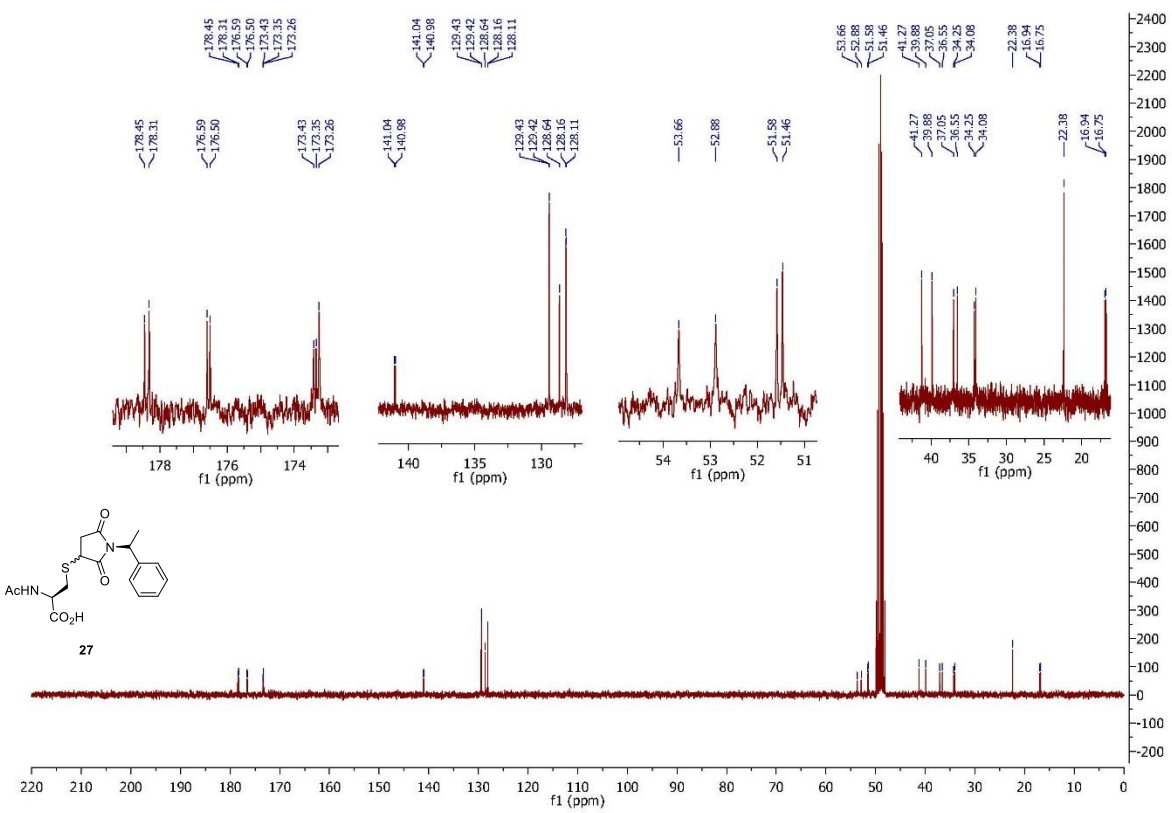
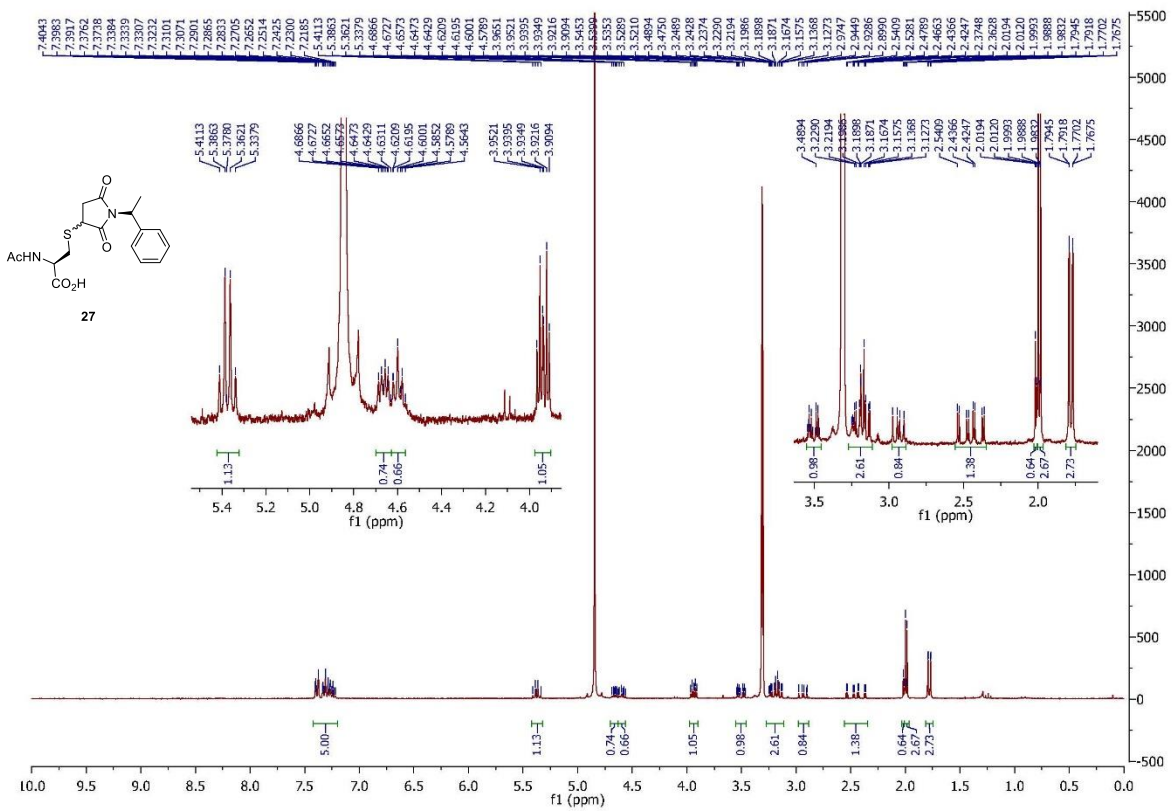


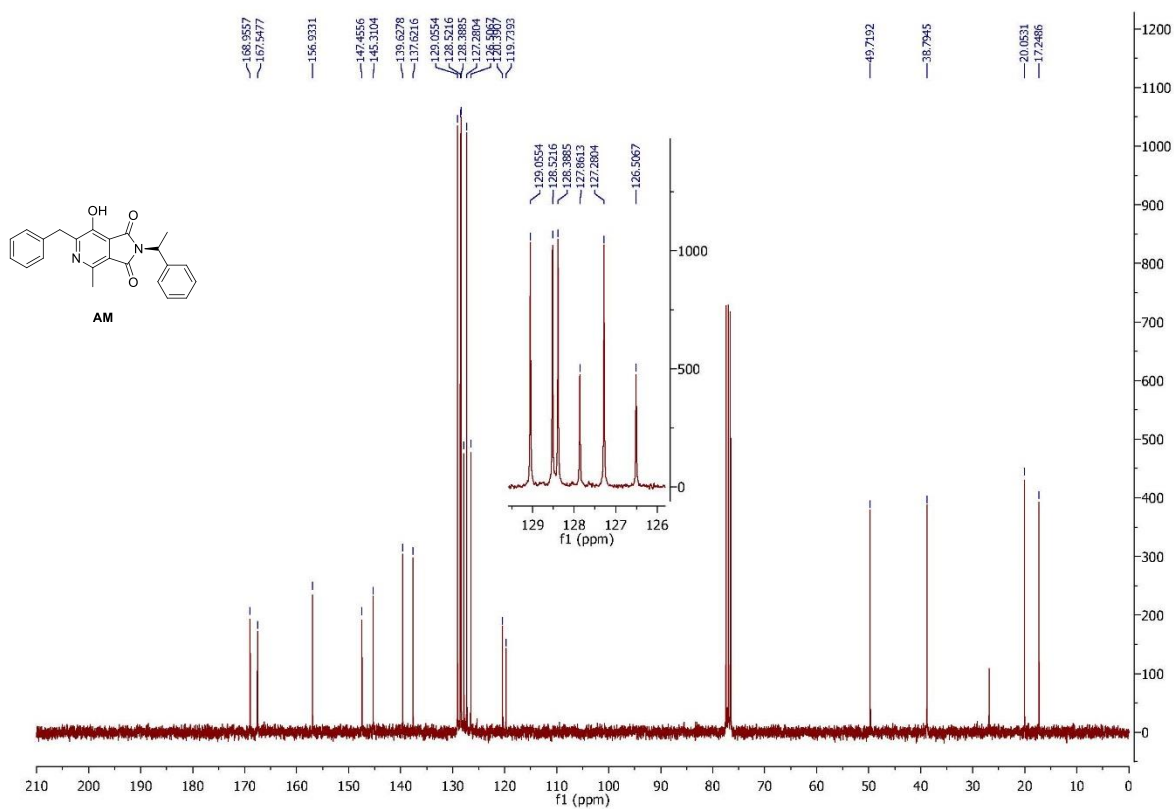
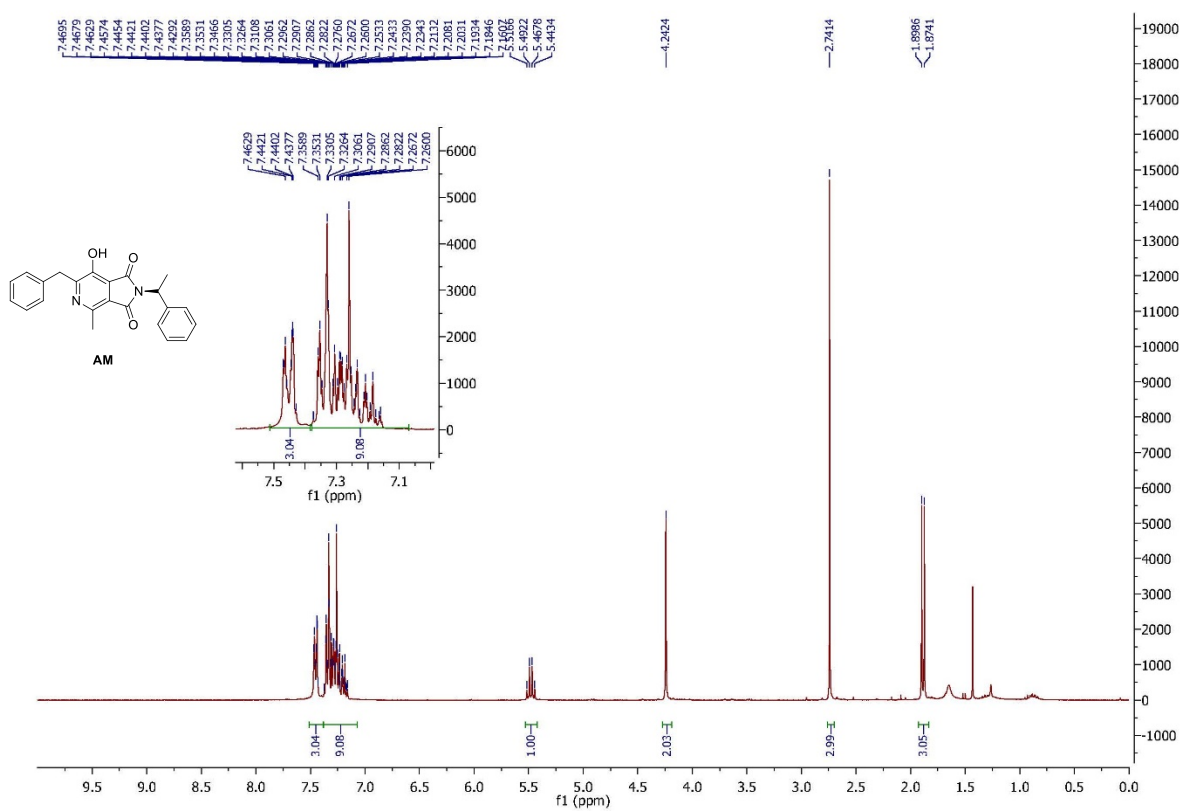
24







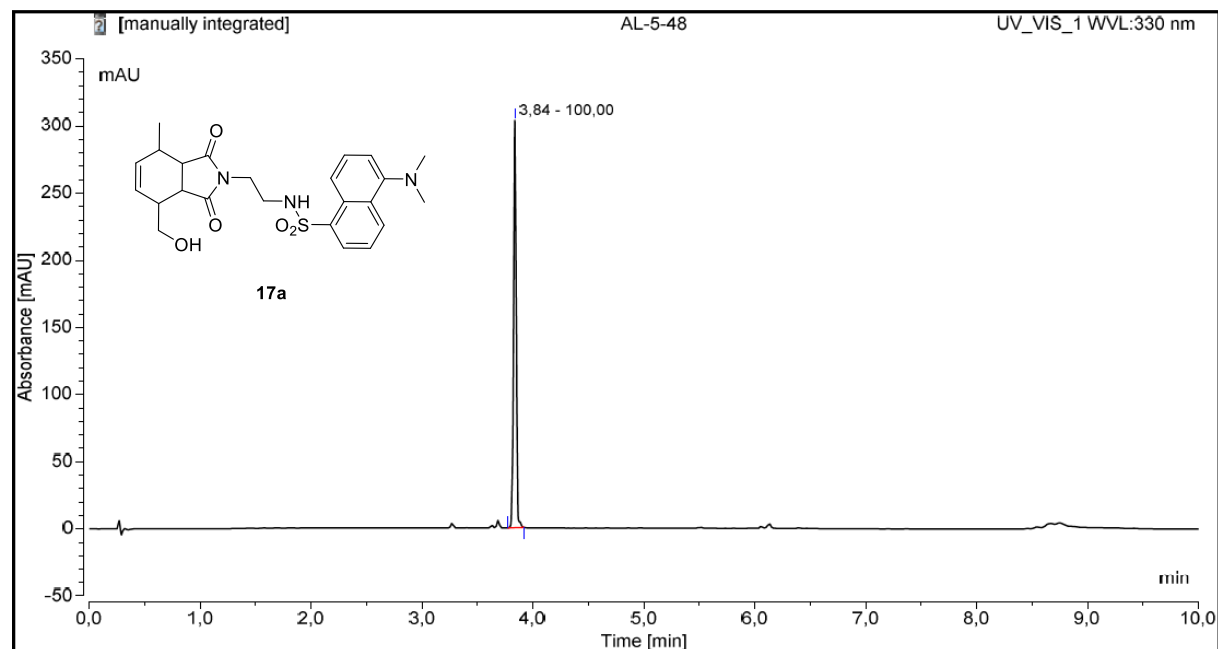




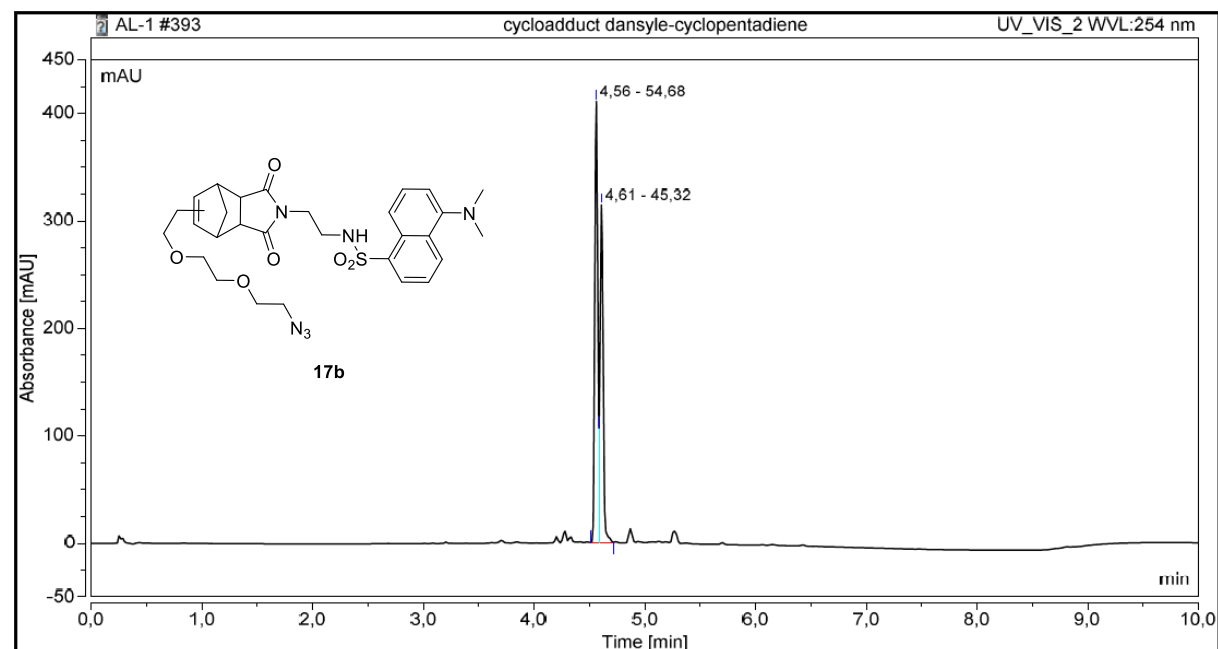
I.2. RP-HPLC chromatograms

HPLC analyses were performed according to described procedure in Materials and Methods, at $\lambda = 254$ and 330 nm. Compounds were dissolved in MeCN (300 - 400 μL) and then with milliQ H_2O (700 - 600 μL). Furfuryl alcohol was not visible by RP-HPLC. For every analyses, RP-HPLC system (A or B) are specified.

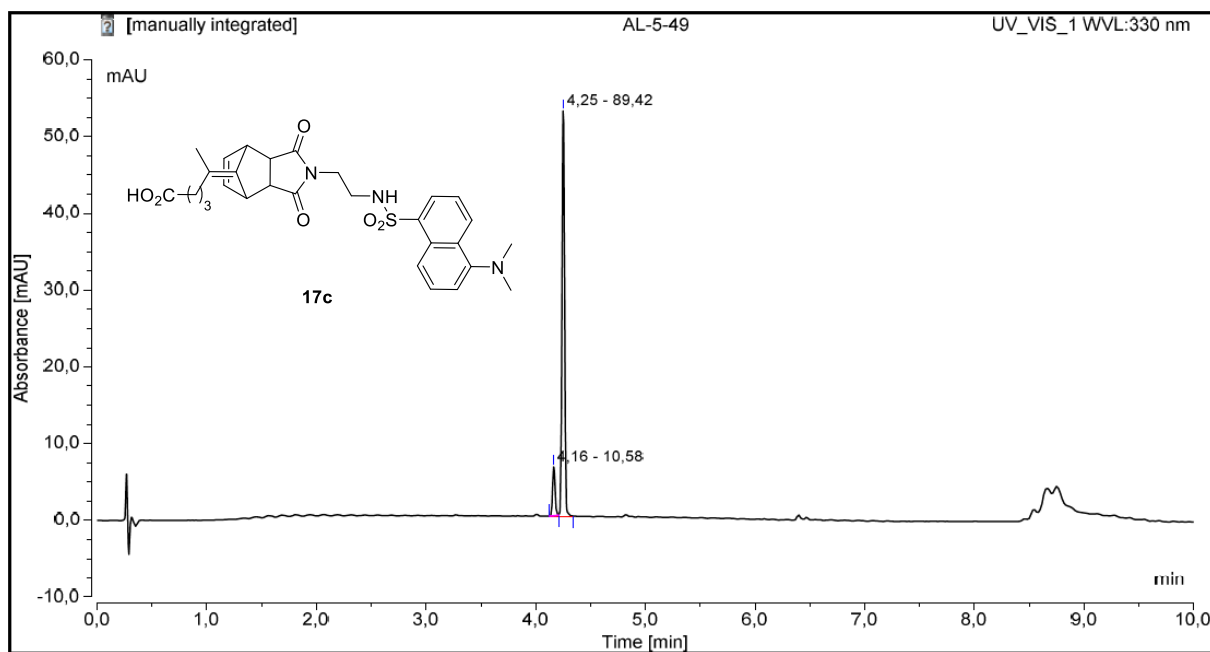
System B



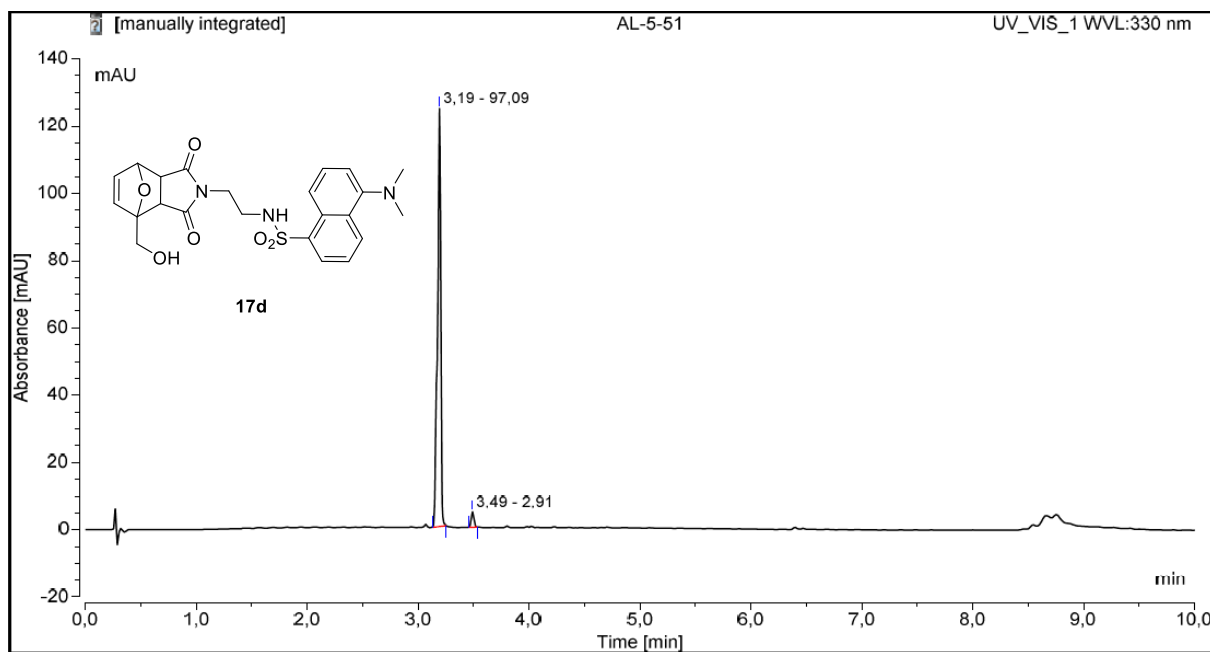
System A



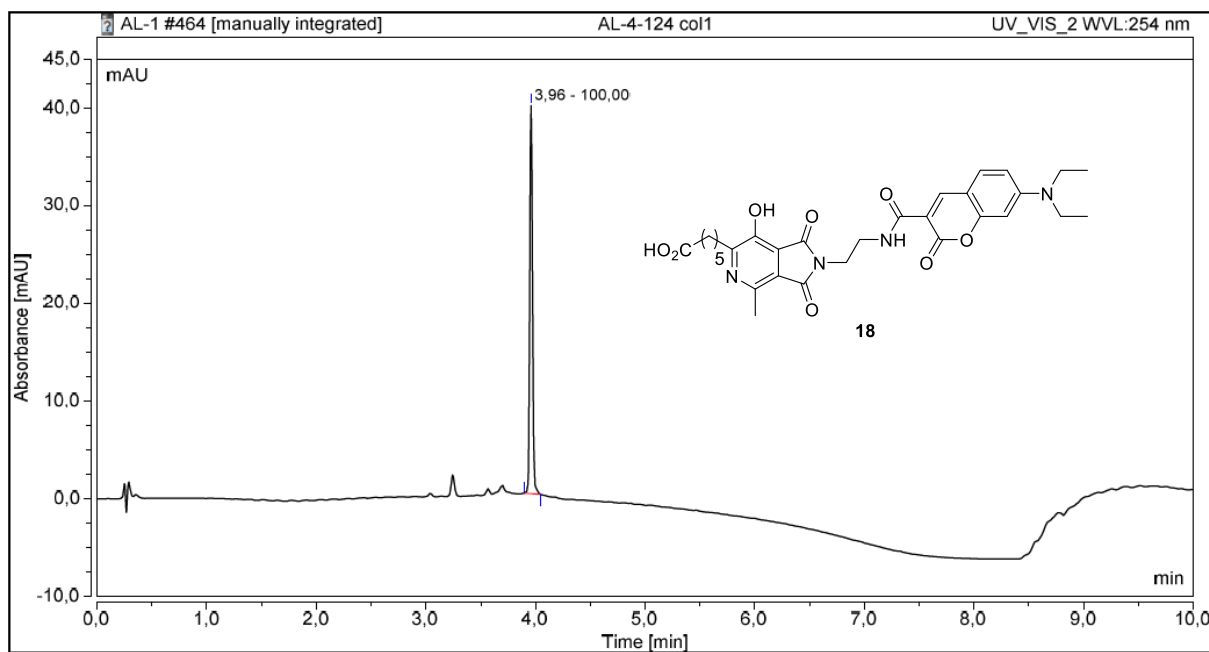
System B



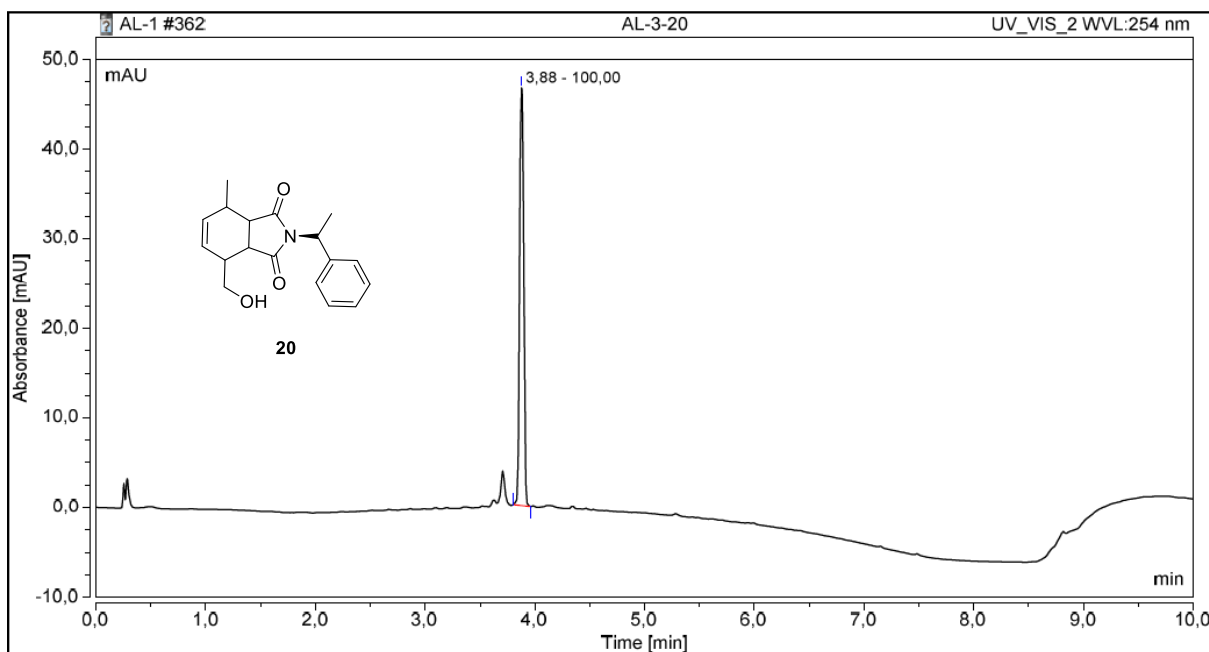
System B



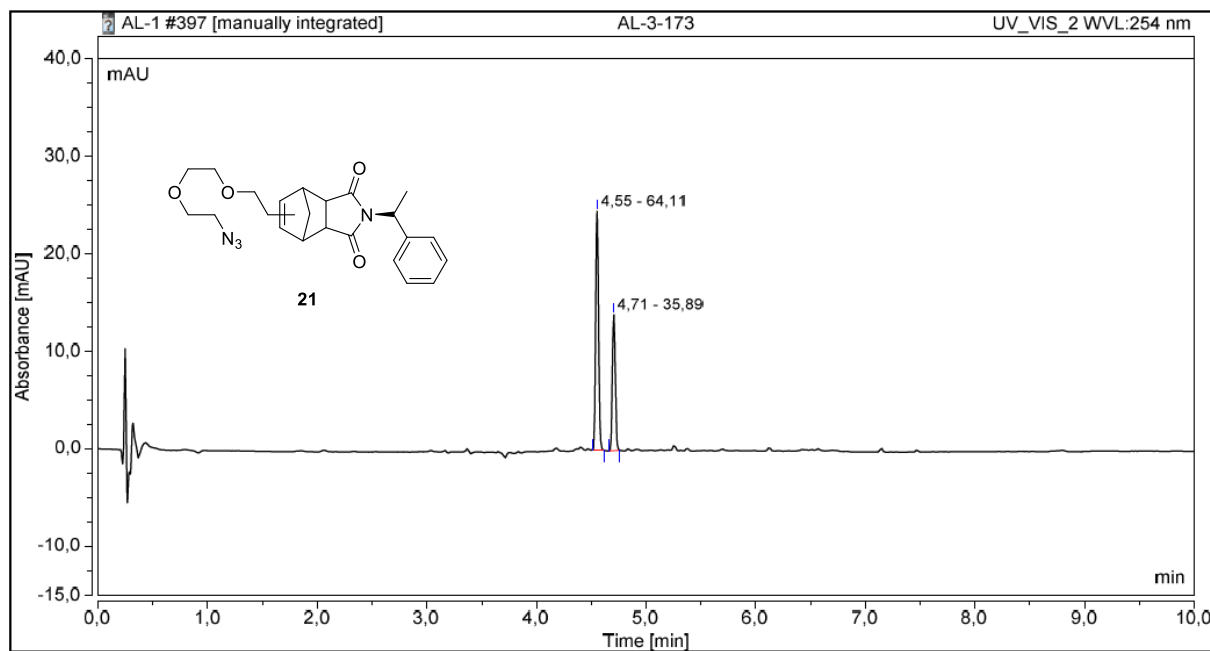
System A



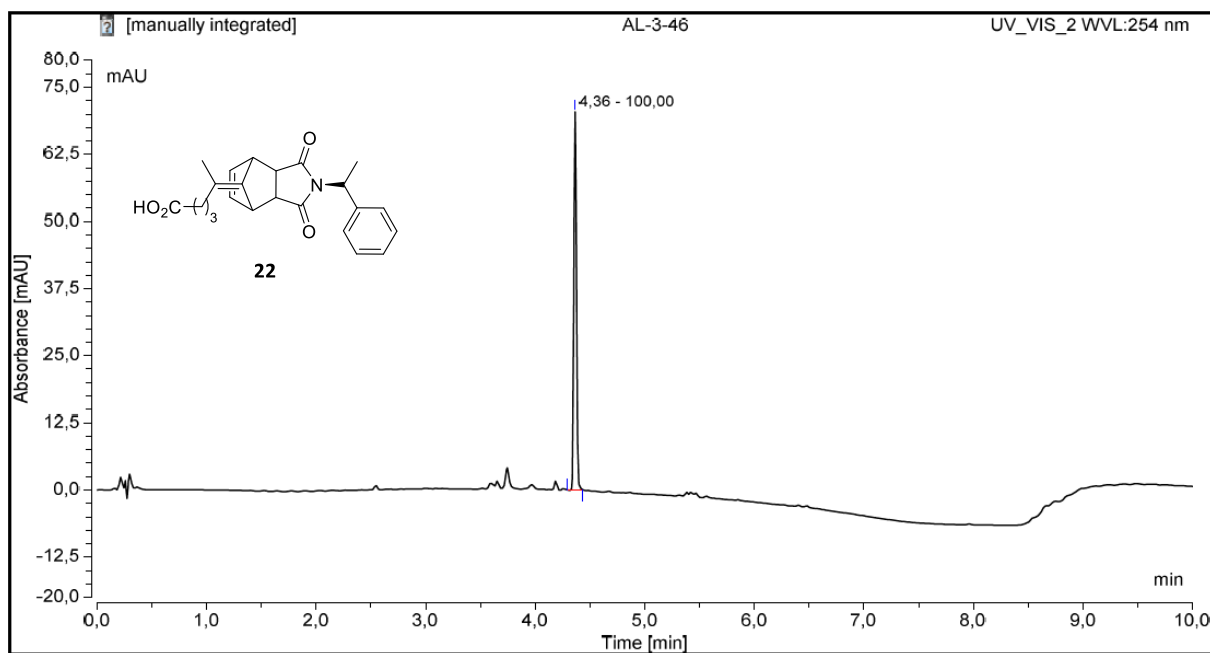
System A



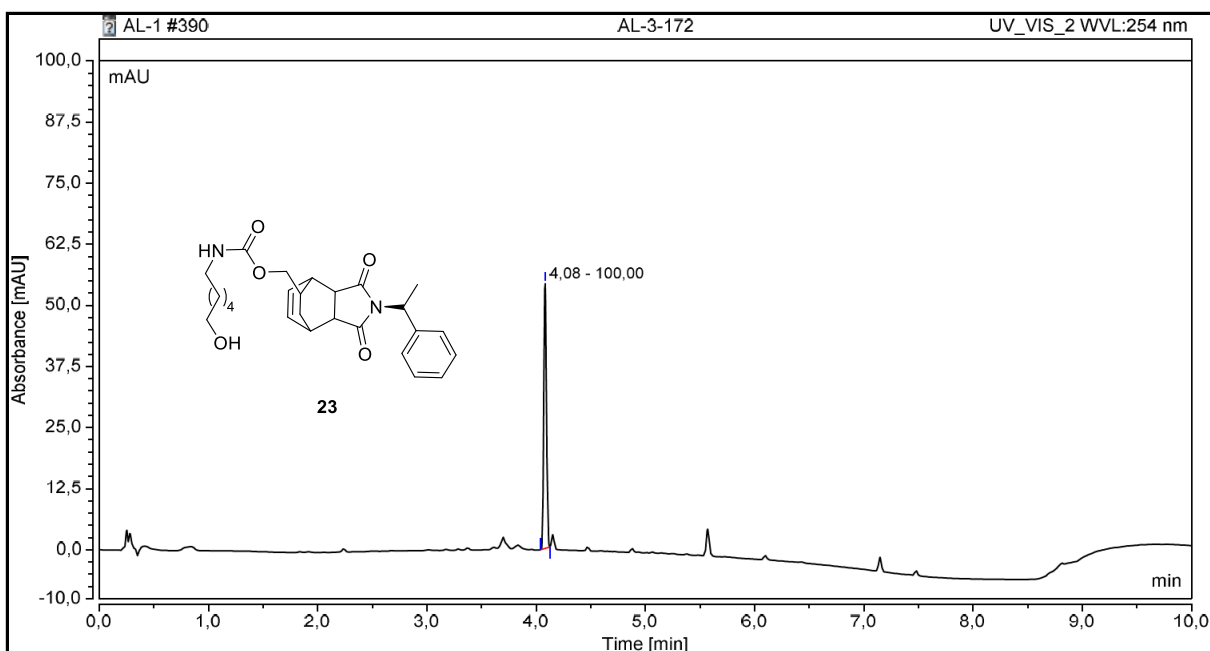
System A



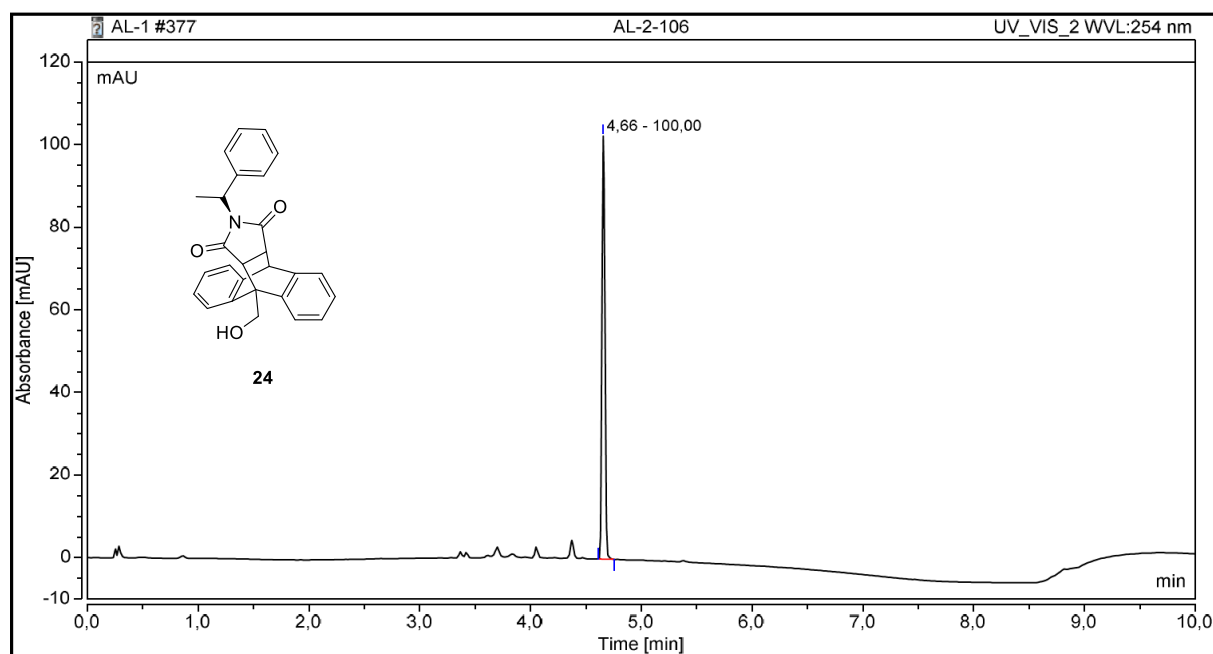
System B



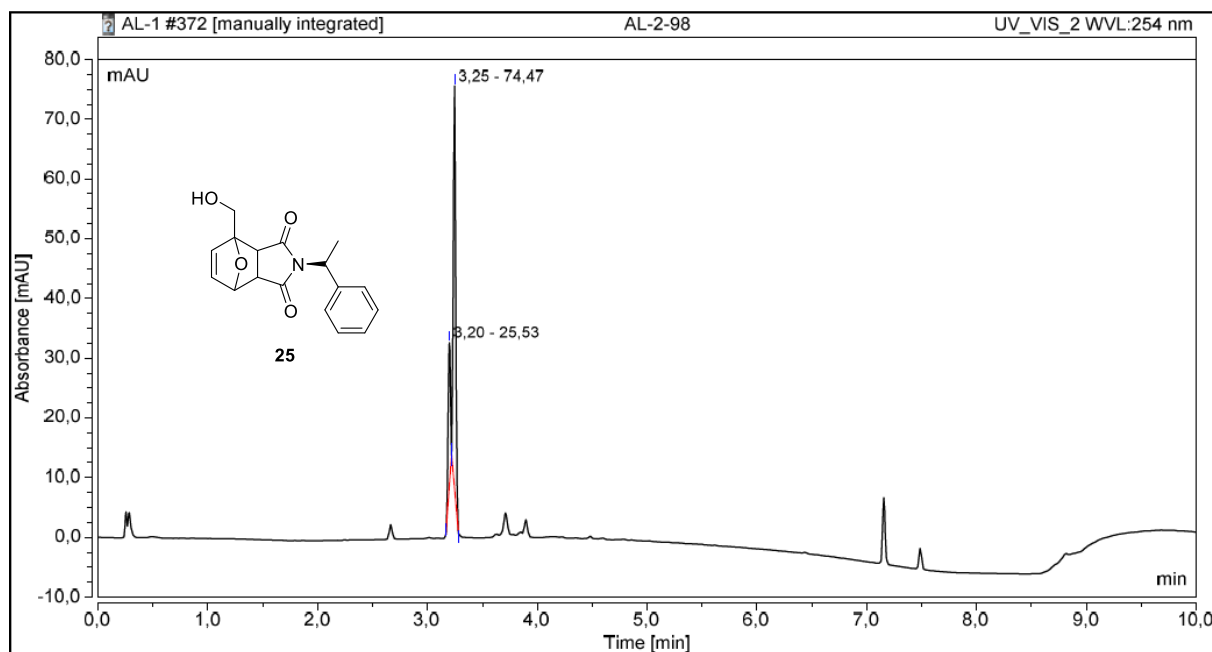
System A



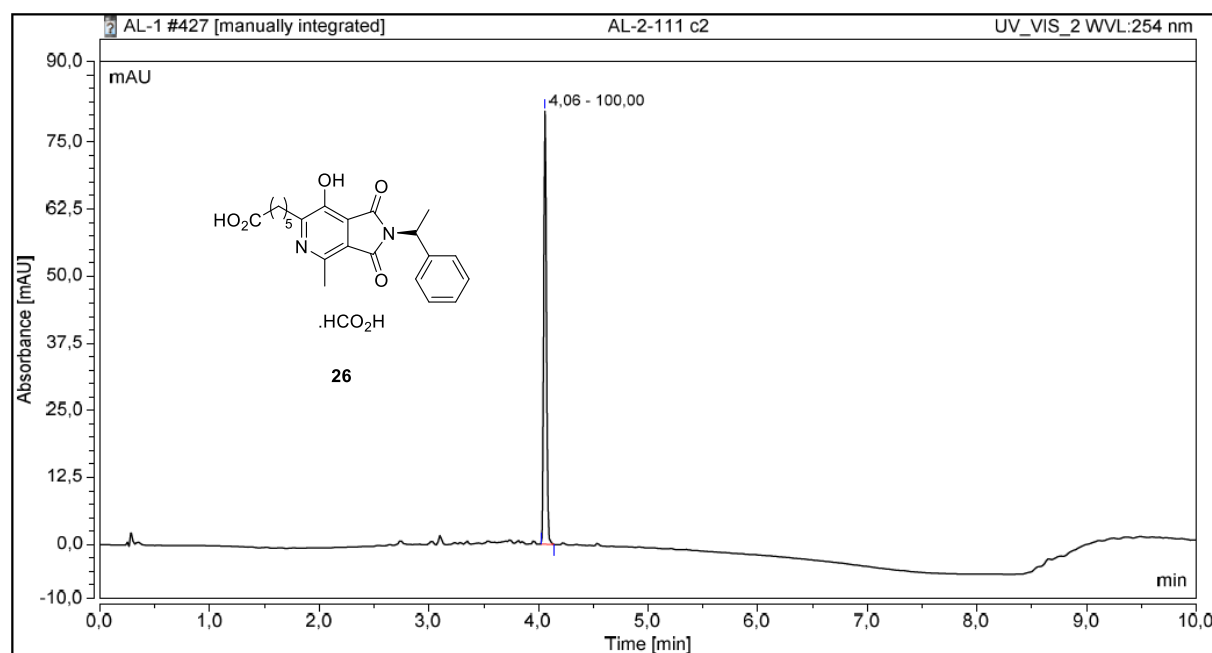
System A



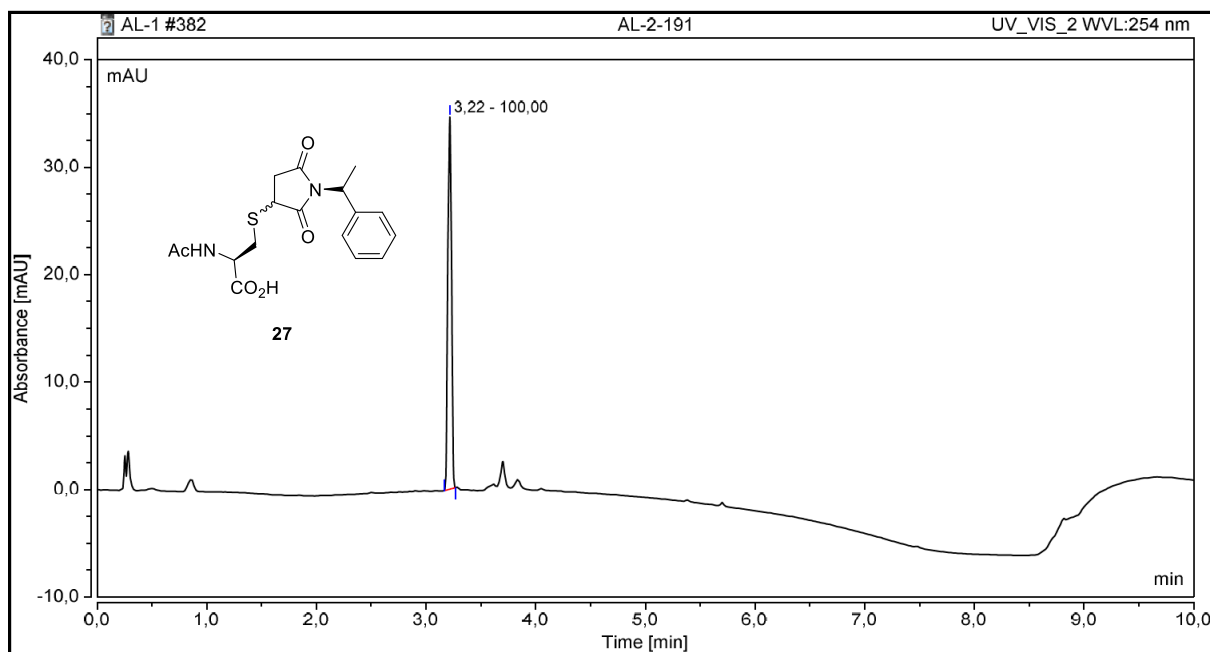
System A



System A



System A



I.3. Photophysical data for compounds **3** and **26**

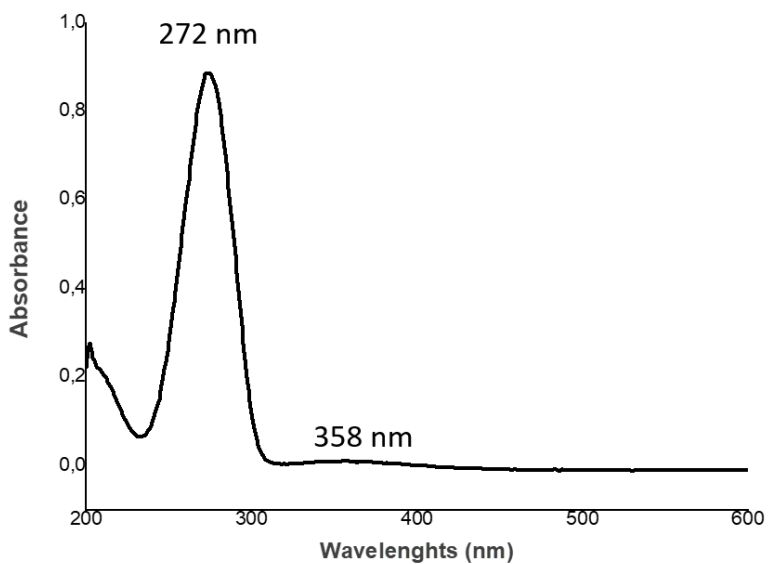


Figure S1: Absorption spectra for compound **3** (20 μ M) in PBS pH 7.4/MeCN (90:10, v.v) at 20 °C.

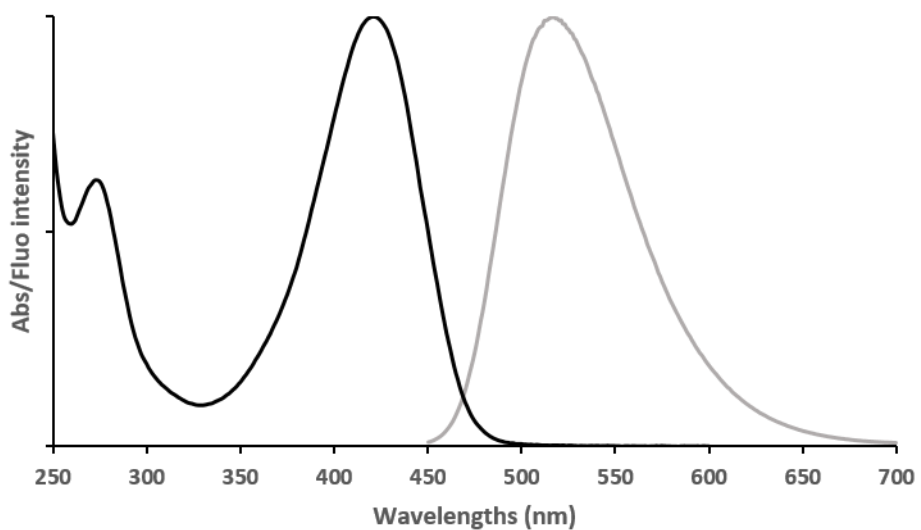
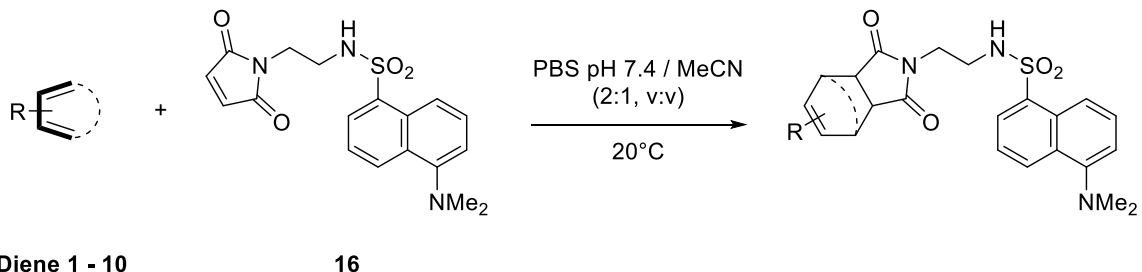


Figure S2: Normalized absorption (black line), emission (grey line, $\lambda_{\text{ex}} = 422$ nm) spectra for compound **26** in PBS pH 7.4 at 25 °C.

II. Kinetic experiments

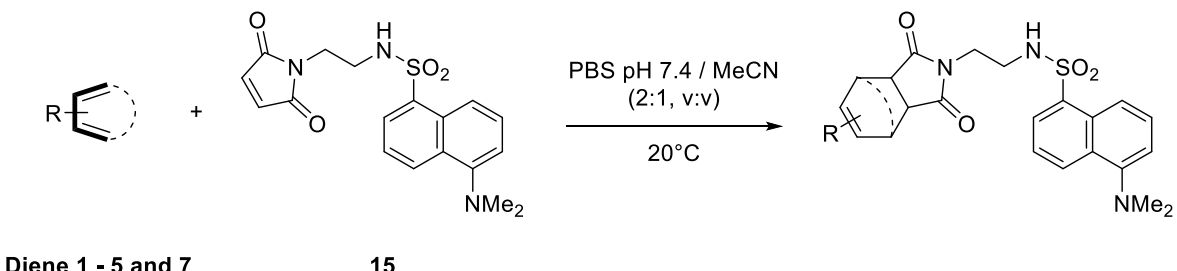
II.1. Monitoring of fluorescence intensity change of Diels-Alder reactions

a) Probe **16** (1 mM) and dienes **1-10** (5 mM)



To a 1.25 mM solution of probe **16** in MeCN/PBS pH 7.4 (2.4 mL, 1:5, v:v) in a fluorescence cell, was added a 25 mM solution of the corresponding diene **1-10** in MeCN (0.6 mL). The resulting mixture was rapidly homogenized and introduced in the spectrophotometer. The resulting composition of the mixture at $t = 0$ min was as follows: MeCN/PBS pH 7.4 (3mL, 1:2, v:v); probe **16** (1 mM); diene (5 mM, 5 equiv.). Diels-Alder reactions were monitored by fluorescence spectroscopy ($\lambda_{\text{ex}} = 330$ nm ; $\lambda_{\text{ex}} = 560$ nm) at $T = 20$ °C.

b) Probe **16** (0.05 mM) and dienes **1-2, 4-6 or 8** (4 mM)



To a 1.4 mM solution of probe **16** in MeCN (50 μ L) in a fluorescence cell, were successively added MeCN (17 μ L), a solution of PBS pH 7.4 (933 μ L) and a 14 mM solution of the corresponding diene **1-2, 4-6 or 8** in MeCN (0.4 mL). The resulting mixture was rapidly homogenized and introduced in the spectrophotometer. The resulting composition of the mixture at $t = 0$ min was as follows: MeCN/PBS pH 7.4 (1.4 mL, 1:2, v:v); probe **16** (0.05 mM); diene (4 mM, 80 equiv.). Diels-Alder reactions were monitored by fluorescence spectroscopy ($\lambda_{\text{ex}} = 330$ nm ; $\lambda_{\text{ex}} = 560$ nm) at $T = 20$ °C.

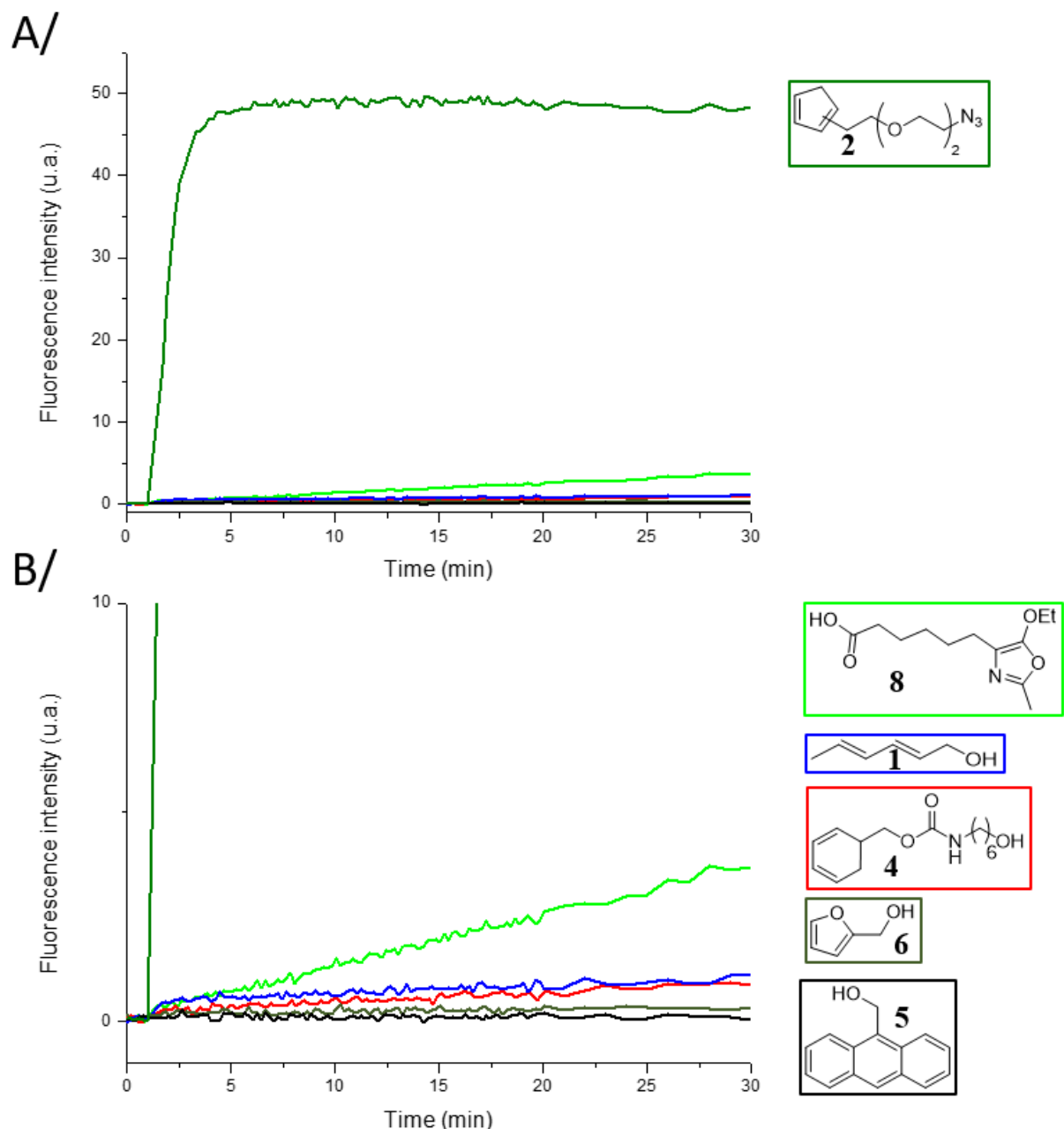


Figure S3. (A) Time-dependent fluorescence intensity changes of dansyl-based probe **16** (0.05 mM) in the presence of dienes **1-2, 4-6** or **8** (4 mM, 80 equiv.) in MeCN/PBS pH 7.4 (1:2, v:v) recorded at λ_{em} 560 nm upon excitation at λ_{ex} 330 nm. (B) Enlarged view of Figure (A).

II.2. RP-HPLC monitoring of cycloadducts formation

Diels-Alder reactions carried out with probe **16** (1 mM) and dienes (5 mM) in PBS/MeCN (2:1, v:v) were also monitored by RP-HPLC at $\lambda_{\text{abs}} = 330$ nm after 1 h (except for diene **2** which was monitored after 10 min) in order to confirm the reaction progress of probe **16** which was observed by fluorescence spectroscopy. System A or B are specified for each experiment (sA or sB, respectively).

Legend:

- Compound **16** ($t_R = 3.19$ to 3.42 min) is labelled with green star (*).
- Dienes are labelled with a purple star (*) when detected at 330 nm.
- Cycloadducts are labelled with a blue star (*) .

Note:

330 nm was selected as the detection wavelength because only dansyle scaffold absorbs, which is not the case for all cycloadduct scaffolds at this wavelength, thus allowing a reliable ratio determination between the dansyl-based maleimide and dansyl-based cycloadduct. Of note, only the fulvene **3** and anthracene **5** were able to absorb at 330 nm but their corresponding cycloadducts scaffolds do not (cf following RP-HPLC).

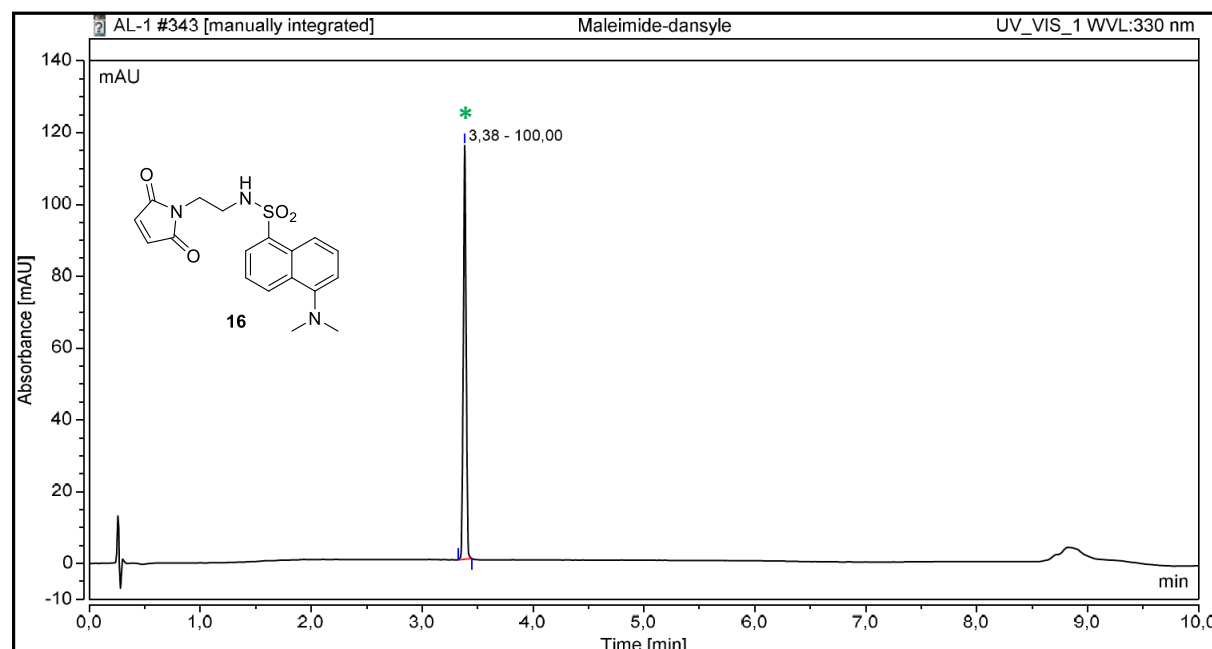


Figure S4. RP-HPLC chromatogram of probe **16** ($\lambda = 330$ nm, sA).

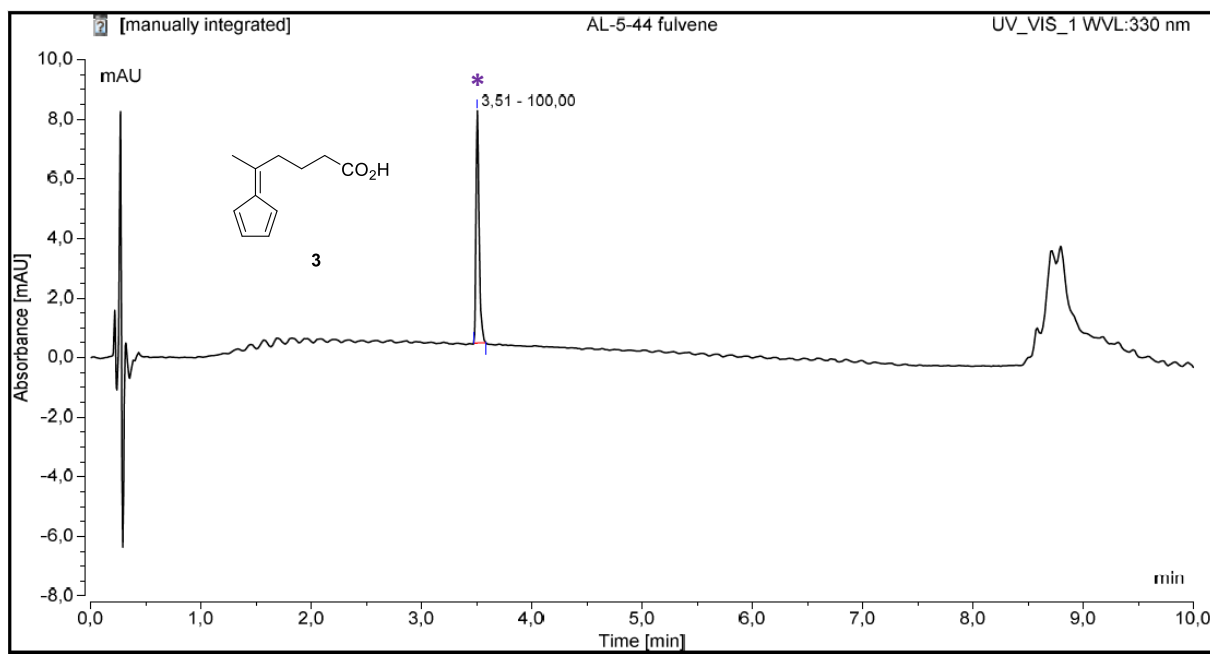


Figure S5. RP-HPLC chromatogram of fulvene **3** ($\lambda = 330$ nm, sB).

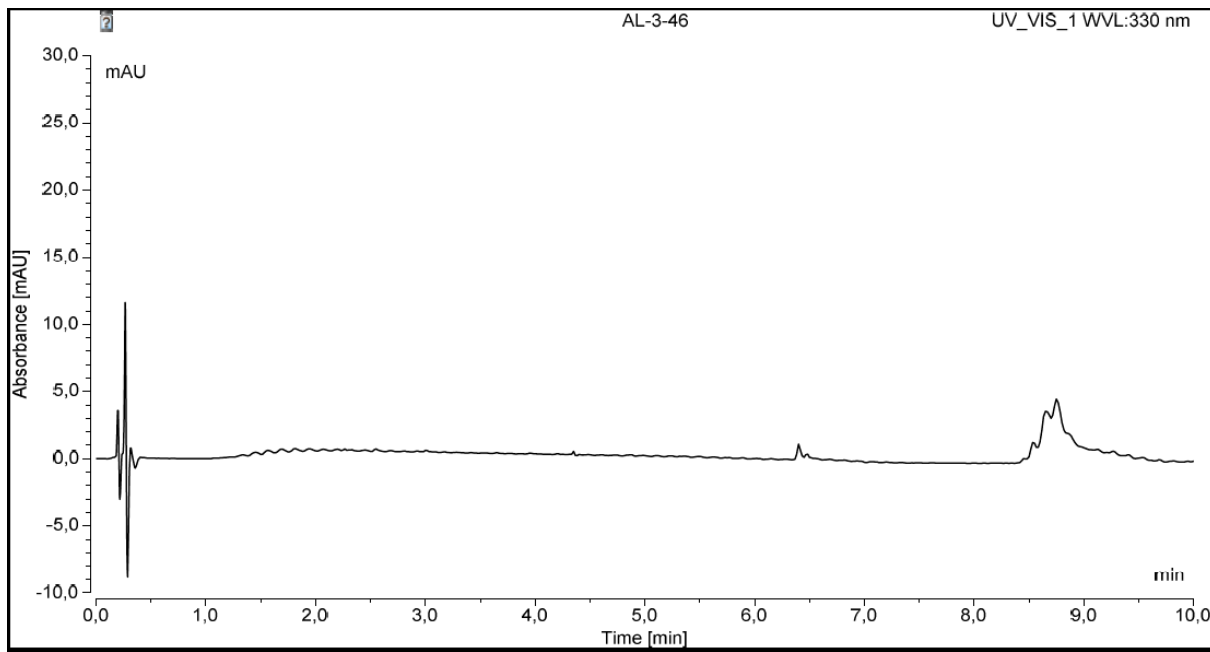


Figure S6. RP-HPLC chromatogram of fulvene-based cycloadduct **22** ($\lambda = 330$ nm, sB).

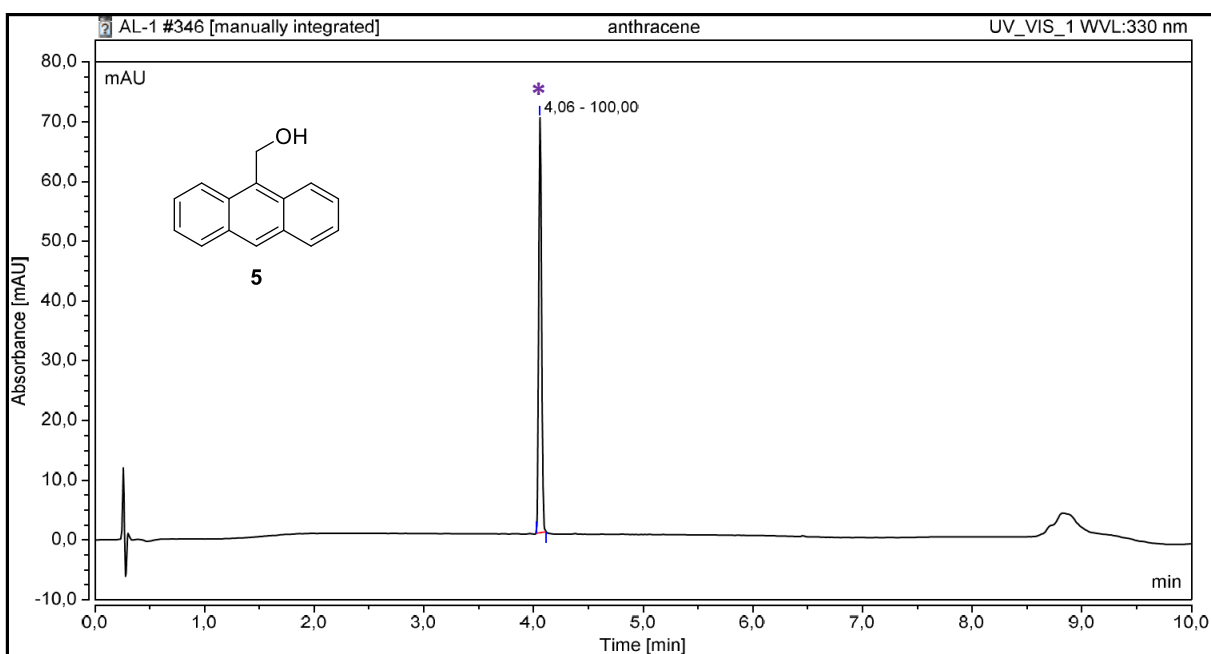


Figure S7. RP-HPLC chromatogram of anthracene **5** ($\lambda = 330$ nm, sA).

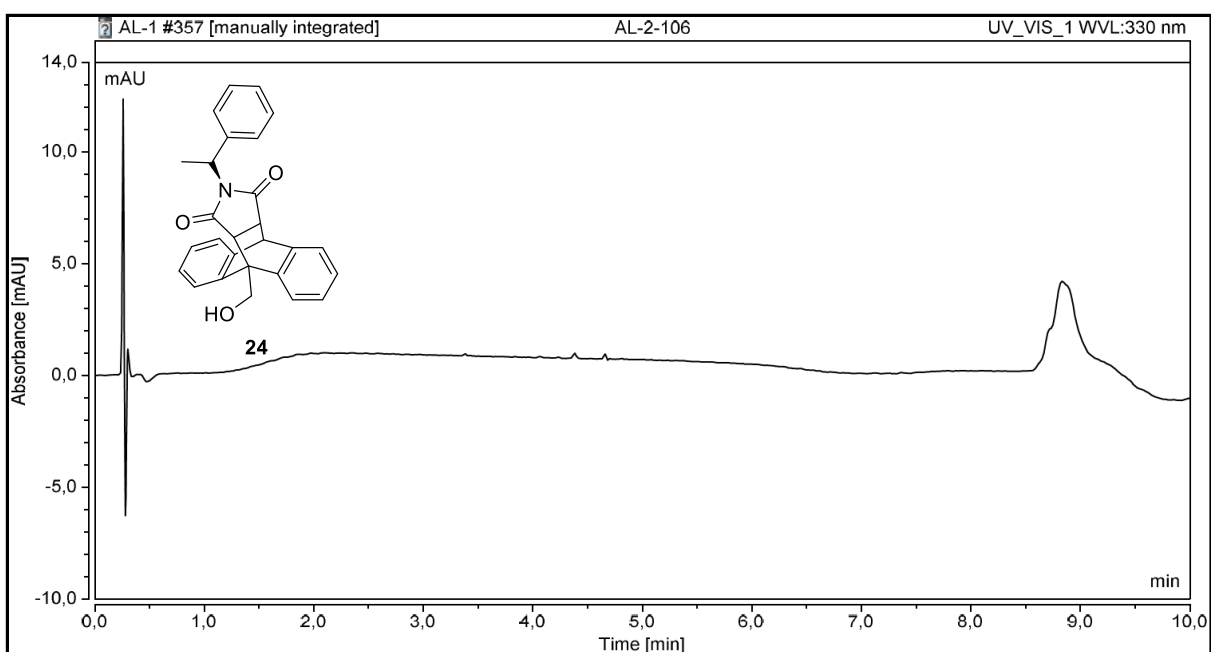
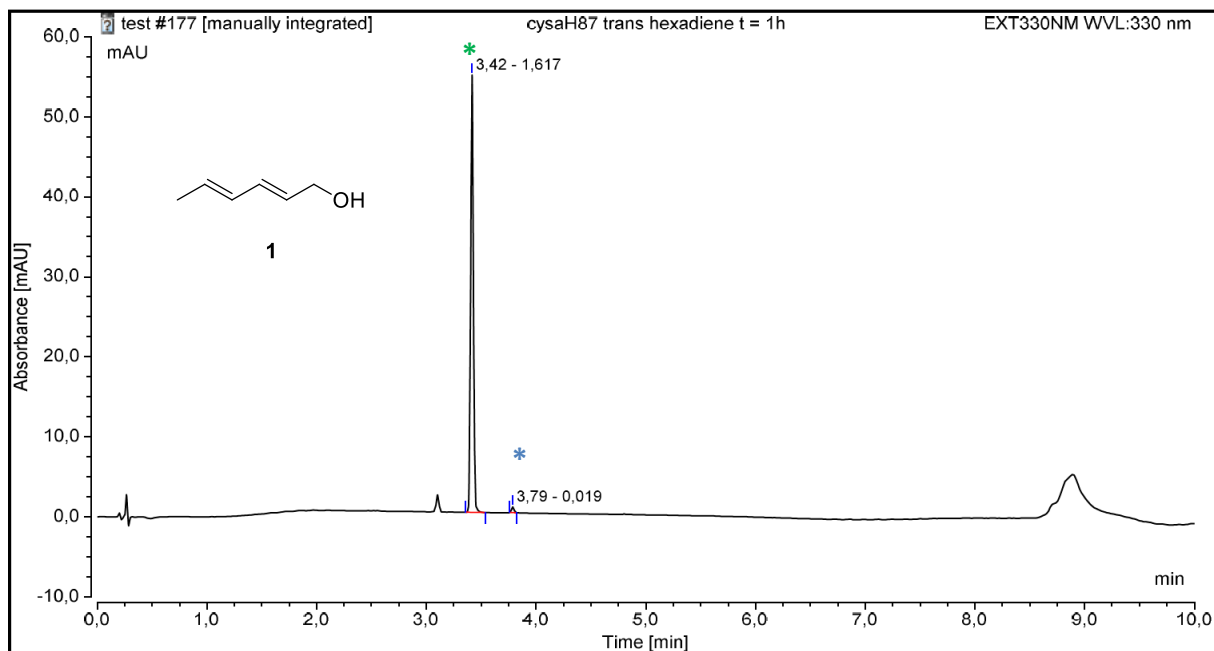


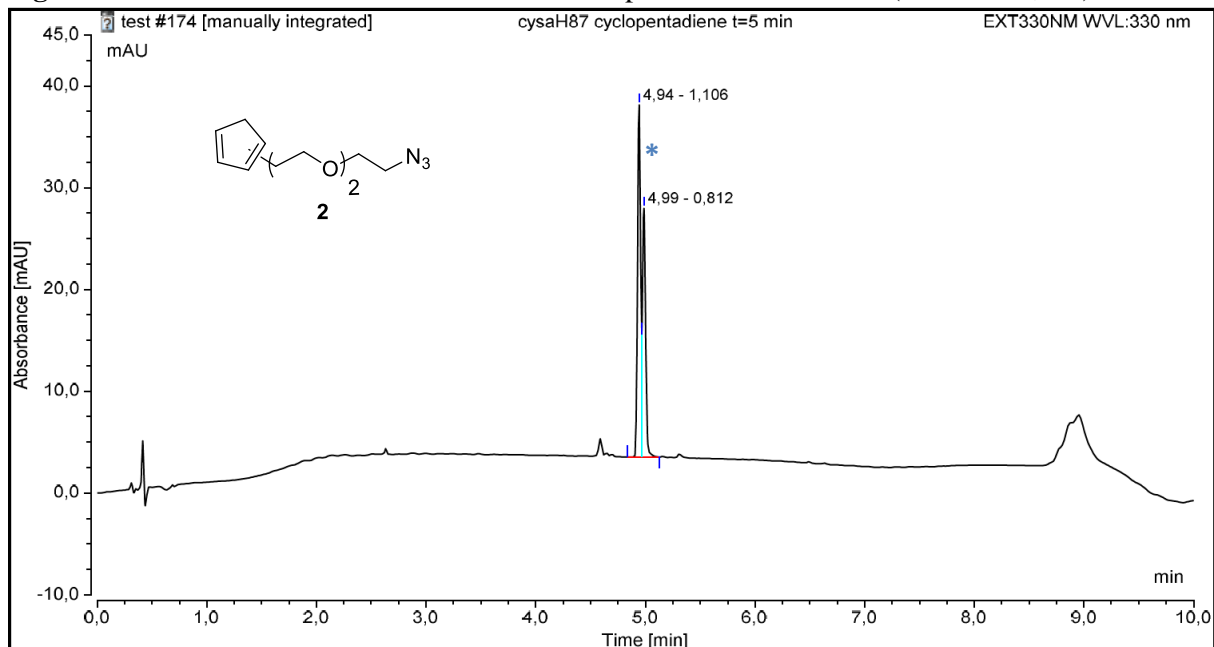
Figure S8. RP-HPLC chromatogram of anthracene-based cycloadduct **24** ($\lambda = 330$ nm, sA).



Integration Results							
No.	Peak Name	Retention Time min	Area mAU*min	Height mAU	Relative Area %	Relative Height %	Amount n.a.
1		3,417	1,617	54,669	98,81	98,70	n.a.
2		3,787	0,019	0,721	1,19	1,30	n.a.
Total:			1,636	55,390	100,00	100,00	

Conversion of 16 = 1.2%

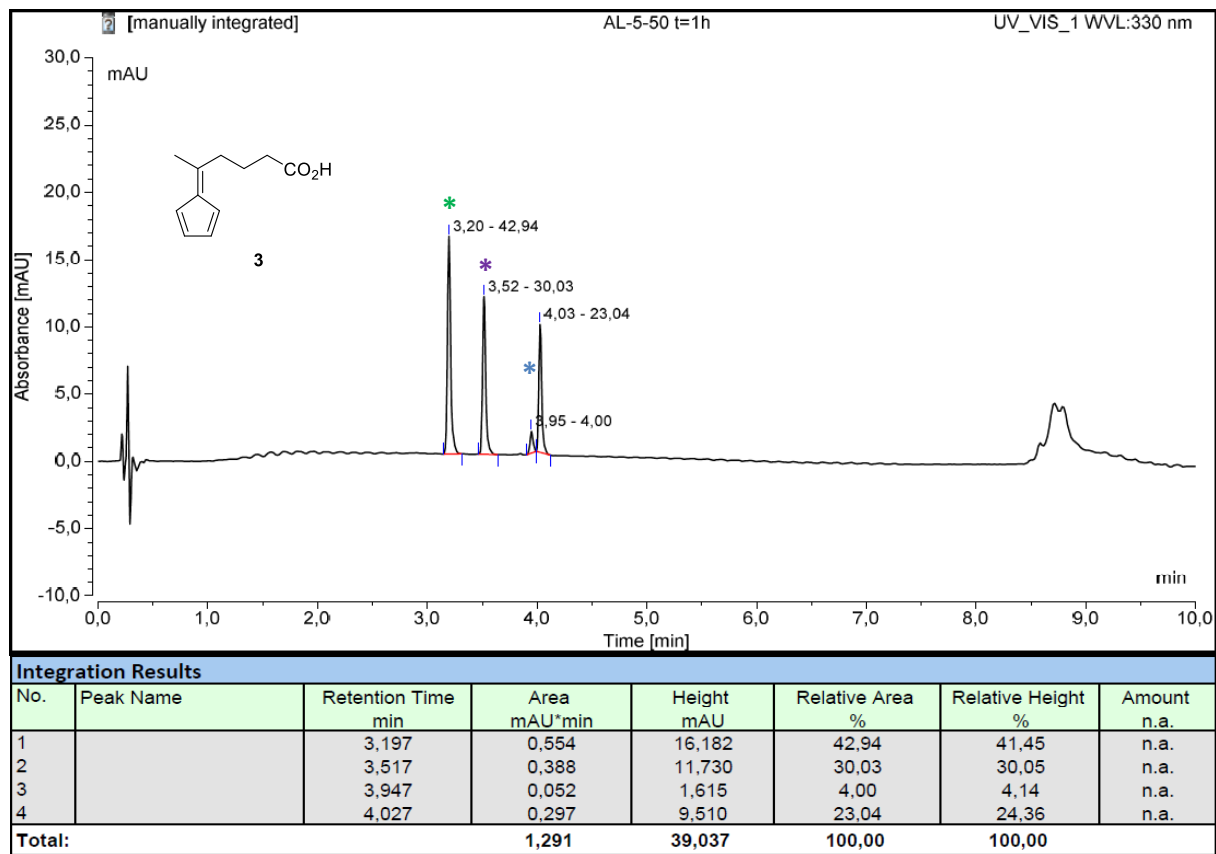
Figure S9. RP-HPLC of the Diels-Alder reaction of probe **16** with diene **1** ($\lambda = 330$ nm, sA).



Integration Results							
No.	Peak Name	Retention Time min	Area mAU*min	Height mAU	Relative Area %	Relative Height %	Amount n.a.
1		4,943	1,106	34,586	57,66	58,59	n.a.
2		4,987	0,812	24,446	42,34	41,41	n.a.
Total:			1,918	59,031	100,00	100,00	

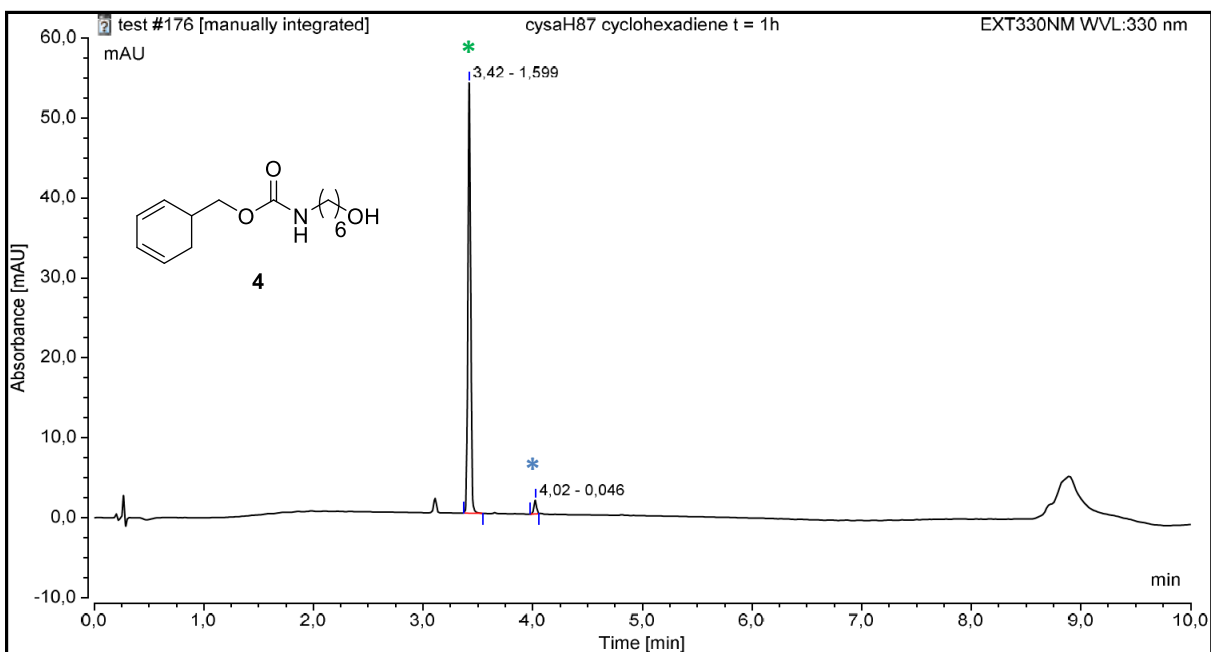
Conversion of 16 = 100%

Figure S10. RP-HPLC of the Diels-Alder reaction of probe **16** with diene **2** ($\lambda = 330$ nm, sA).



Conversion of 16 = 39%

Figure S11. RP-HPLC of the Diels-Alder reaction of probe **16** with diene **3** ($\lambda = 330$ nm, sB)

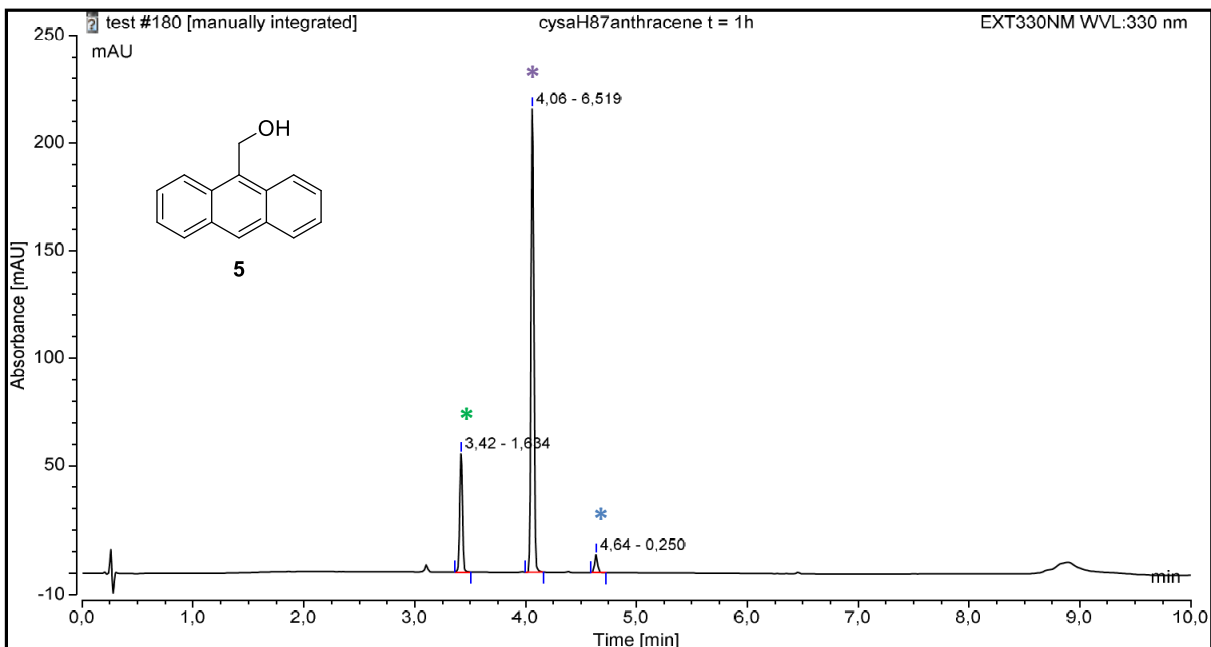


Integration Results

No.	Peak Name	Retention Time min	Area mAU*min	Height mAU	Relative Area %	Relative Height %	Amount n.a.
1		3,420	1,599	53,838	97,21	96,92	n.a.
2		4,023	0,046	1,709	2,79	3,08	n.a.
Total:			1,645	55,547	100,00	100,00	

Conversion of 16 = 2.8%

Figure S12. RP-HPLC of the Diels-Alder reaction of probe **16** with diene **4** ($\lambda = 330$ nm, sA).

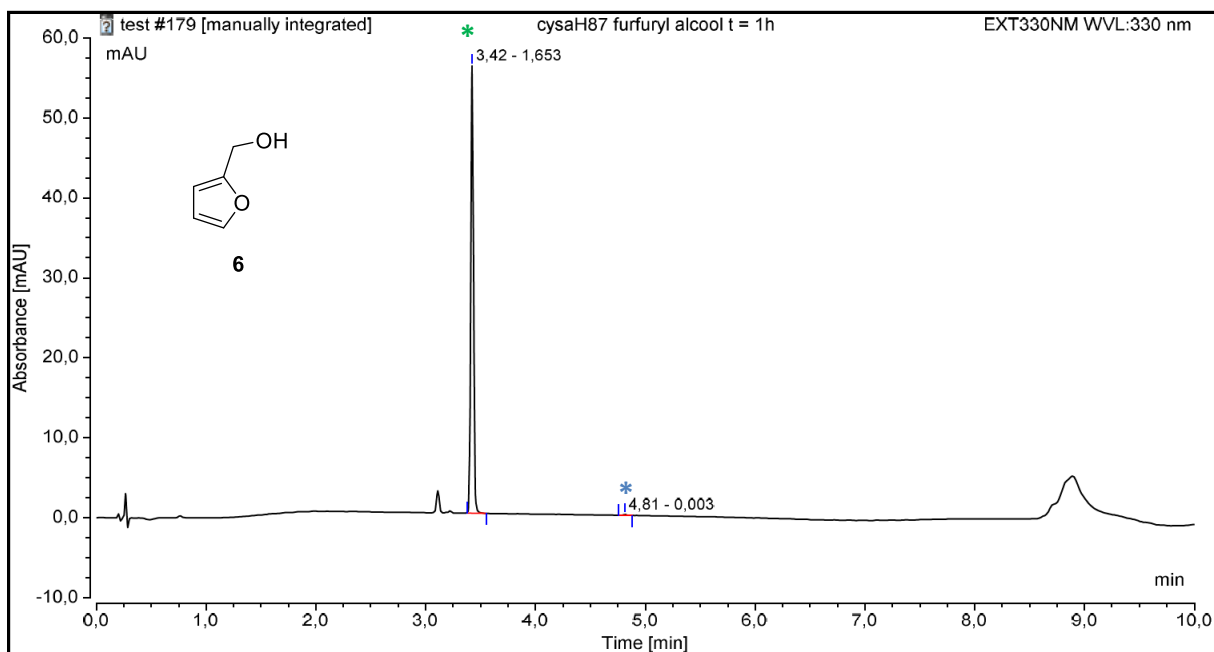


Integration Results

No.	Peak Name	Retention Time min	Area mAU*min	Height mAU	Relative Area %	Relative Height %	Amount n.a.
1		3,417	1,634	55,006	19,45	19,73	n.a.
2		4,060	6,519	215,430	77,58	77,28	n.a.
3		4,637	0,250	8,322	2,97	2,99	n.a.
Total:			8,404	278,758	100,00	100,00	

Conversion of 16 = 13.2%

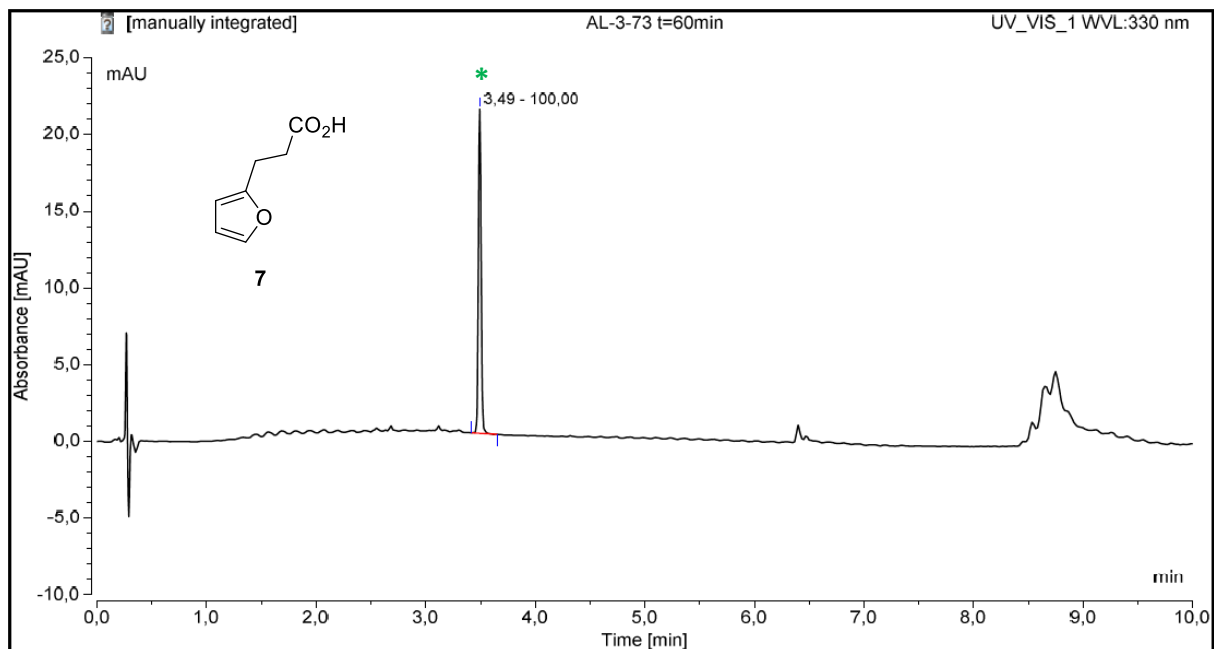
Figure S13. RP-HPLC of the Diels-Alder reaction of probe **16** with diene **5** ($\lambda = 330$ nm, sA)



Integration Results							
No.	Peak Name	Retention Time min	Area mAU*min	Height mAU	Relative Area %	Relative Height %	Amount n.a.
1		3,423	1,653	55,961	99,79	99,80	n.a.
2		4,813	0,003	0,110	0,21	0,20	n.a.
Total:			1,656	56,071	100,00	100,00	

Conversion of 16 = 0.2%

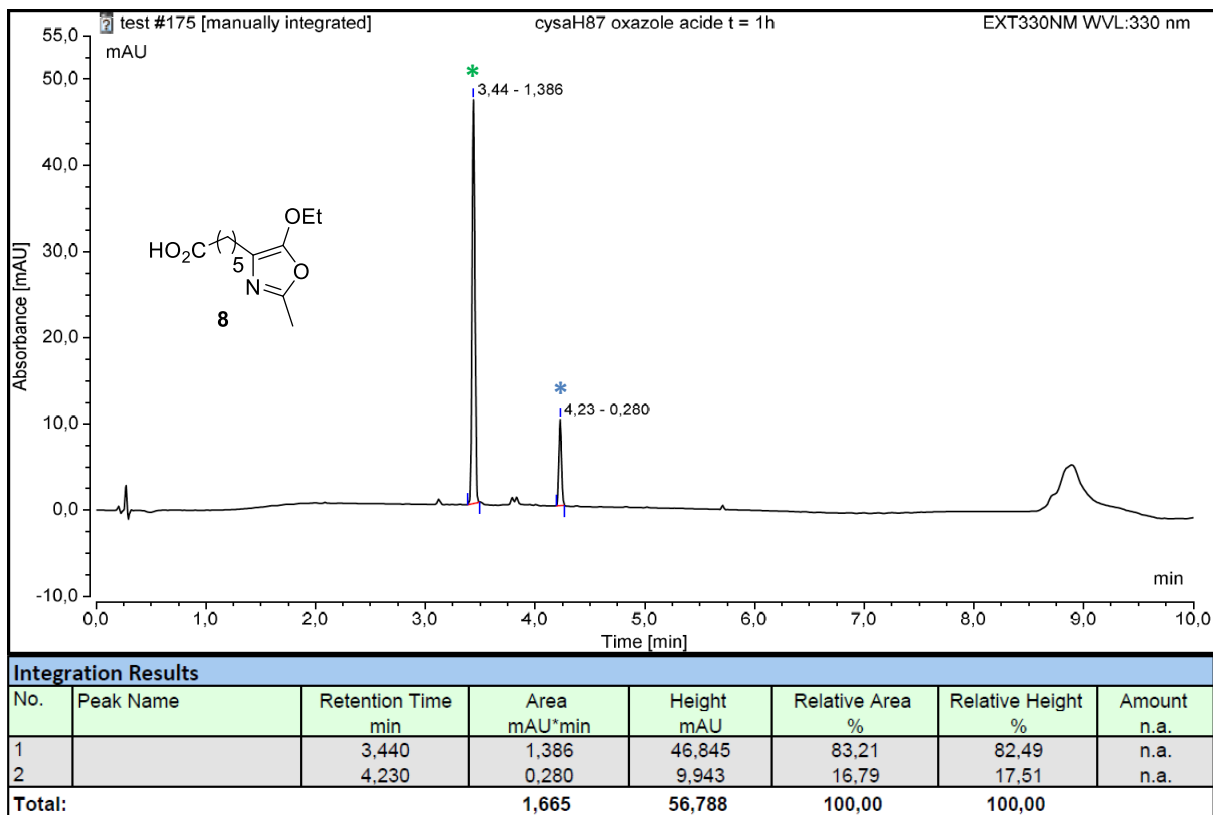
Figure S14. RP-HPLC of the Diels-Alder reaction of probe **16** with diene **6** ($\lambda = 330$ nm, sA)



Integration Results							
No.	Peak Name	Retention Time min	Area mAU*min	Height mAU	Relative Area %	Relative Height %	Amount n.a.
1		3,493	0,610	21,131	100,00	100,00	n.a.
Total:			0,610	21,131	100,00	100,00	

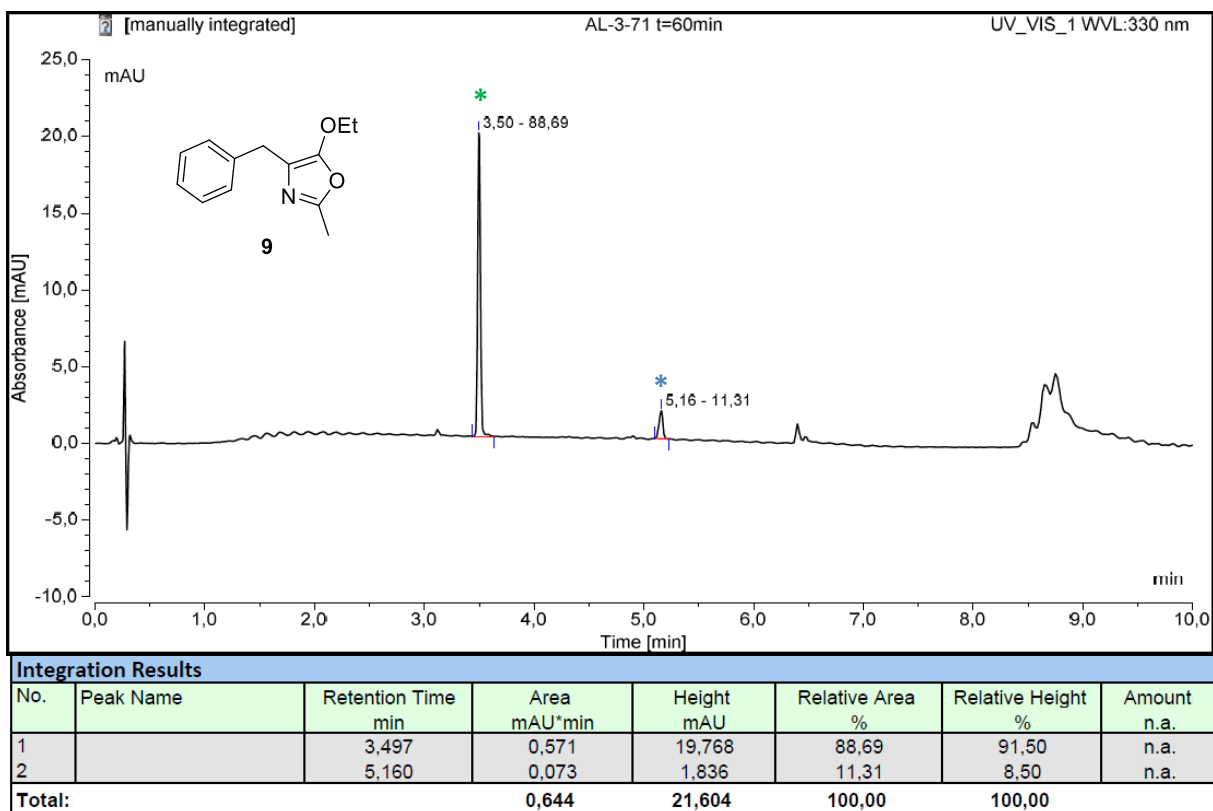
Conversion of 16 = not detectable

Figure S15. RP-HPLC of the Diels-Alder reaction of probe **16** with diene **7** ($\lambda = 330$ nm, sB)



Conversion of 16 = 16.8%

Figure S16. RP-HPLC of the Diels-Alder reaction of probe 16 with diene 8 ($\lambda = 330$ nm, sA)



Conversion of 16 = 11.3%

Figure S17. RP-HPLC of the Diels-Alder reaction of probe 16 with diene 9 ($\lambda = 330$ nm, sB)

II.3. Reaction rate determination of cycloaddition of probe **16** with dienes **1-3, 6, and 8-9**

*a) Reaction rate determination of cycloaddition of probe **16** with cyclopentadiene **2** in aqueous/organic medium*

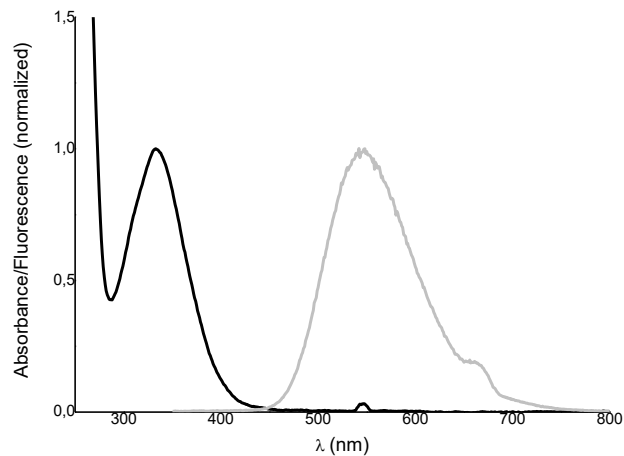
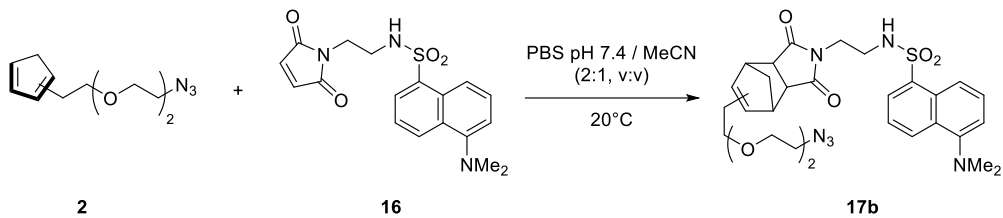


Figure S18. Normalized absorption (black line) and emission (grey line) spectra of **17b** in MeCN/PBS pH 7.4 (1:2, v:v) at T = 20 °C and at $\lambda_{\text{ex}} = 330$ nm

- Calibration curve between fluorescent intensity and concentration of cycloadduct **17**.

From a 1.4 mM stock solution of **17b** in MeCN were prepared five diluted solutions (from 10 to 50 μ M in PBS/MeCN, 2:1). A fluorescence emission spectrum was recorded for each diluted solution ($\lambda_{\text{ex}} = 330$ nm, T = 20 °C) in a 1.4 mL Hellma fluorescence cell. Then, the fluorescence intensity observed at $\lambda_{\text{em}} = 560$ nm for $\lambda_{\text{ex}} = 330$ nm was plotted against concentration to afford linear relation.

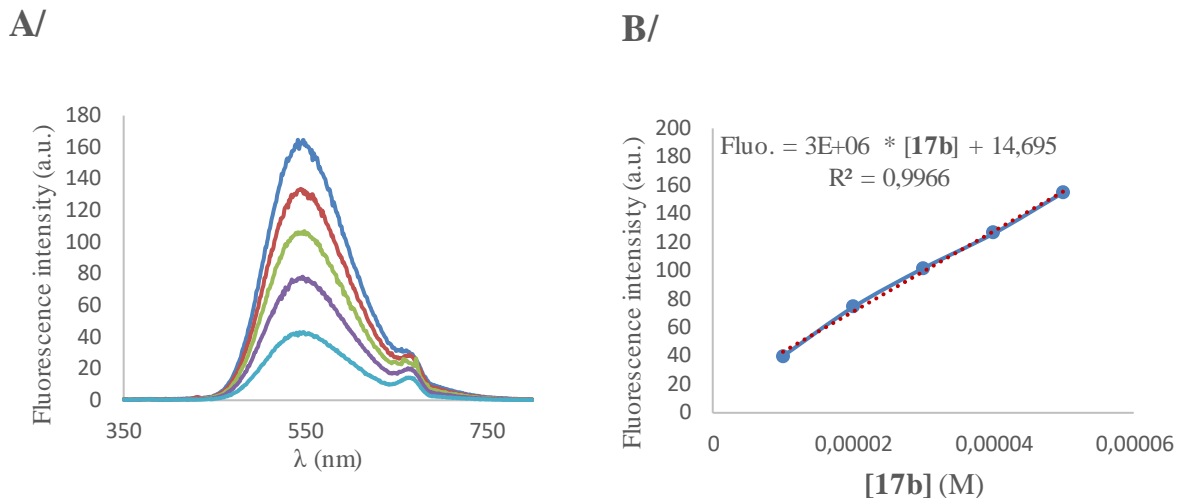


Figure S19. (A) Fluorescence intensity for **17b** at five concentrations (from 10 to 50 μM in PBS/MeCN, 2:1) for $\lambda_{\text{ex}} = 330$ nm. (B) Fluorescence intensity for **17b** plotted against concentration ($\lambda_{\text{ex}} = 330$, $\lambda_{\text{em}} = 560$ nm).

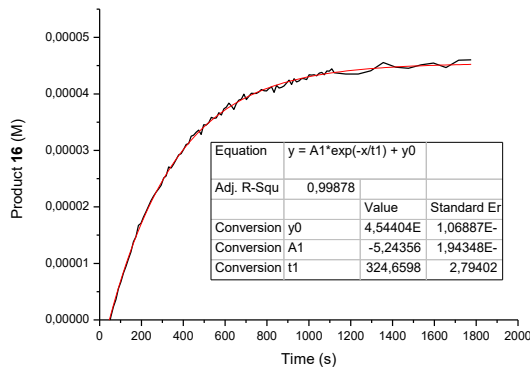
- Second order reaction rate k_2 determination via k_{obs}

To a 1.4 mM solution **16** in MeCN (50 μL) in a 1.4 mL fluorescence cell, were added MeCN (X μL , cf Table) and a solution of PBS pH 7.4 (933 μL). Then, a 14 mM solution of **2** in MeCN (Y μL , cf Table) was added and the reactional mixture was directly introduced into the spectrophotometer after homogenization. The resulting composition of the mixture at $t = 0$ min was as follows: MeCN/PBS pH 7.4 (1.4 mL, 1:2, v:v) ; $[\mathbf{16}] = 50 \mu\text{M}$; $[\mathbf{2}] = 500 \mu\text{M}, 750 \mu\text{M}, 875 \mu\text{M}$ or $1000 \mu\text{M}$. The Diels-Alder reaction was monitored by fluorescence spectroscopy ($\lambda_{\text{ex}} = 330$ nm ; $\lambda_{\text{em}} = 560$ nm) at $T = 20^\circ\text{C}$.

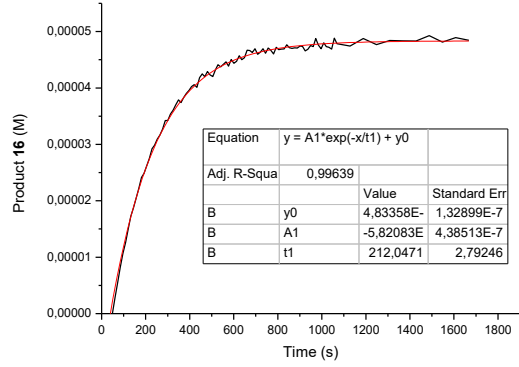
Final concentration of 2 (μM)	Volume X of MeCN (μL)	Volume Y of the 14 mM solution of 2 in MeCN (μL)
500	367	50
750	342	75
875	329.5	87.5
1000	317	100

Resulting fluorescence curves were converted to the conversion against time thanks to the calibration relation. Conversion curves were fitted with non-linear exponential correlation, which afforded t_1 values and then k_{obs} ($= 1 / t_1$). k_{obs} values were plotted against concentration of **2** and the line was fitted with linear regression, affording a slope $= k_2$ ($\text{M}^{-1} \cdot \text{s}^{-1}$).

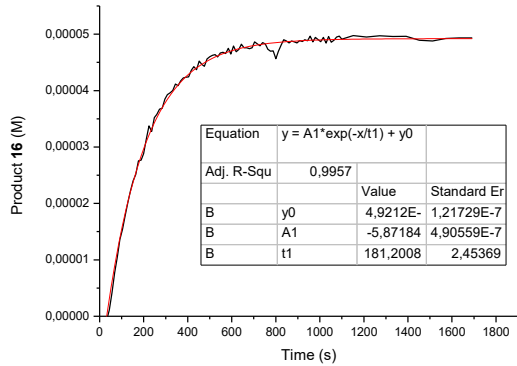
A/ [2] = 500 μM



B/ [2] = 750 μM



C/ [2] = 875 μM



D/ [2] = 1000 μM

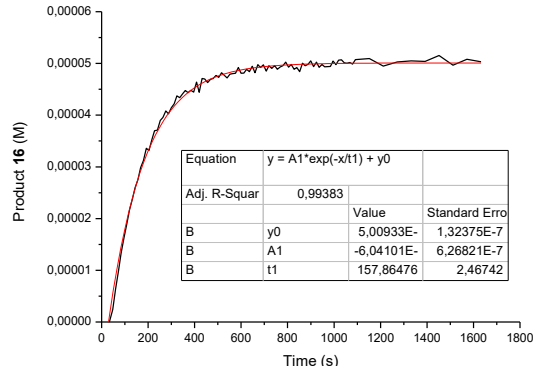


Figure S20. Time course formation of product **17b** at different concentrations of **2**: 500, 750, 875 and 1000 μM for (A), (B), (C), and (D), respectively.

[2] (μM)	t_1 (s)	k_{obs} (s^{-1})
500	324,6598	0,00308015
750	212,0471	0,00471593
875	181,20086	0,00551874
1000	157,86476	0,00633454

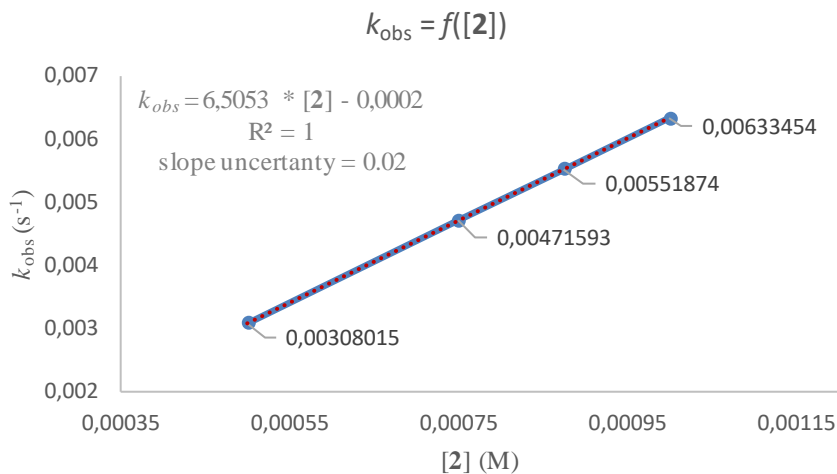


Figure S21. Plot of the k_{obs} values against the cyclopentadiene **2** concentration. The slope of the linear fit is the second-order rate constant.

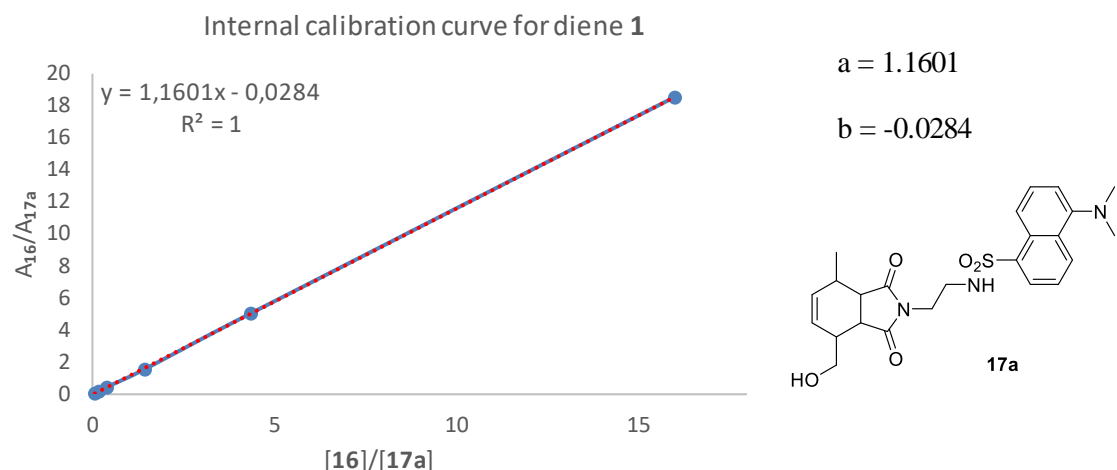
$$\text{Slope} = k_2 = \mathbf{6.50 \pm 0.02 \text{ M}^{-1} \text{s}^{-1}}$$

b) Reaction rate determination of cycloaddition of probe **16** with diene **1**, **3**, **6**, **8**, **9** in aqueous/organic medium

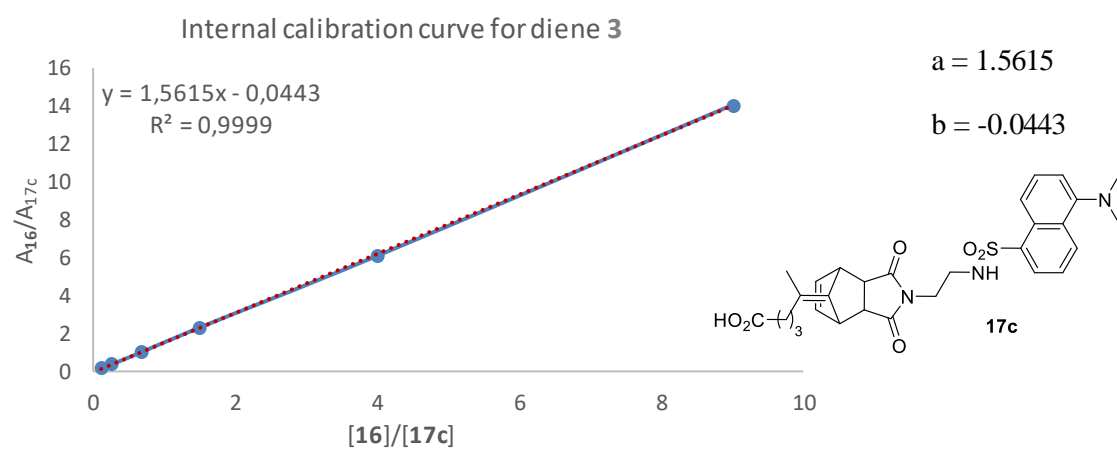
- Internal calibration procedure for kinetic HPLC monitoring

For each diene (**1**, **3** and **6**), a range of titrated solution containing the corresponding isolated dansyl-based cycloadduct (**17a**, **17c** and **17d**, respectively) and probe **16** was prepared in H₂O/MeCN (2:1, v:v). The range was established according to the solubility of diene and the kinetic experiment. Every titrated mixtures were analyzed by HPLC ($\lambda = 330$ nm, System B) and the ratios of HPLC areas ($A_{15}/A_{\text{cycloadduct}}$) were plotted against the corresponding concentration ratios ([**16**]/[cycloadduct]). Parameters a and b are employed for kinetic calculations.

A/



B/



C/

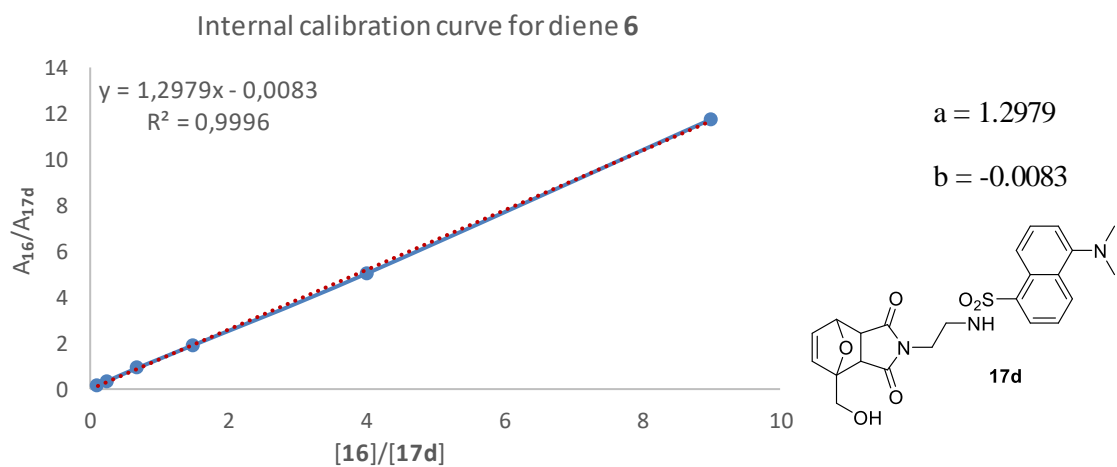


Figure S22. Internal calibration curves for (A) diene 1; (B) diene 3; and (C) diene 6.

- External calibration procedure for kinetic HPLC monitoring

Corresponding cycloadducts for dienes **8** and **9** could not be isolated. A range of titrated solution containing the probe **16** and commercial **coumarin** (external HPLC reference, CAS number: 91-64-5) was prepared in H₂O/MeCN (2:1, v:v). The range was established according to the solubility of diene and the kinetic experiment, with [coumarin] = constant = 5.0 mM. Every titrated mixtures were analyzed by HPLC (λ = 330 nm, System B) and the ratios of HPLC areas ($A_{16}/A_{\text{coumarin}}$) were plotted against the corresponding concentration ratios ([**16**]/[coumarin]). Parameters a and b are employed for kinetic calculations.

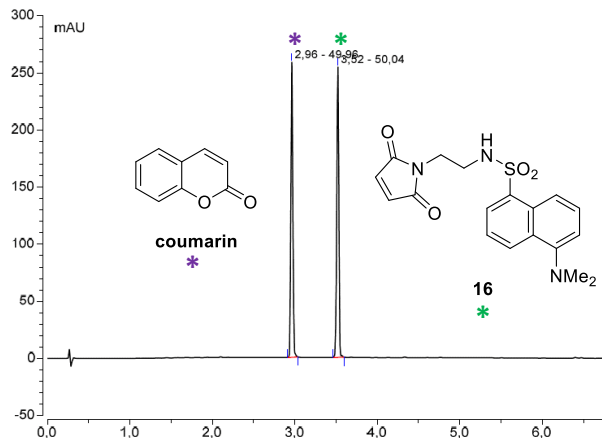


Figure S23. Chromatogram (λ = 330 nm, System B) of equimolar mixture of **coumarin** + probe **16**.

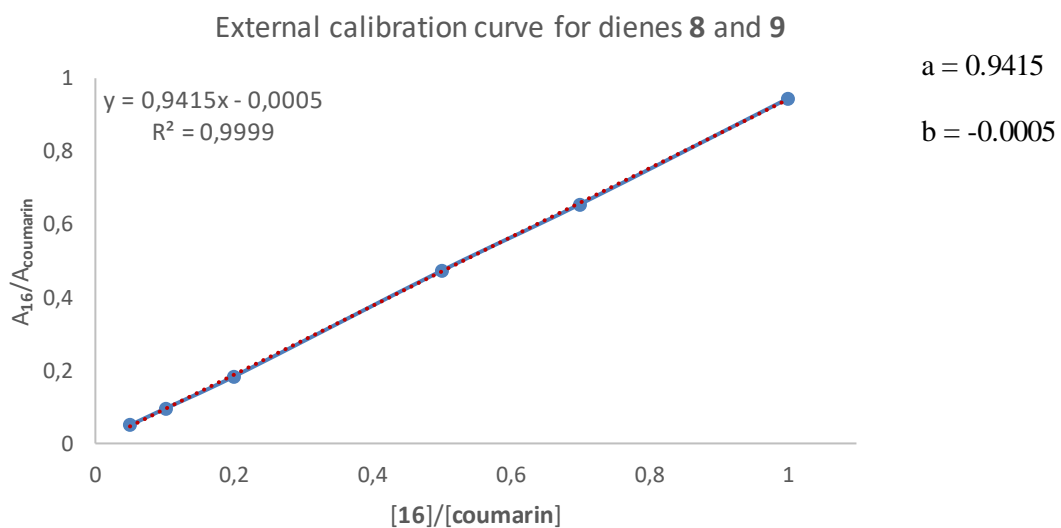
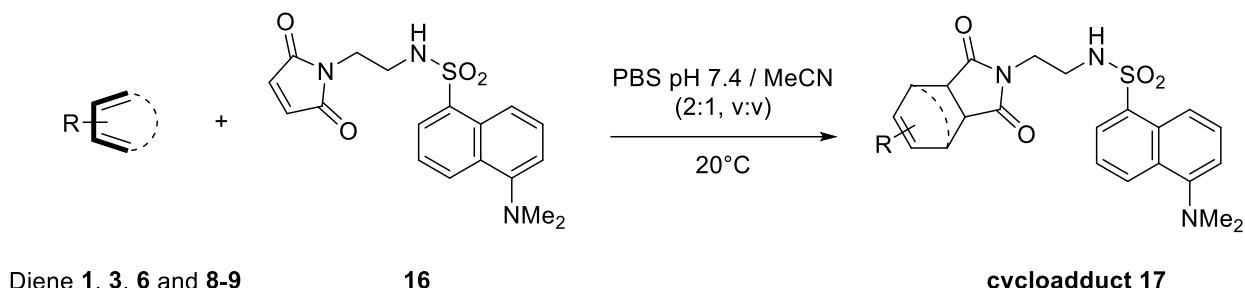


Figure S24. External calibration curve with **coumarin** for dienes **8** and **9**.

- Direct second order reaction rate k_2 determination.



In a flask containing a stirring bar were added PBS pH 7.4 (666 µL) and MeCN (volume calculation: $V_{\text{MeCN}} = 333 - V_{\text{16}} - V_{\text{diene}}$ µL so as to reach a final ratio PBS/MeCN, 2:1). For every experiments, titrated stock solutions of dienes and probe **16** were prepared in MeCN. Titrated stock solutions of diene (volume V_{diene}) and probe **16** (volume V_{16}) were sequentially added (final volume = 999 µL, PBS/MeCN, 2:1). Reaction time was immediately measured with a chronometer. Starting concentrations for T = 0 are specified for each experiments ($[\text{16}]_0 = [\text{diene}]_0$). The Diels-Alder reactions were monitored by HPLC ($\lambda = 330$ nm, System B) at T = 20 °C.

HPLC aliquots were prepared as follows:

- Internal calibration: 30 µL reactional mixture + 120 µL H₂O + 50 µL MeCN
- External calibration: 30 µL reactional mixture + 120 µL H₂O + 20 µL MeCN + 30 µL coumarin solution (5 mM in H₂O/MeCN, 2:1)

Equations for internal calibrations:

- Concentration of dansyl dye at any time:

$$[\text{16}]_0 = [\text{16}] + [\text{cycloadduct}]$$
- Linear relation from internal calibration (with a and b the parameters from calibration curves):

$$A_{16}/A_{\text{cycloadduct}} = a * ([\text{16}]/[\text{cycloadduct}]) + b$$
- [cycloadduct] at any time with the previous relations:

$$[\text{cycloadduct}] = [\text{16}]_0 / (((A_{16}/A_{\text{cycloadduct}}) - b) / a) + 1$$
- [16] at any time with the previous relations:

$$[\text{16}] = [\text{16}]_0 - [\text{cycloadduct}]$$

Equations for external calibration:

- Linear relation from external calibration (with a and b the parameters from calibration curves and [coumarin] = constant):

$$A_{16}/A_{\text{coumarin}} = a * ([\text{16}]/[\text{coumarin}]) + b$$
- Concentration of probe **16** at any time with the previous relation:

$$[\text{16}] = [\text{coumarin}] * (((A_{16}/A_{\text{coumarin}}) - b) / a)$$

[16] in each kinetic experiments were calculated thanks to these correlations (internal and external calibrations) and plotted against time (s).

Typical kinetic equation for a second order reaction is:

- $d[C]/dt = k_2 \cdot [16] \cdot [\text{diene}]$

With $[16] = [\text{diene}]$ (for $[16]_0 = [\text{diene}]_0$), the previous equation becomes:

- $d[C]/dt = k_2 \cdot [16]^2$

The following relation is found after integration:

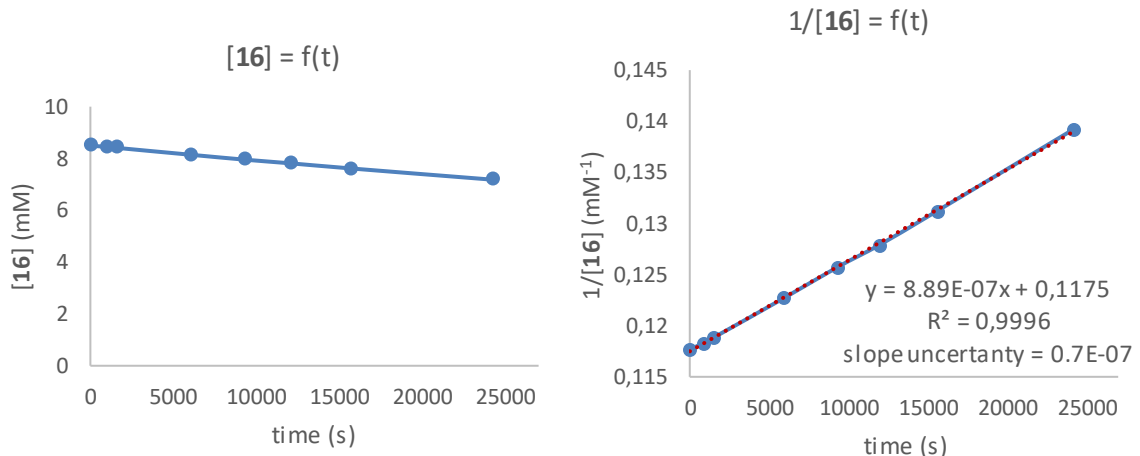
- $1/[16] = k_2 \cdot t + 1/[16]_0$

with:

- k_2 in $M^{-1} \cdot s^{-1}$
- t in s
- $[16]$, $[\text{diene}]$ and $[\text{coumarin}]$ in mM

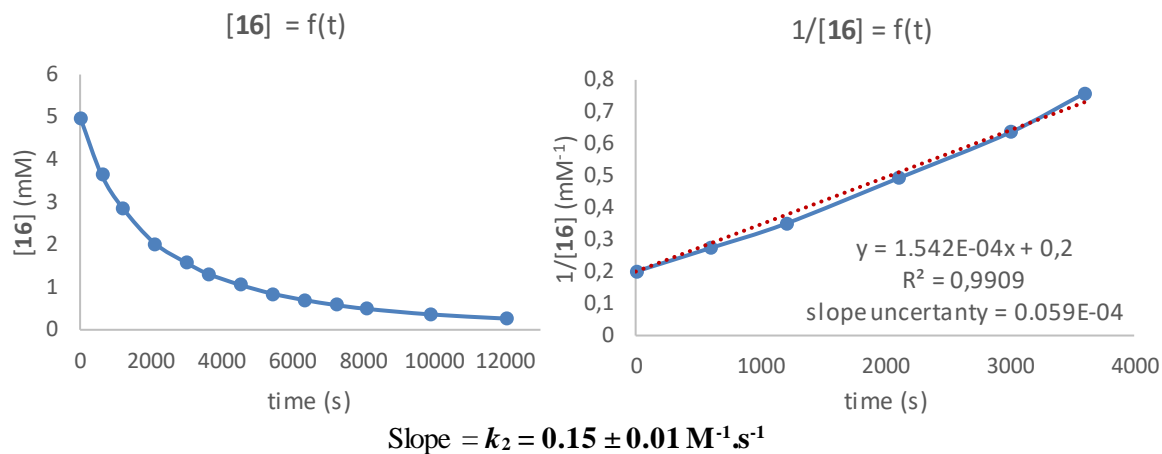
$1/[16]$ were plotted against time for each kinetic experiments. The slope of the resulting right affords the k_2 value.

A/ Diene 1 ($[16]_0 = [1]_0 = 8.5 \text{ mM}$)

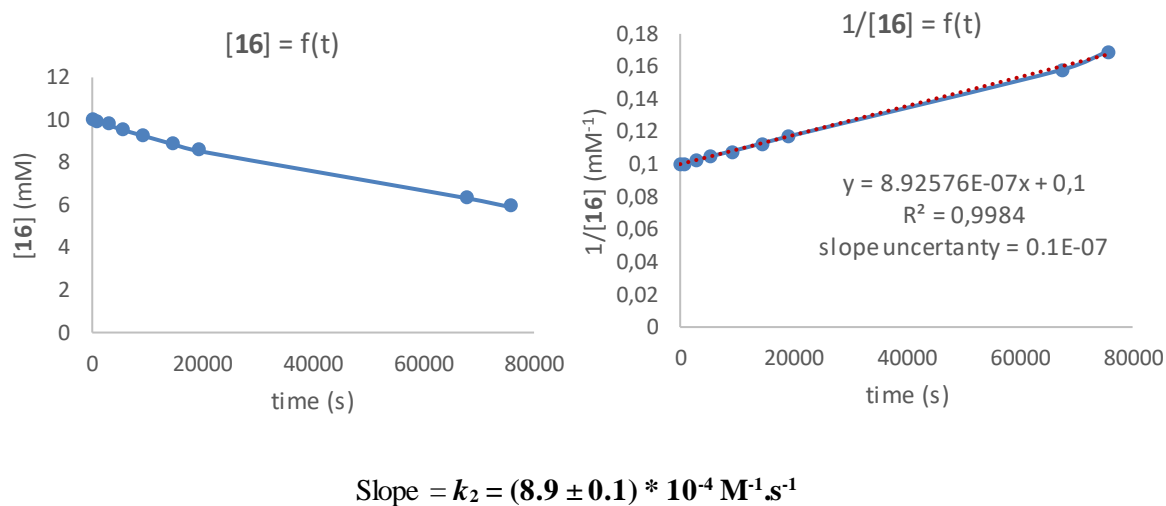


$$\text{Slope} = k_2 = (8.9 \pm 0.7) * 10^{-3} \text{ M}^{-1} \cdot \text{s}^{-1}$$

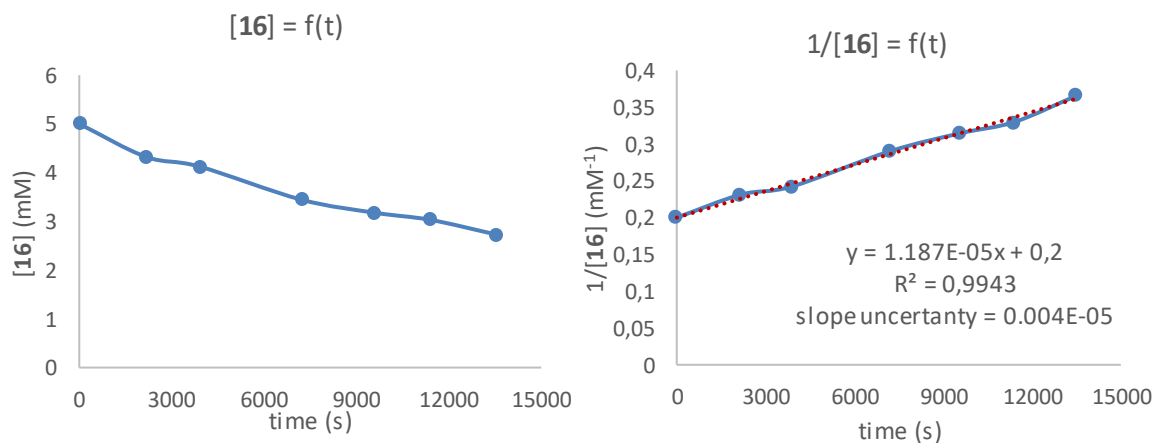
B/ Diene **3** ($[16]_0 = [3]_0 = 5 \text{ mM}$)



C/ Diene **6** ($[16]_0 = [6]_0 = 10 \text{ mM}$)

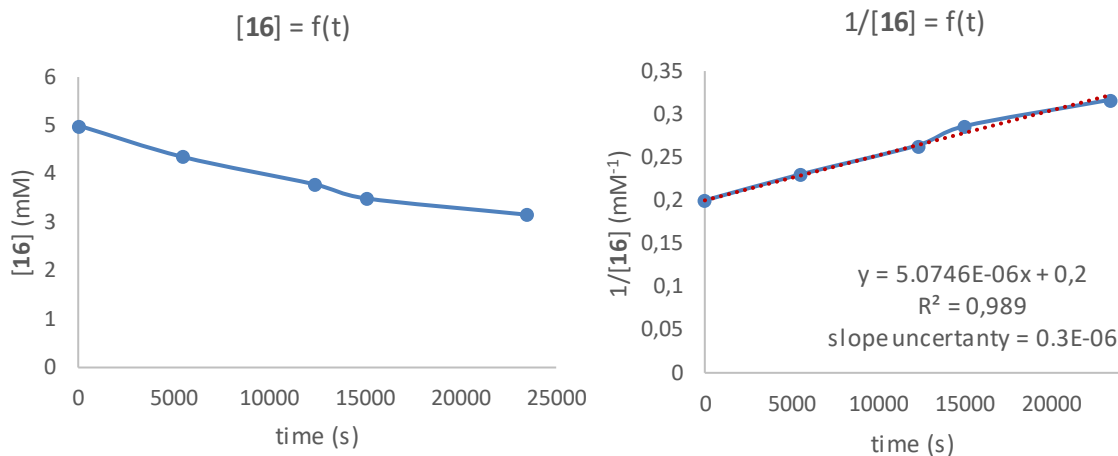


D/ Diene **8** ($[16]_0 = [8]_0 = 5 \text{ mM}$)



$$\text{Slope} = k_2 = (1.2 \pm 0.4) * 10^{-2} \text{ M}^{-1}\text{s}^{-1}$$

E/ Diene **9** ($[16]_0 = [9]_0 = 5 \text{ mM}$)



$$\text{Slope} = k_2 = (5.1 \pm 0.3) * 10^{-3} \text{ M}^{-1}\text{s}^{-1}$$

Figure S25. Second order kinetic rate constant calculations for (A) diene **1**, (B) diene **3**, (C) diene **6**, (D) diene **8** and (E) diene **9**.

II.4. One-pot double labeling strategy with dienes **2** and **8**

a) Full experiment

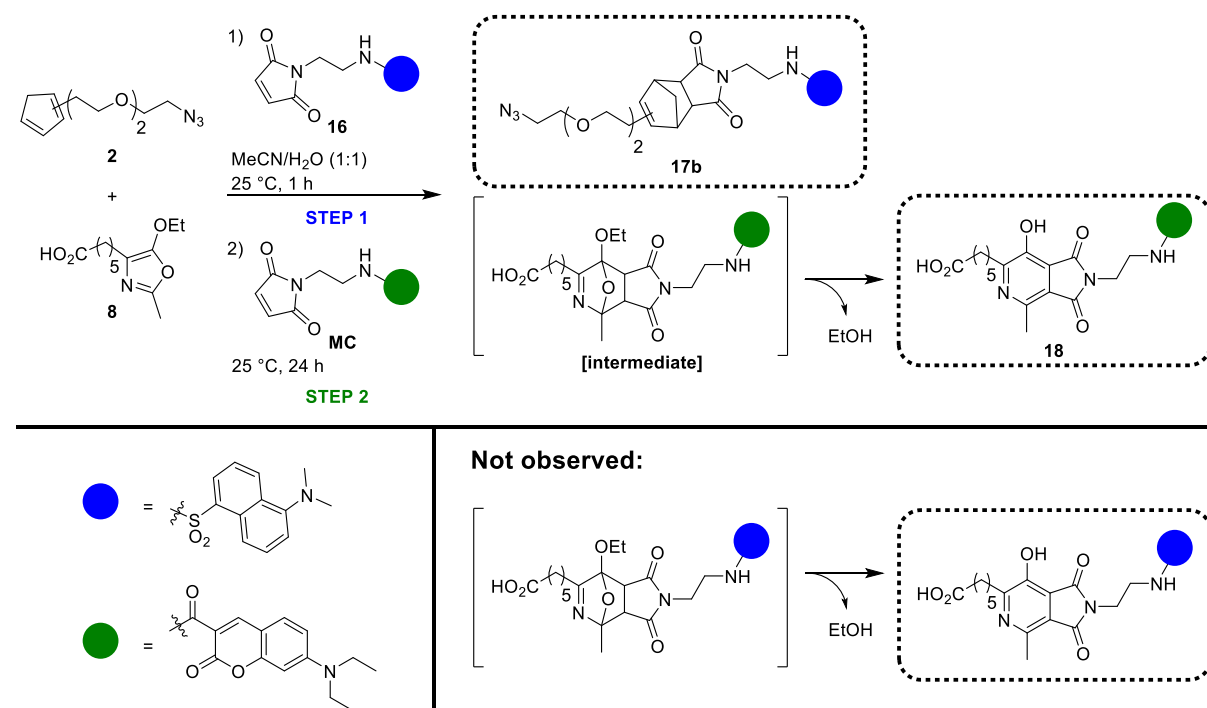


Figure S26. Sequential labeling experiment from dienes **2** and **8** and maleimides **16** and **MC**.

To a mixture of H₂O (250 µL) and MeCN (190 µL) were added a 25 mM solution of **2** (20 µL) and a 25 mM solution of **8** (20 µL). After 1 min of stirring, a 20 mM solution of **16** (25 µL, 1 equiv.) was added and the mixture was stirred at room temperature (T ≈ 25 °C). After completion of **STEP 1** (1 h), maleimide-based coumarine **MC** (1 mg, 2.6 µmol, 5 equiv.) was added to the mixture for the **STEP 2** and the reaction further stirred for 24 h at 25 °C. Diels-Alder reactions were monitored by RP-HPLC (system A).

Final concentration for time = 0:

- [2] = 1 mM (STEP 1)
- [8] = 1 mM (STEP 1 and 2)
- [16] = 1 mM (STEP 1)
- [MC] = 5 mM (STEP 2)
- 500 µL H₂O/MeCN (1:1, v:v)

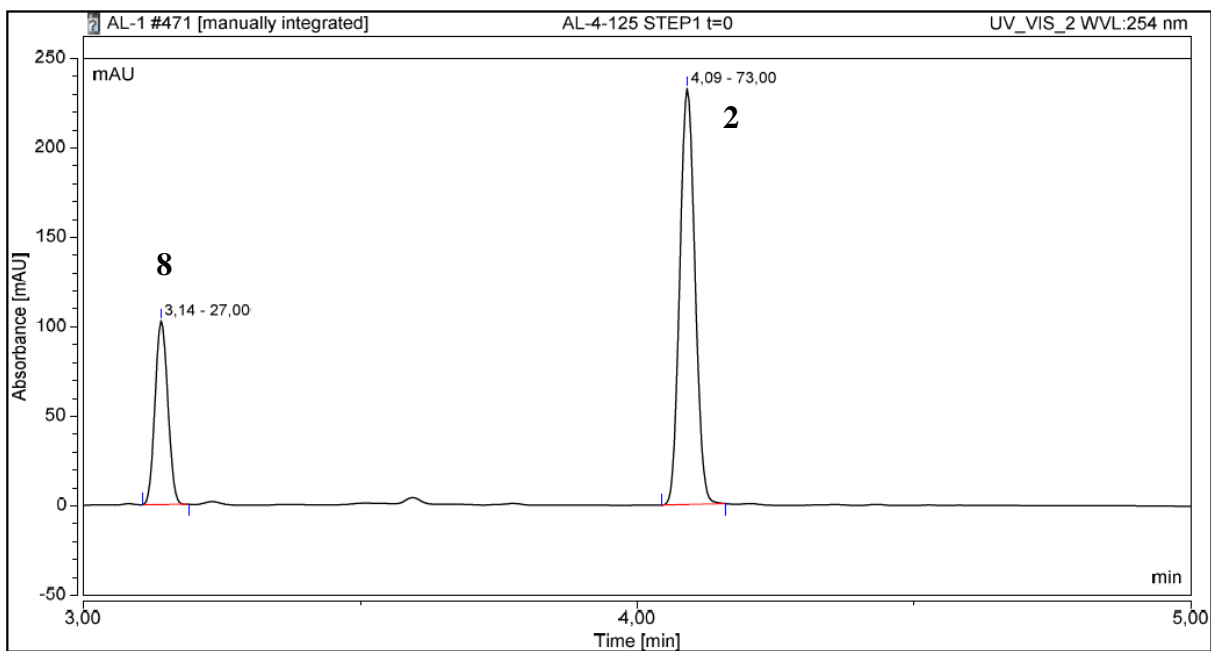


Figure S27. RP-HPLC chromatogram of a mixture of **2** and **8** ($\lambda = 254$ nm, sA) at $T = 0$.

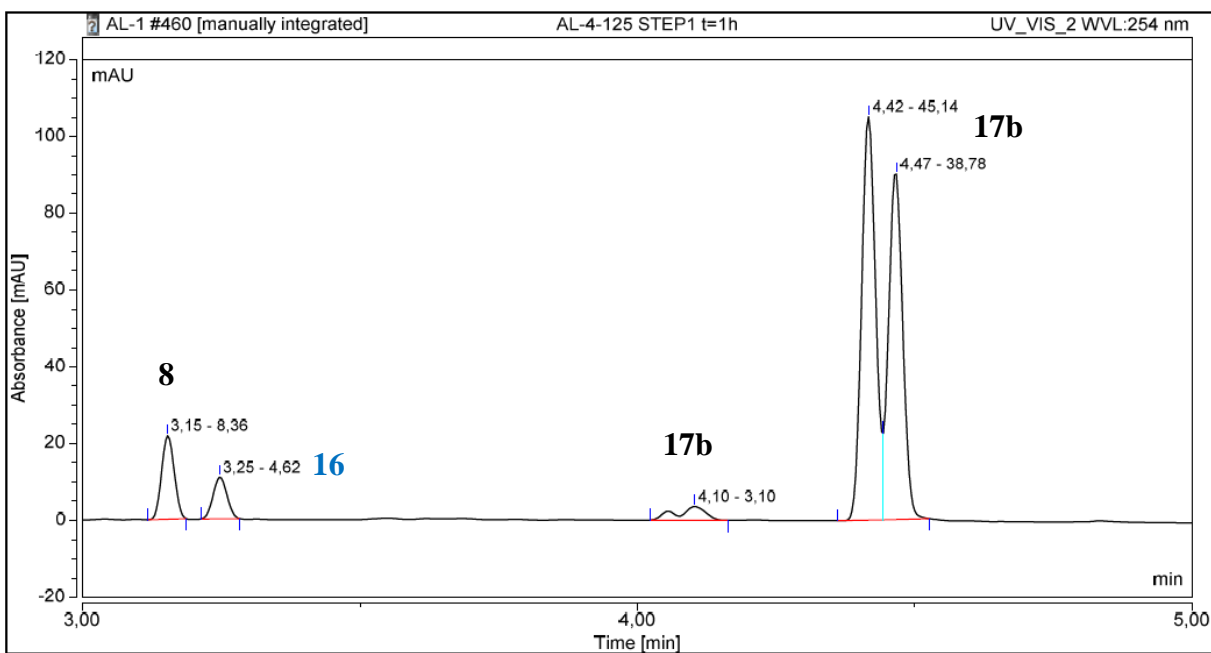


Figure S28. RP-HPLC chromatogram of a mixture of **2**, **8**, and **16** ($\lambda = 254$ nm, sA) at $T = 1$ h (STEP 1).

STEP 2, T = 8 h

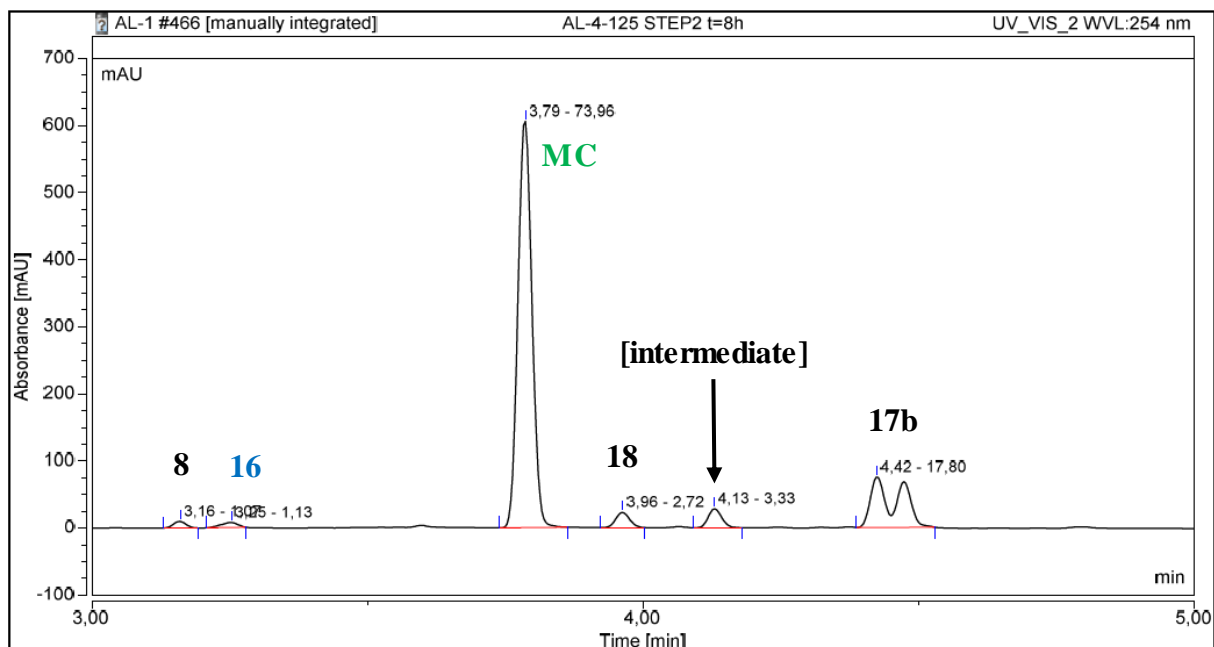


Figure S29. RP-HPLC chromatogram of a mixture of **2**, **8**, **16**, and **MC** ($\lambda = 254$ nm, sA) at $T = 8$ h (STEP 2).

STEP 2, T = 24 h

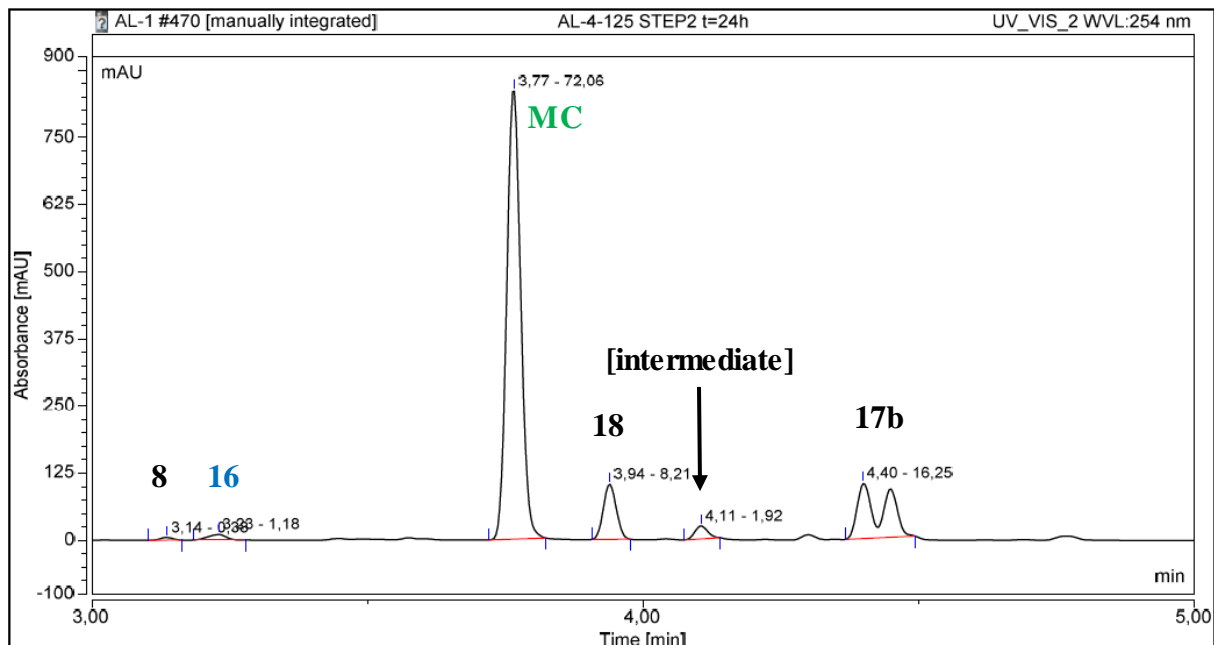


Figure S30. RP-HPLC chromatogram of a mixture of **2**, **8**, **16**, and **MC** ($\lambda = 254$ nm, sA) at $T = 24$ h (STEP 2).

b) Control experiment

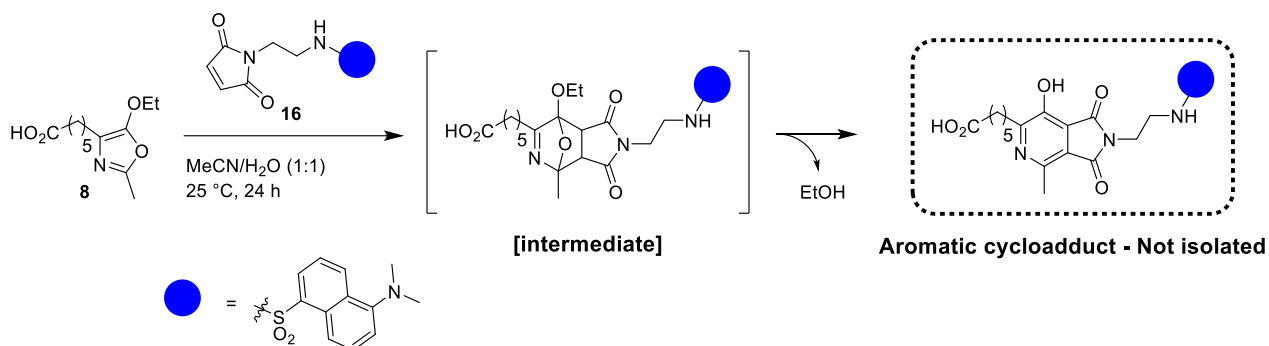


Figure S31. Control experiment regarding the plausible formation the azaphthalimide generated from the Diels-Alder reaction of **8** and **16**.

To a 25 mM solution of **8** (20 µL) in a solution of H₂O/MeCN (250:105 µL) was added a 20 mM solution of **16** (125 µL, 5 equiv.) and the mixture was stirred at room temperature (≈ 25 °C). Diels-Alder reactions were monitored by RP-HPLC after 5 and 24 h.

Final concentration for time = 0:

- [8] = 1 mM
- [16] = 5 mM
- 500 µL H₂O/MeCN (1:1, v:v)

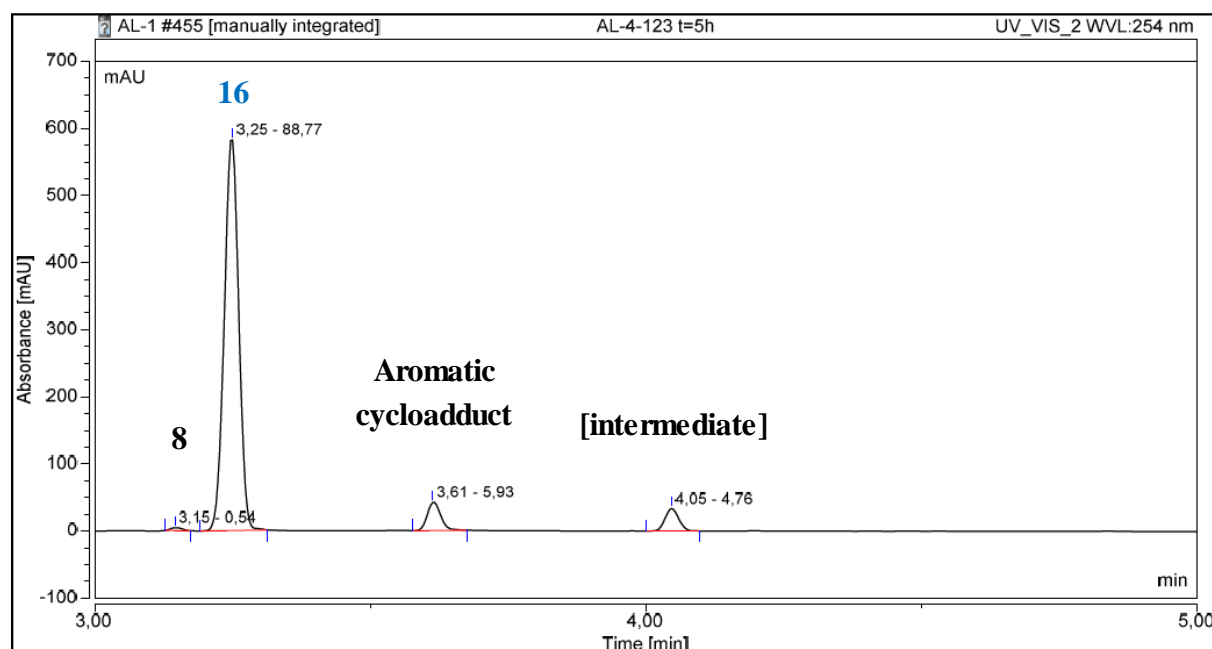


Figure S32. RP-HPLC chromatogram of a mixture of **8** and **16** ($\lambda = 254$ nm, sA) after T = 5 h.

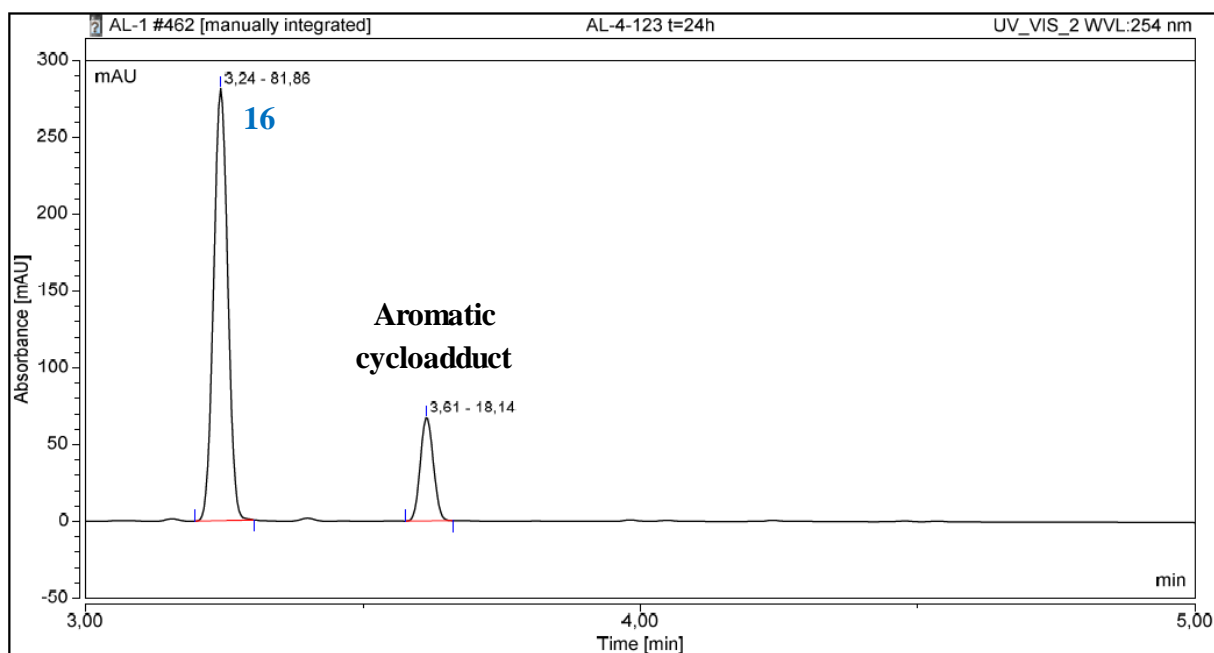


Figure S33. RP-HPLC chromatogram of a mixture of **8** and **16** ($\lambda = 254$ nm, sA) after $T = 24$ h.

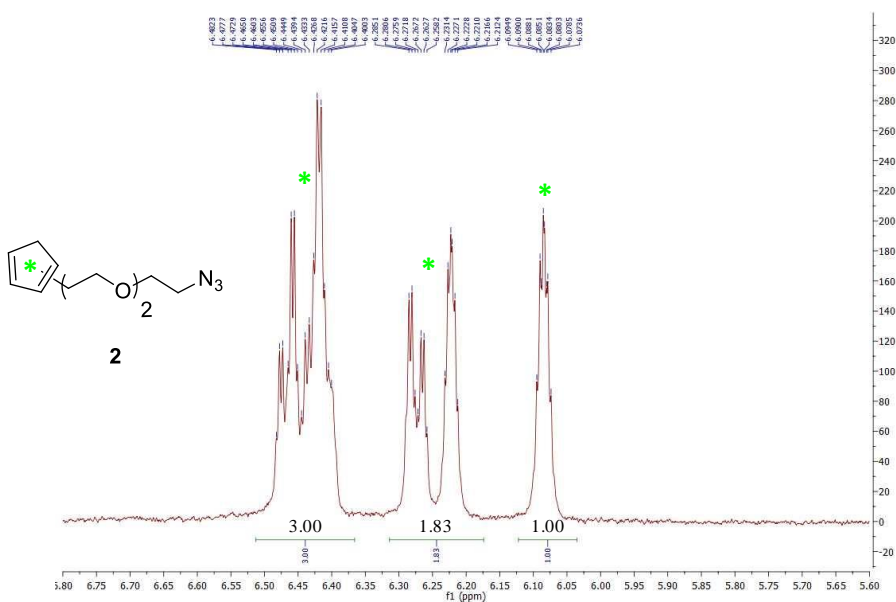
III. Study of stability of dienes **2**, **3**, **8**, **9** and conjugates **19-24**

III.1 Study of stability of dienes **2**, **3**, **8**, and **9**

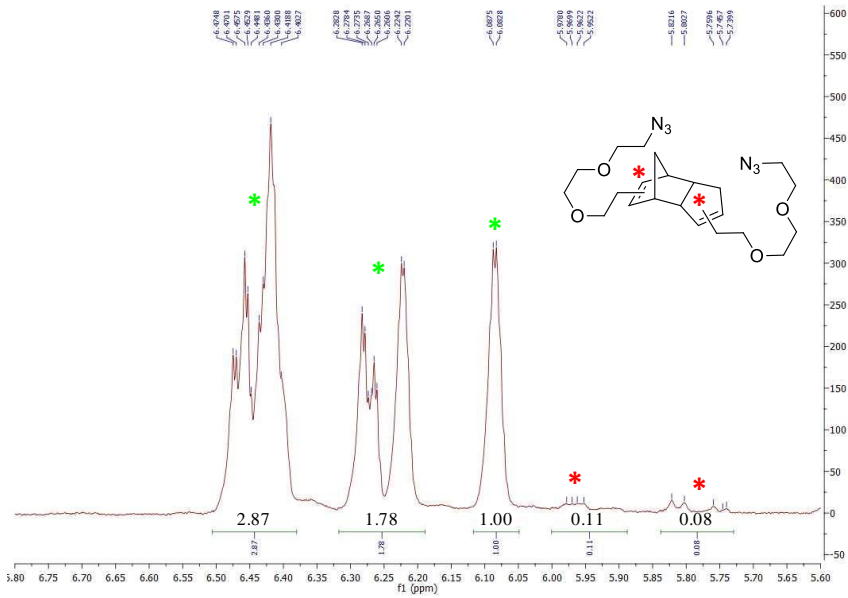
All non-commercial dienes were conserved at -25 °C after their synthesis.

a) Cyclopentadiene **2**

A/



B/



C/

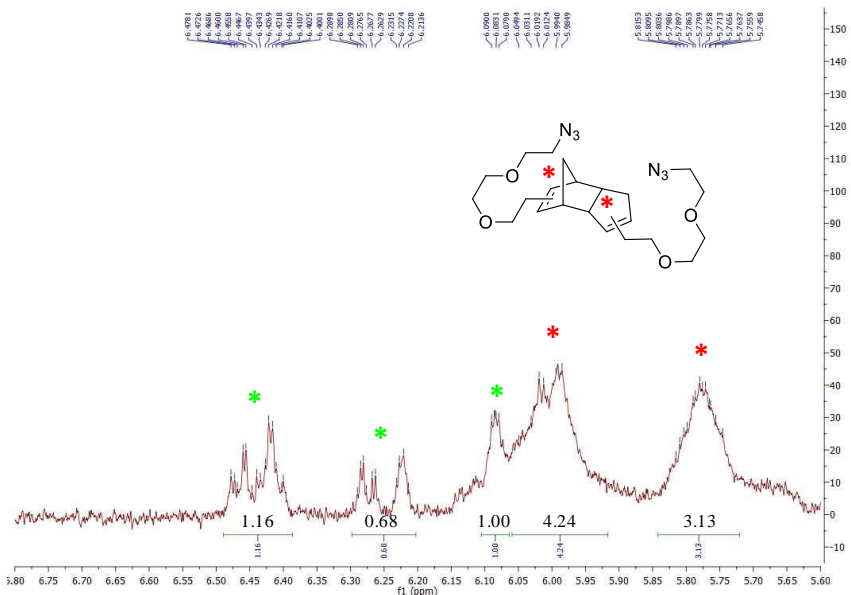


Figure S34. ^1H NMR analysis in CDCl_3 (300 MHz) of (A) isolated cyclopentadiene **2**; (B) cyclopentadiene **2** stored for 9 months at -25°C ; (C) cyclopentadiene **2** stored for 36 h at room temperature.

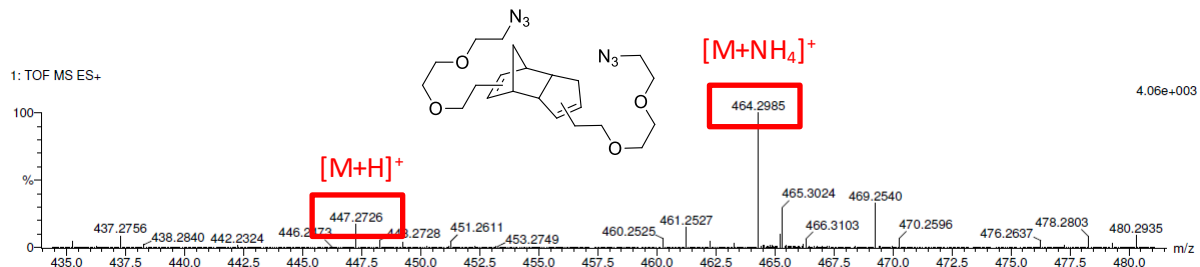
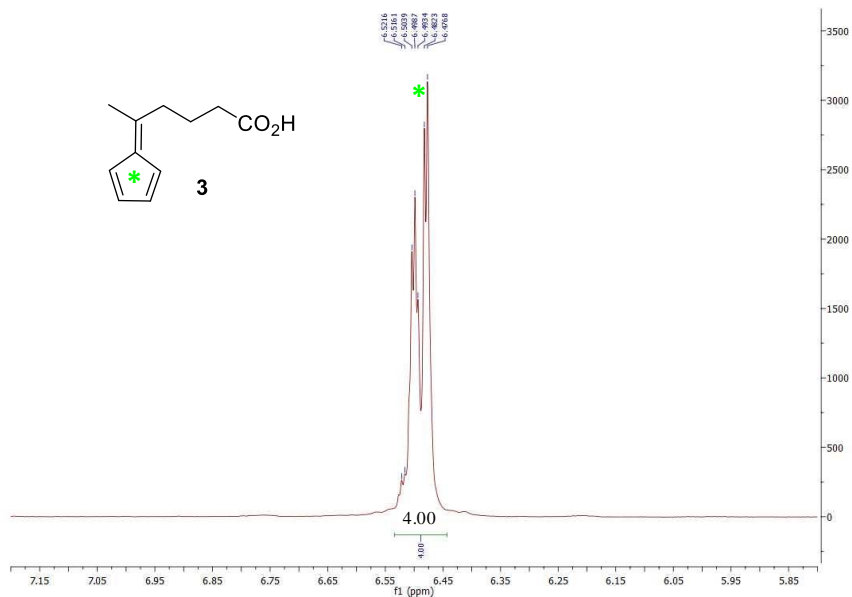


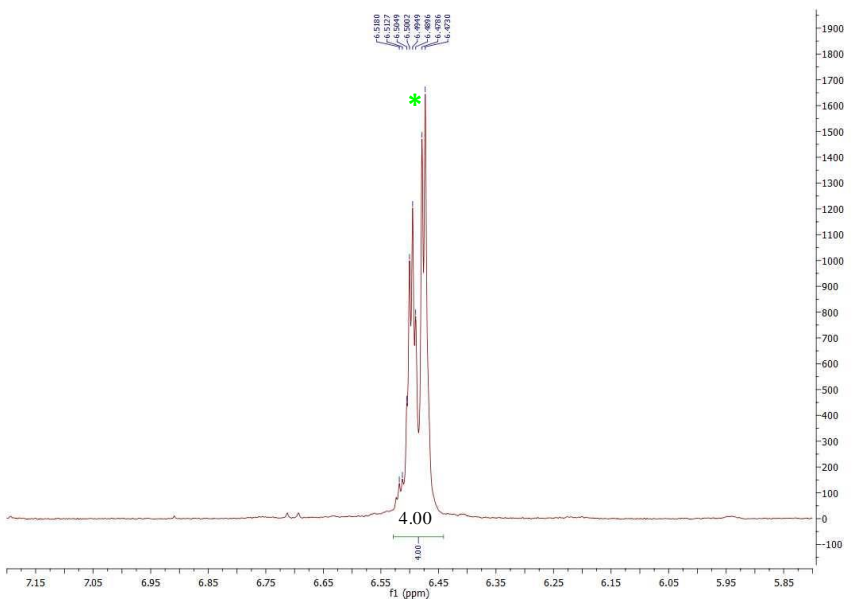
Figure S35. HRMS (ESI⁺) mass spectrum of compound **2** after 36 h at room temperature.

b) Fulvene 3

A/



B/



C/

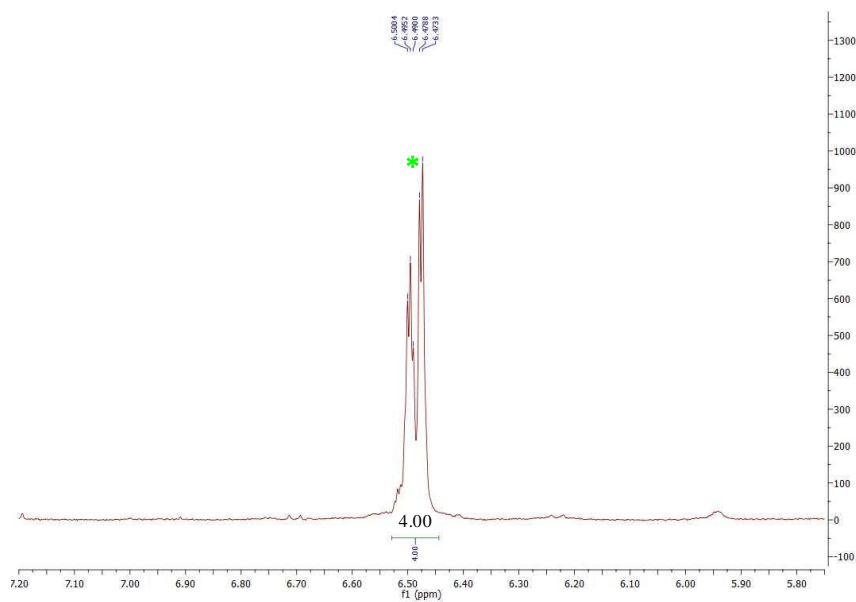
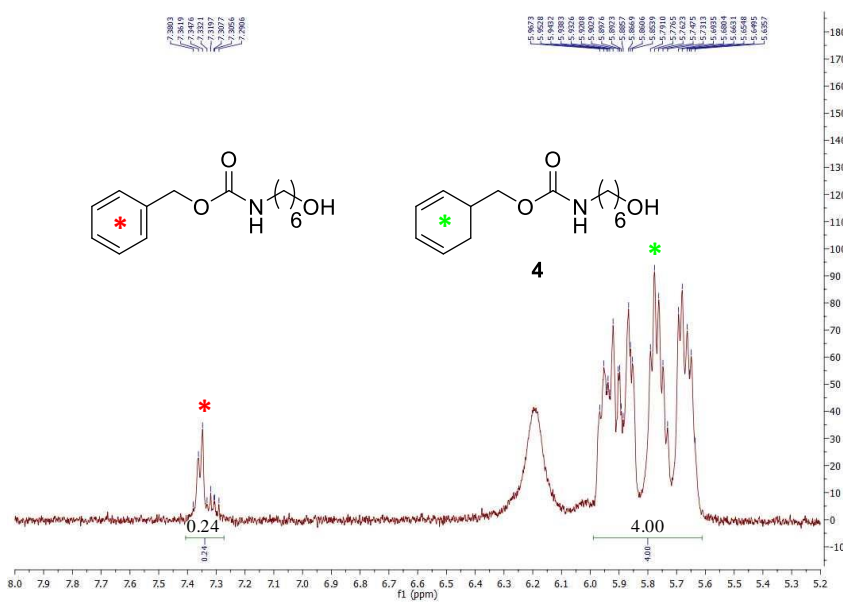


Figure S36. ¹H NMR analysis in CDCl₃ (300 MHz) of (A) isolated fulvene **3**; (B) fulvene **3** stored for 36 h at room temperature; (C) fulvene **3** stored for 16 days at room temperature.

c) Cyclohexadiene **4**

A/



B/

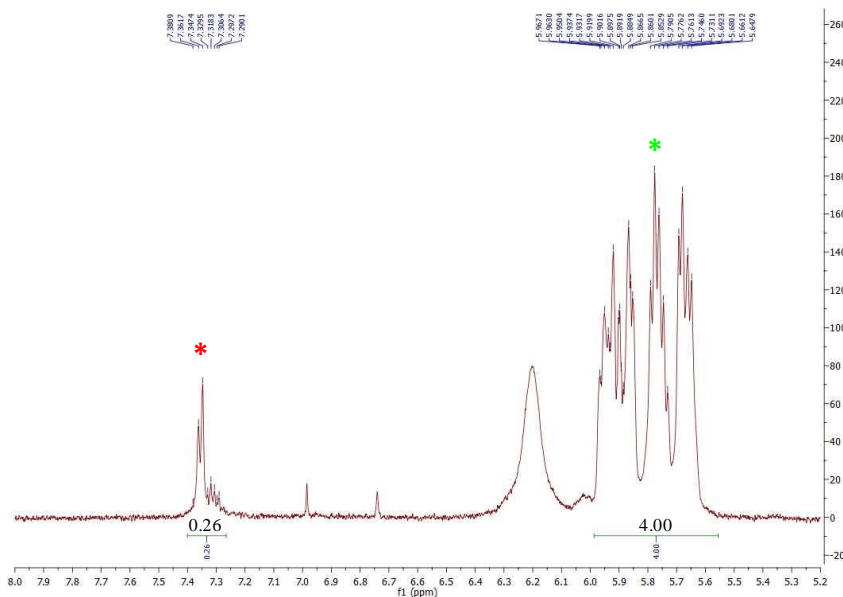
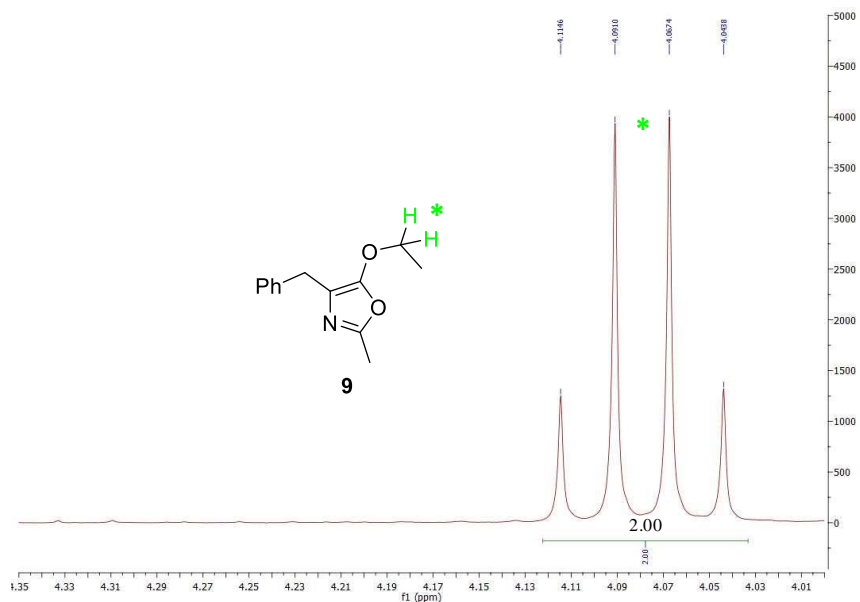


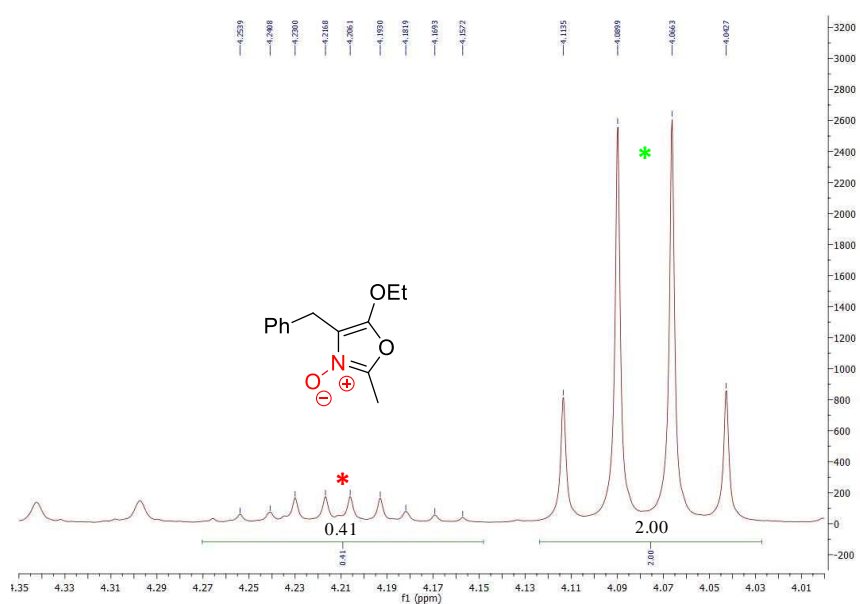
Figure S37. ^1H NMR analysis in CDCl_3 (300 MHz) of (A) isolated cyclohexadiene **4**; (B) cyclohexadiene **4** stored for 3 months at -25°C .

d) Oxazole 9

A/



B/



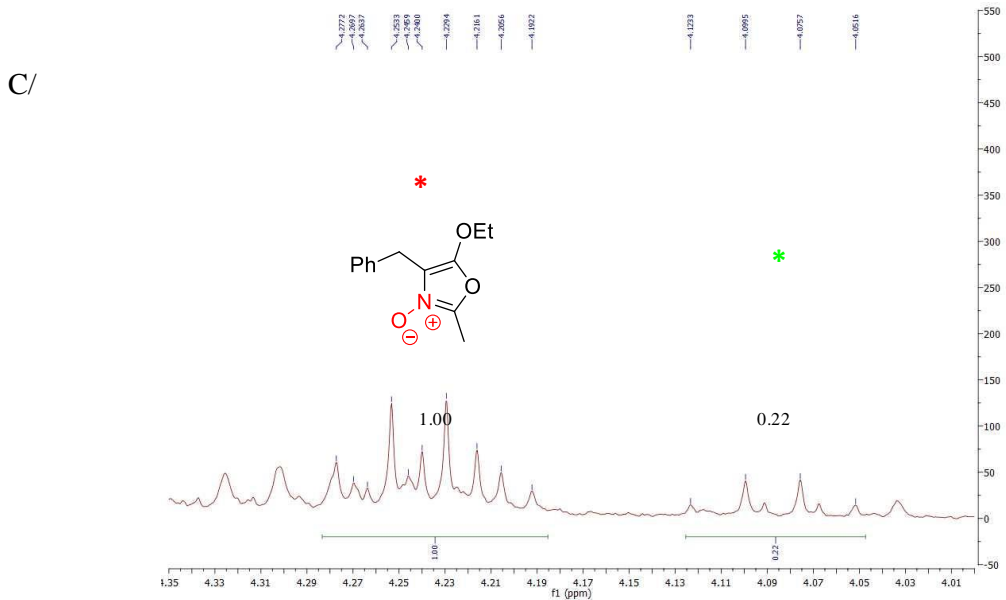
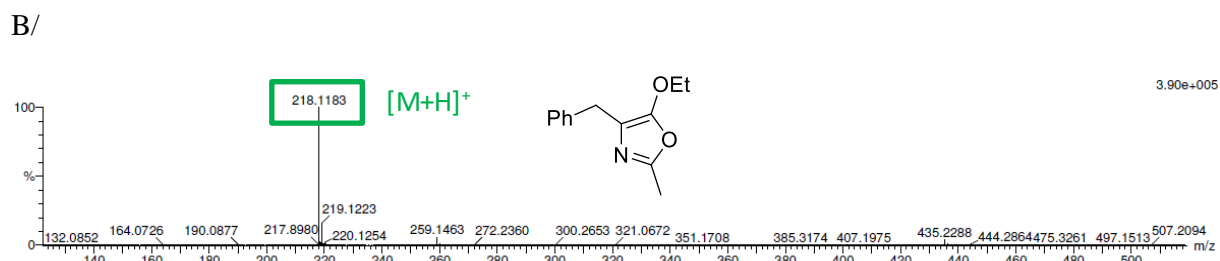
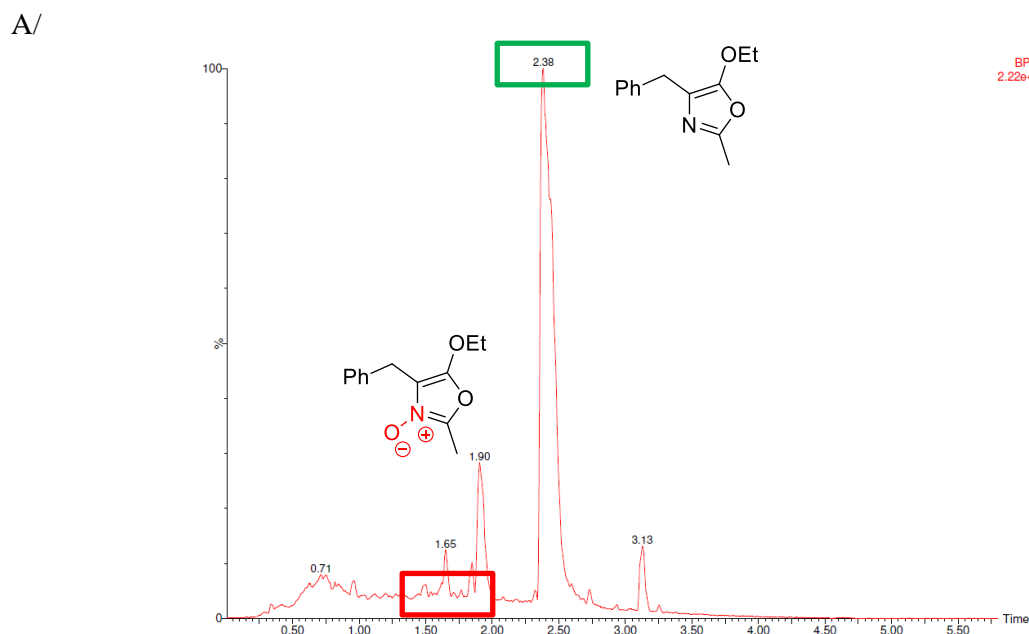


Figure S38. ^1H NMR analysis in CDCl_3 (300 MHz) of (A) isolated oxazole **9**; (B) oxazole **9** with AcOH (1 equiv.) stored for 9 months at -25°C ; (C) oxazole **9** stored for 9 months at -25°C .



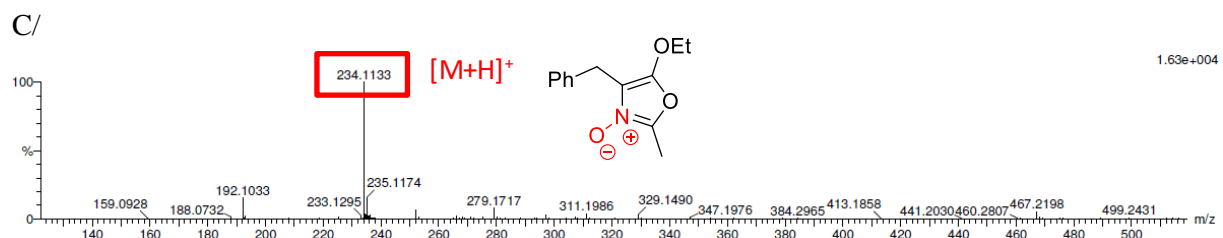


Figure S39. (A) TIC chromatogram of compound **9**, (B) HRMS (ESI+) mass spectrum of compound **9** at $t = 2.38$ min, (C) HRMS (ESI+) mass spectrum of compound **9** at $t = 1.65$ min, after 36 h at room temperature.

e) Oxazole **10**

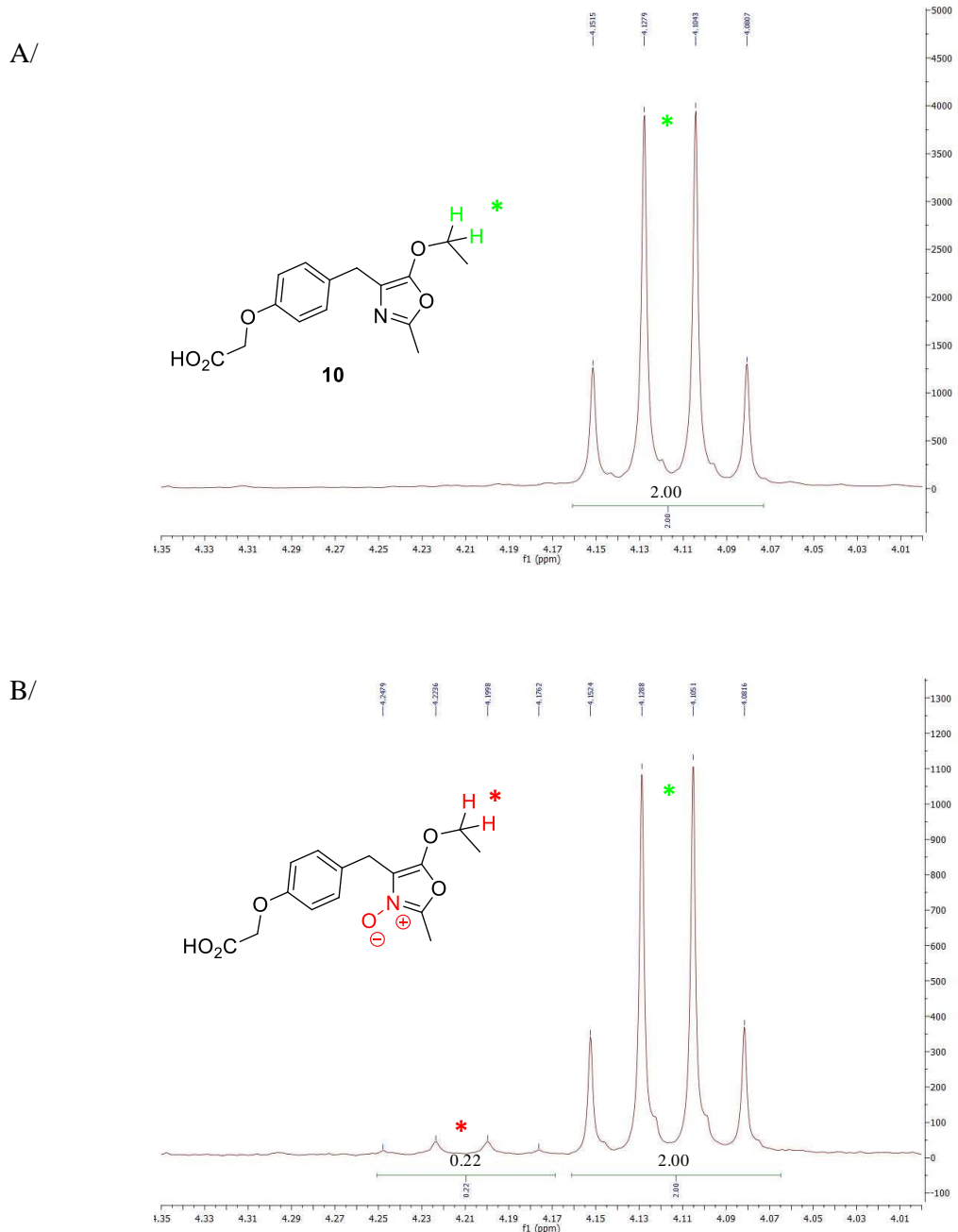


Figure S40. ^1H NMR analysis in CDCl_3 (300 MHz) of (A) isolated oxazole **10**; (B) oxazole **10** stored for 9 months at -25°C .

III.2. Study of stability of conjugates **20-26**

a) LC-MS (System C) of starting conjugates **20-26**

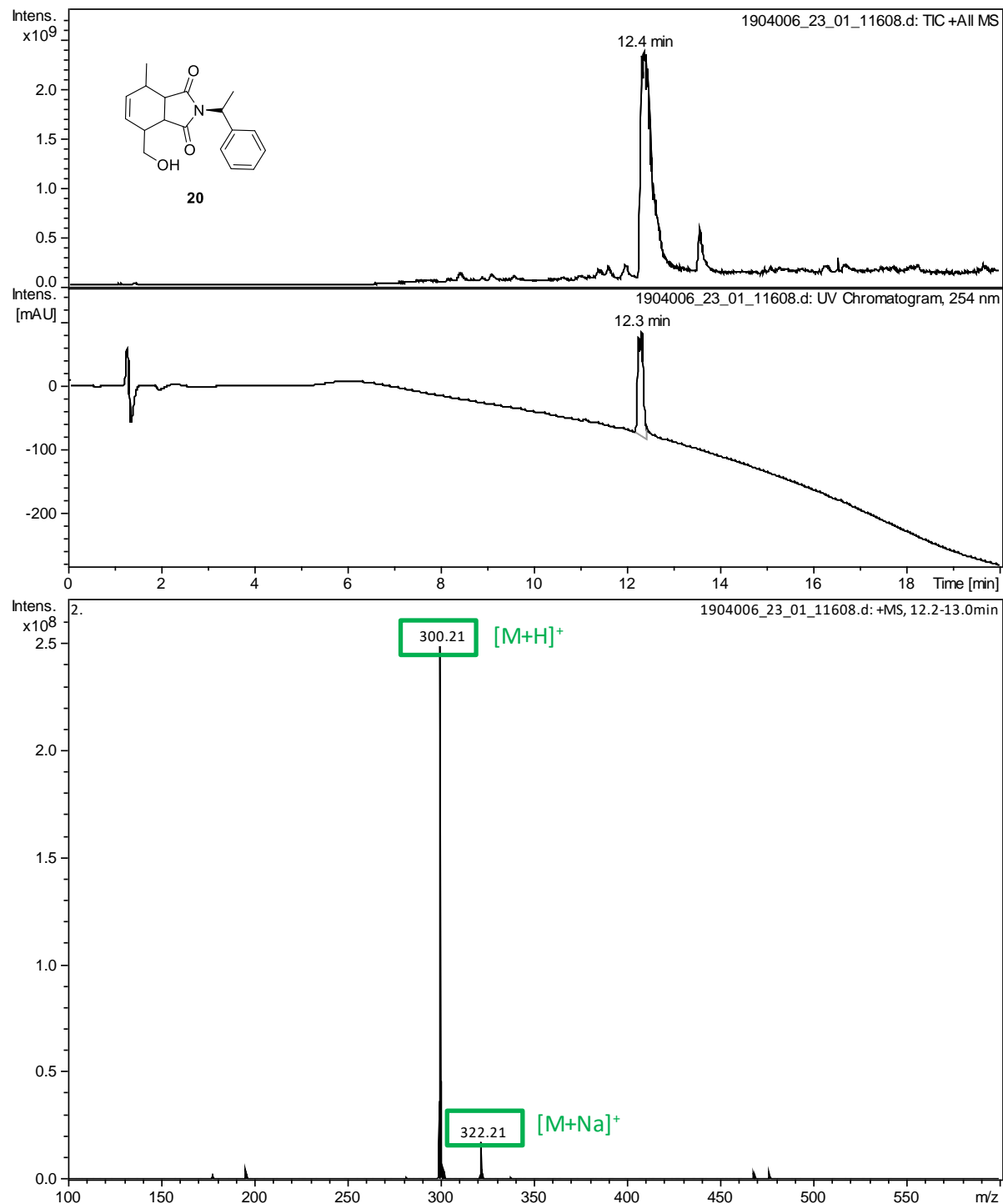
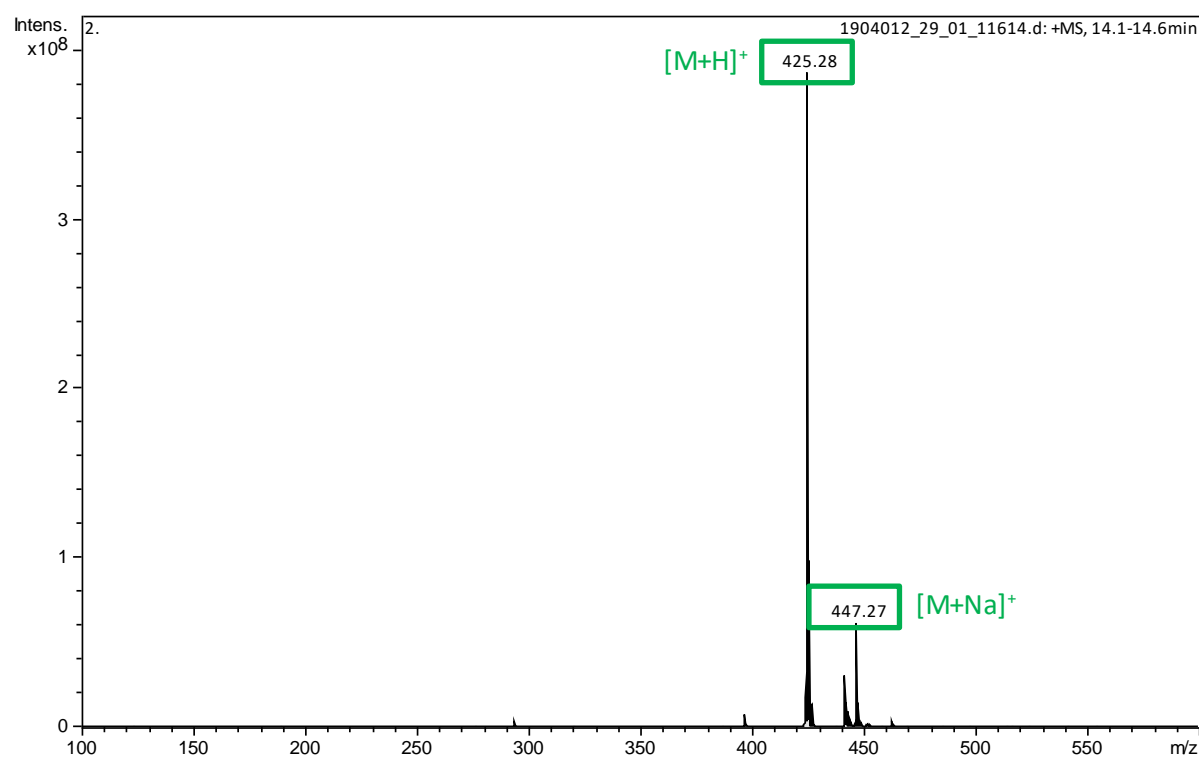
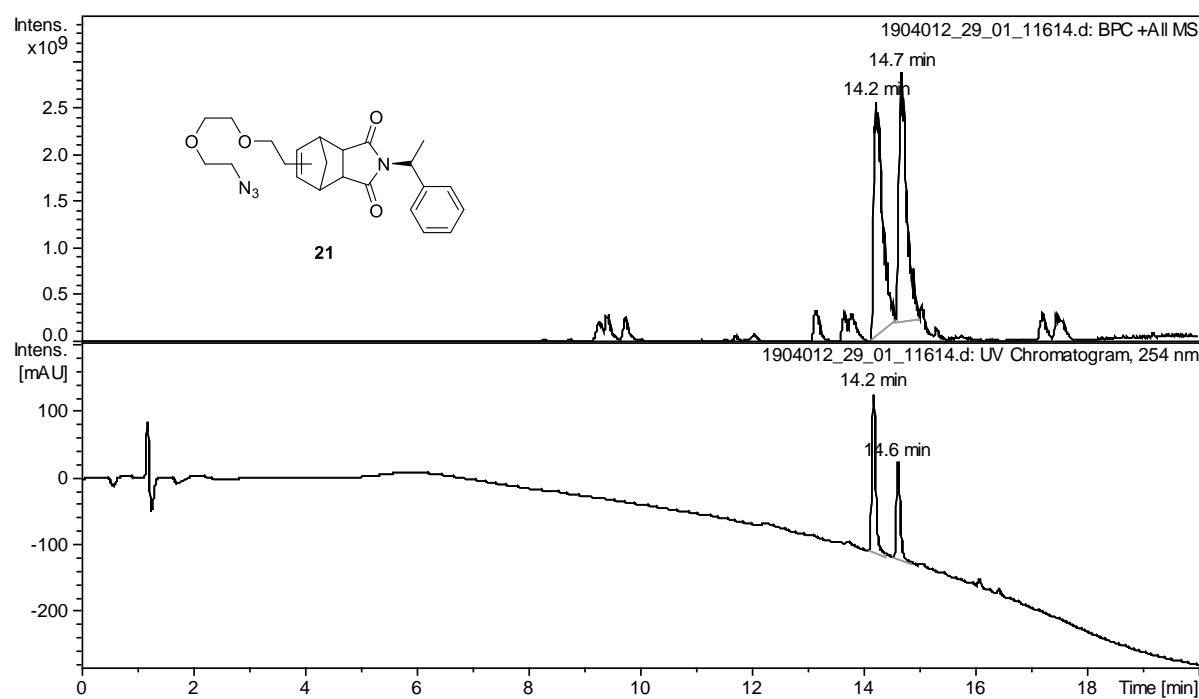


Figure S41. TIC, UV (254 nm) chromatograms and HRMS (ESI+) mass spectrum of compound **20**.



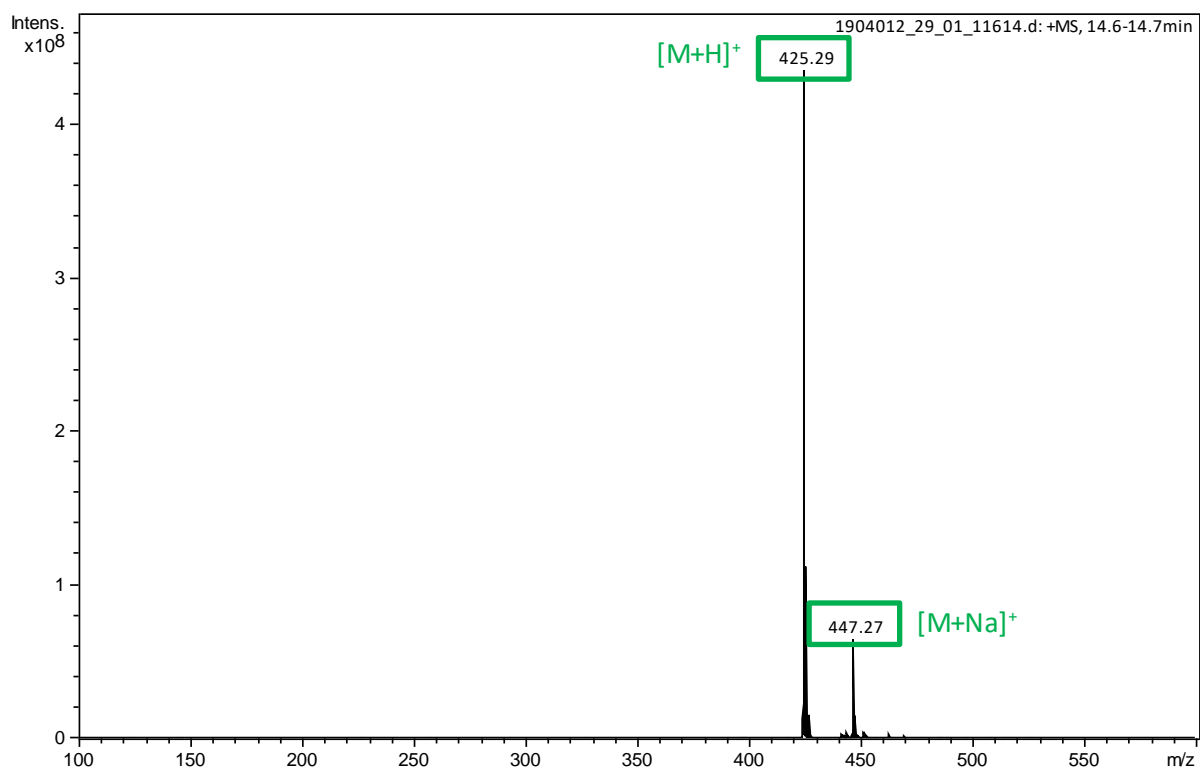


Figure S42. TIC UV (254 nm) chromatograms and HRMS (ESI+) mass spectra of compound **21**.

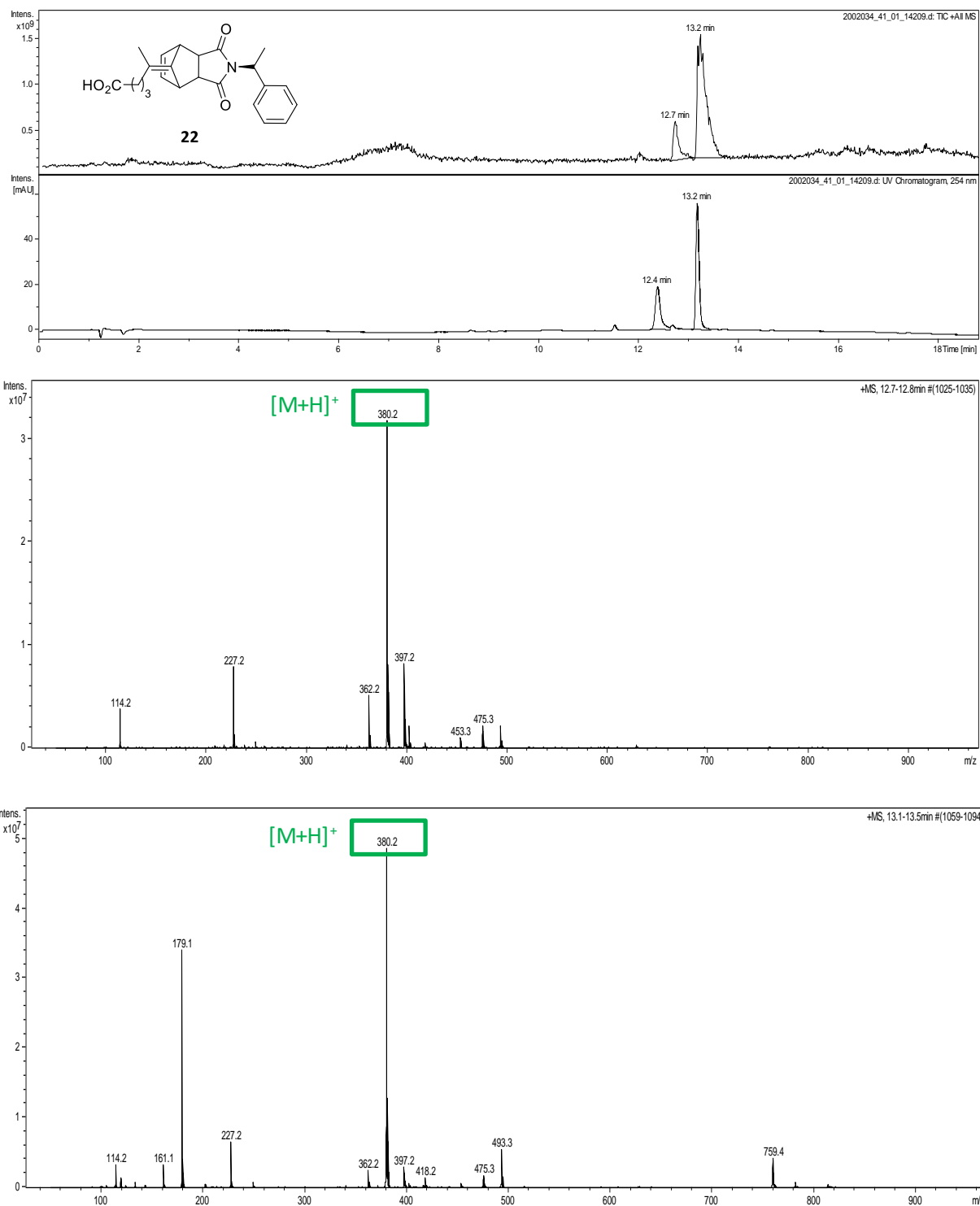
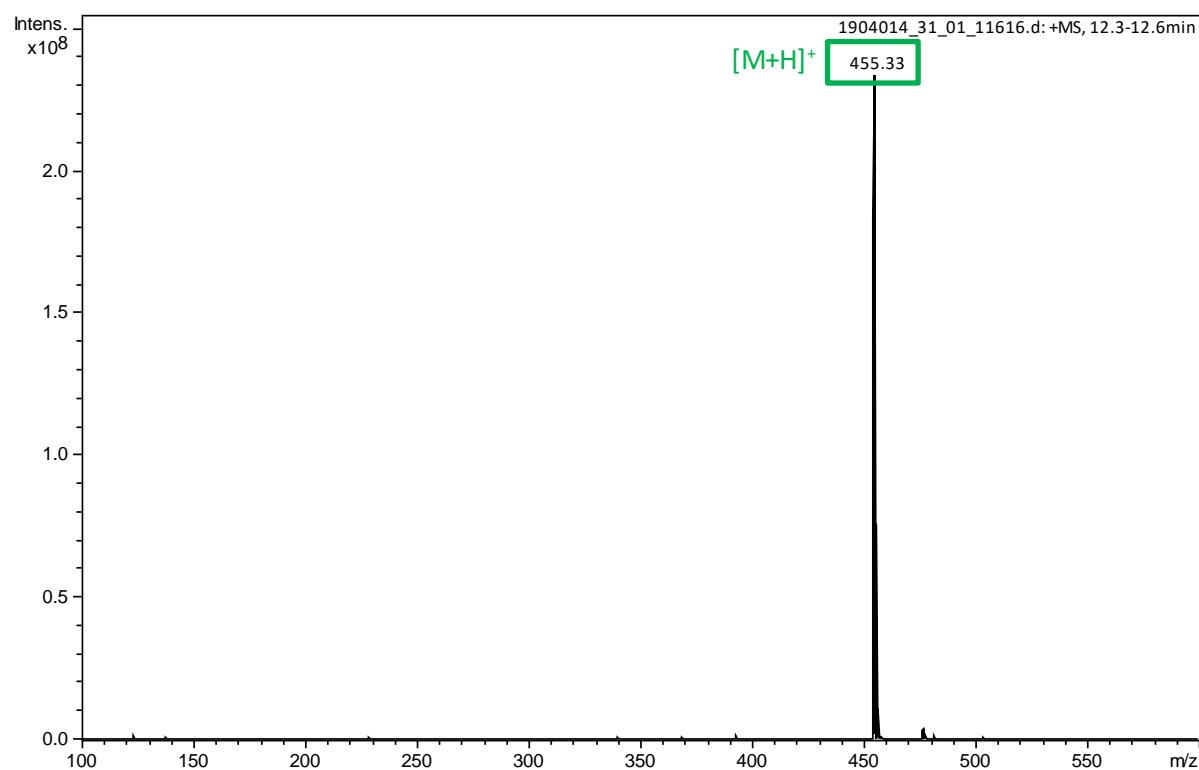
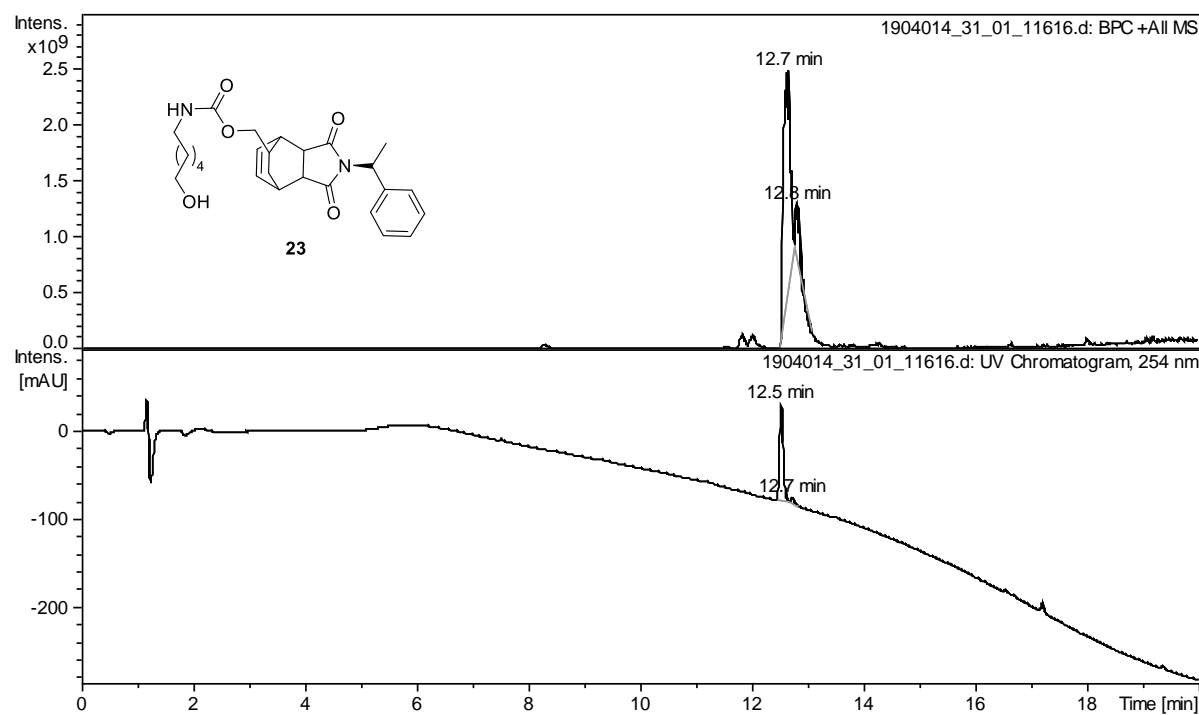


Figure S43. TIC UV (254 nm) chromatograms and HRMS (ESI+) mass spectra of compound **22**.



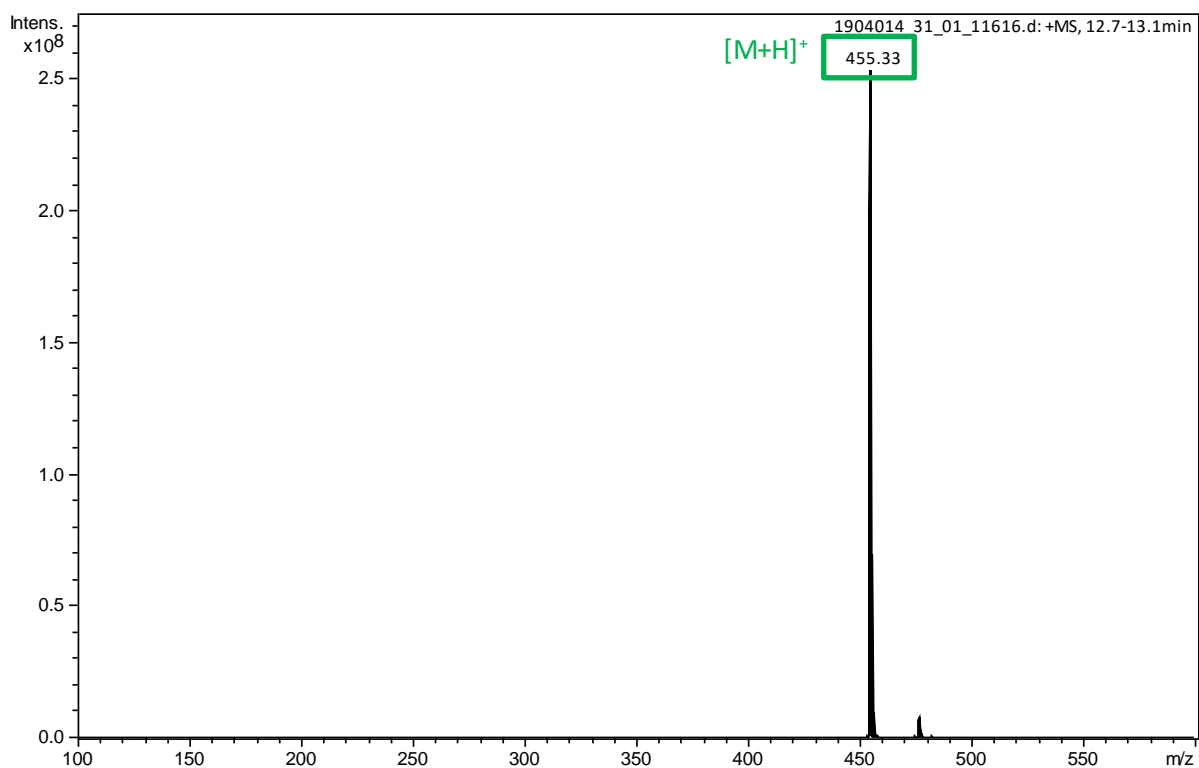


Figure S44. TIC, UV (254 nm) chromatograms and HRMS (ESI+) mass spectra of compound **23**.

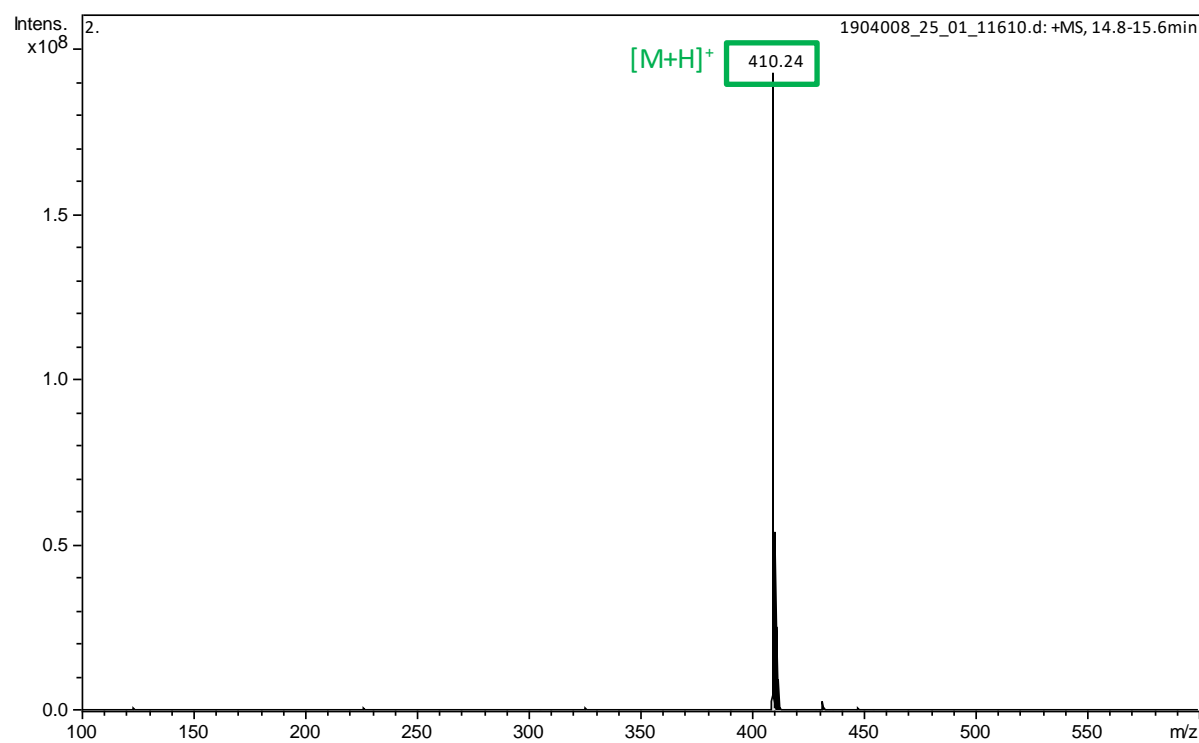
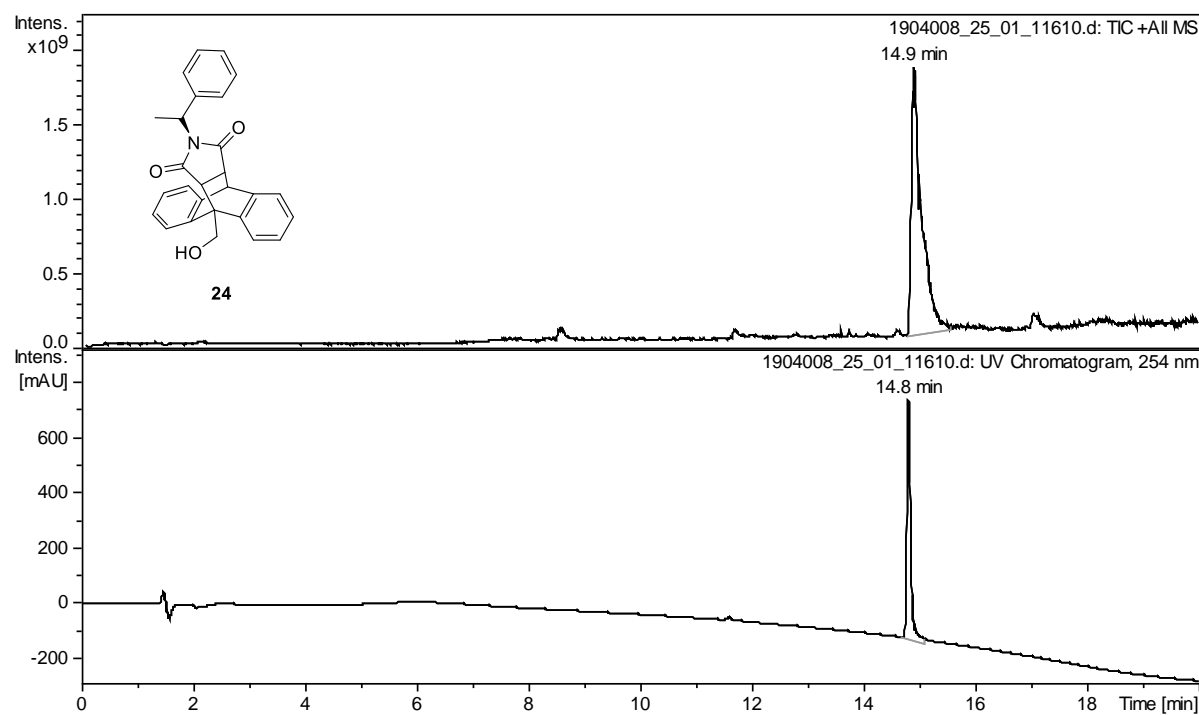


Figure S45. TIC, UV (254 nm) chromatograms and HRMS (ESI+) mass spectrum of compound **24**.

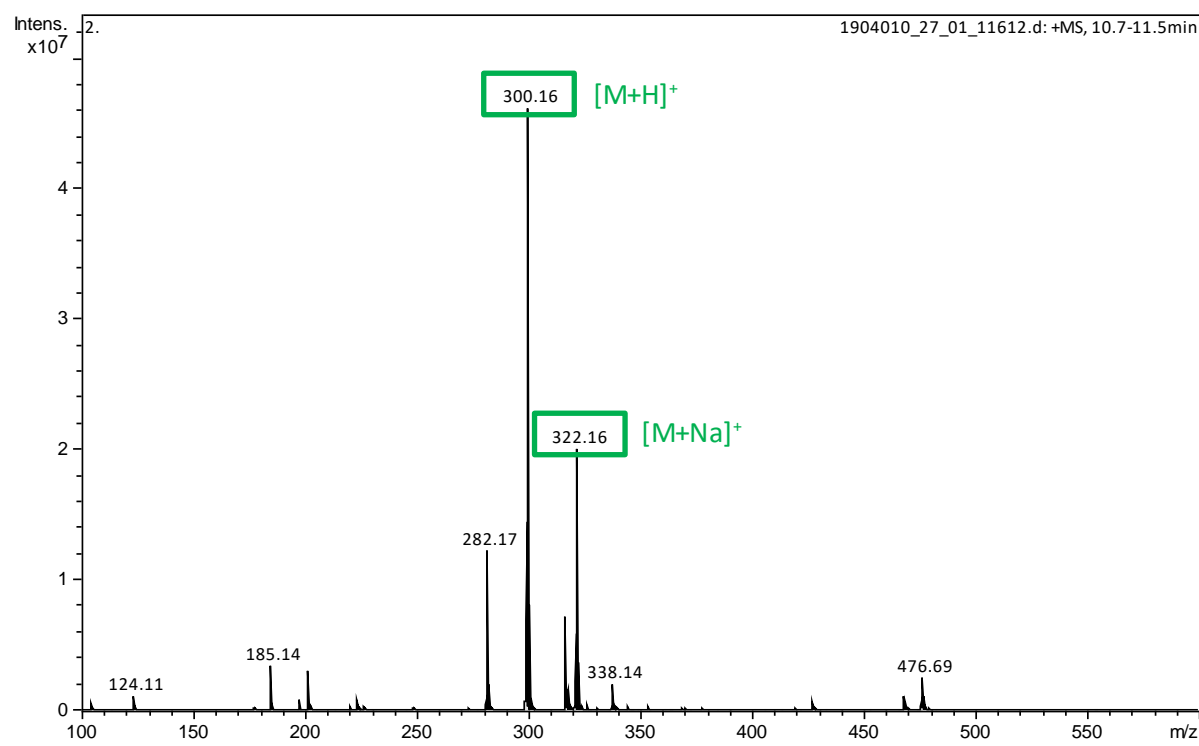
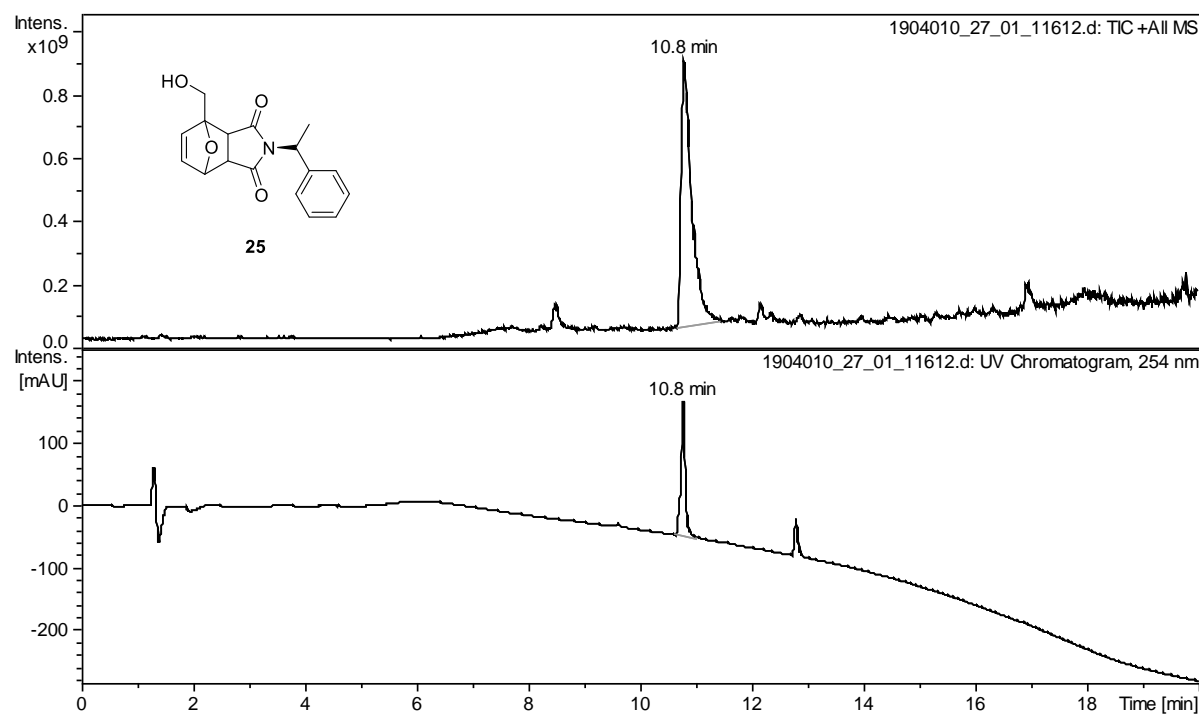


Figure S46. TIC, UV (254 nm) chromatograms and HRMS (ESI+) mass spectrum of compound **25**.

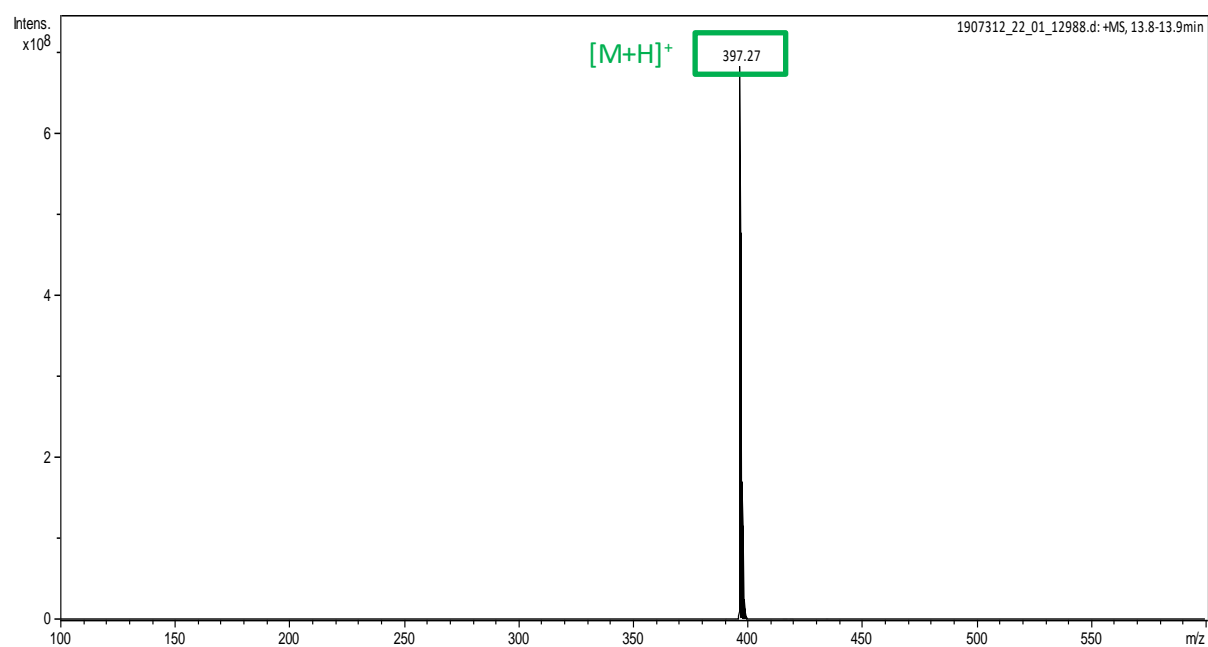
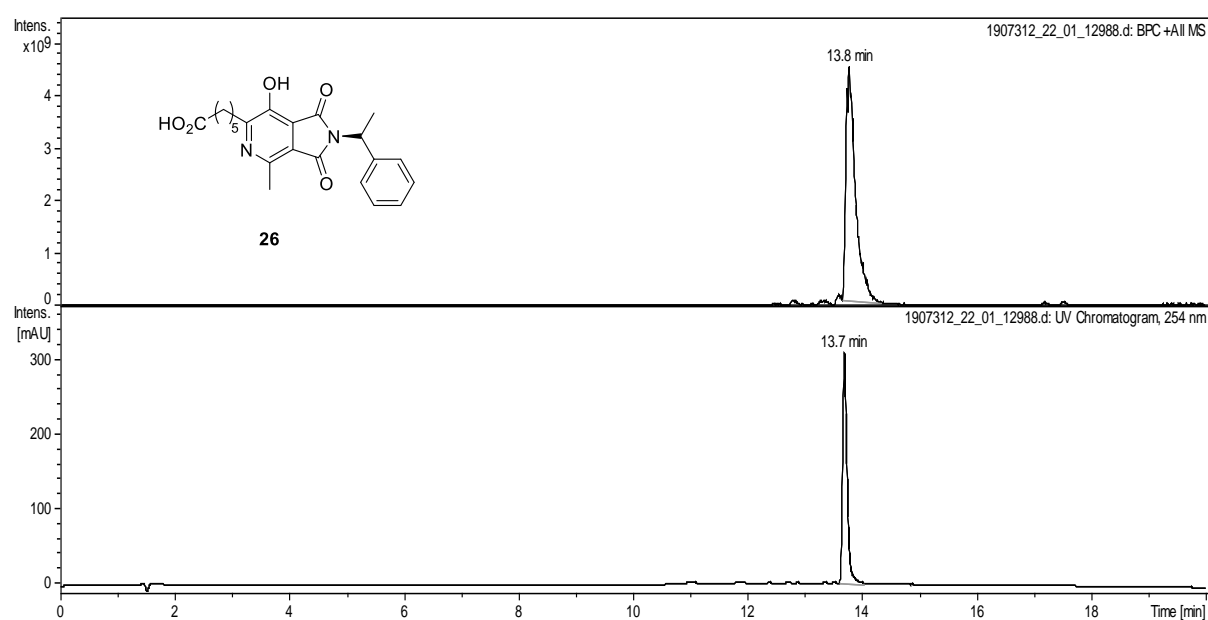


Figure S47. TIC, UV (254 nm) chromatograms and HRMS (ESI+) mass spectrum of compound **26**.

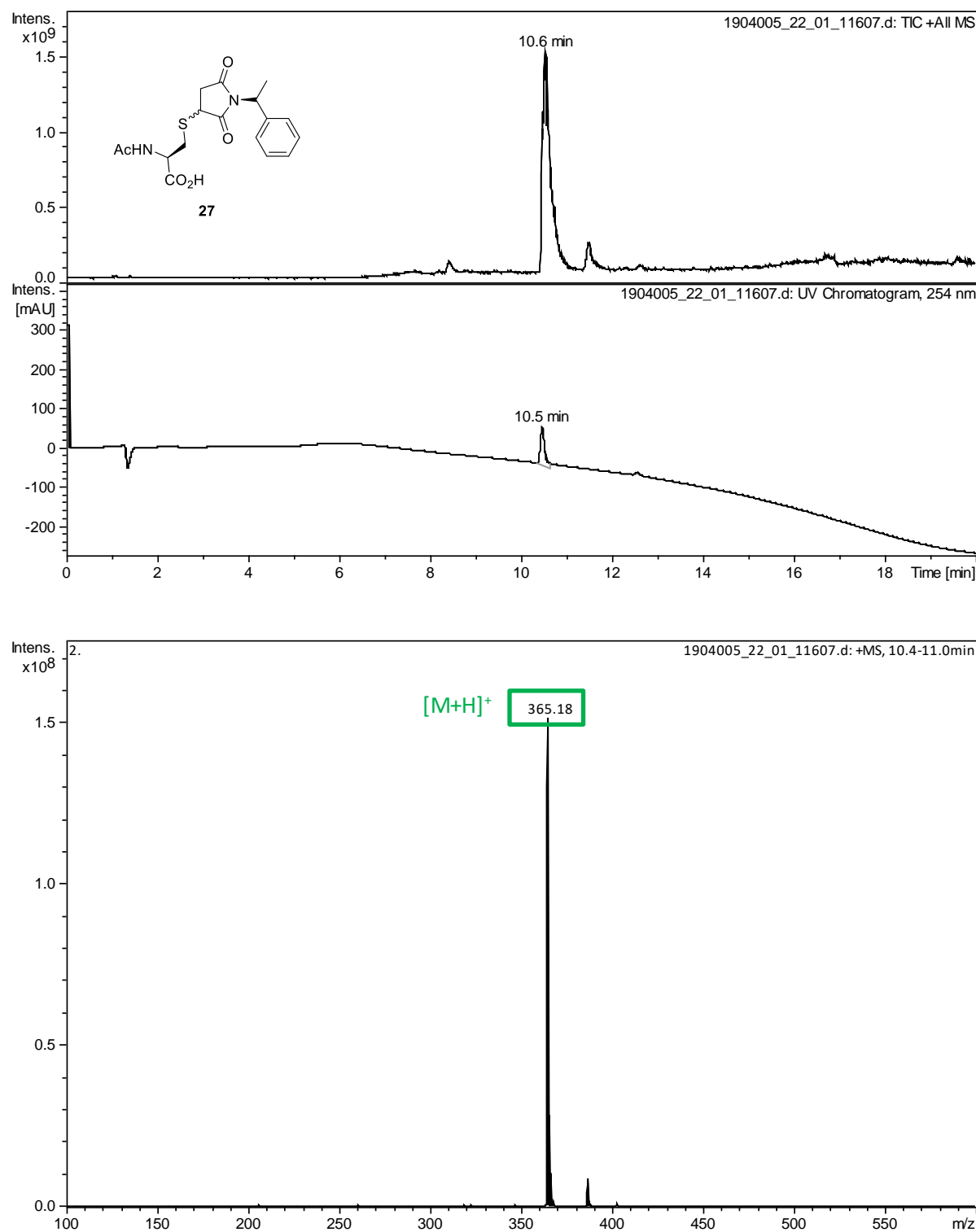


Figure S48. TIC, UV (254 nm) chromatograms and HRMS (ESI+) mass spectrum of compound **27**.

b) Study of retro-Diels-Alder reactions under physiological conditions

The reaction rate of Michael addition between *N*-acetylcysteine (NAC) and maleimide **16** was qualitatively studied following similar conditions as retro-Diels-Alder experiments. To a mixture of iPrOH/PBS pH 7.4 (1388 µL and 1174 µL respectively) at T = 37 °C was added a solution of probe **16** (112 µL, 26.8 mM in iPrOH). After 2 minutes of incubation, a solution of NAC (326 µL, 91.9 mM in PBS pH 7.4) was added. Final concentrations for t = 0 min were 1 mM for probe **16**, 10 mM (10 equiv.) for NAC and solvents ratio was iPrOH/PBS (1:1, v:v). The reaction was monitored by fluorescence spectroscopy and RP-HPLC after 8 minutes of reaction.

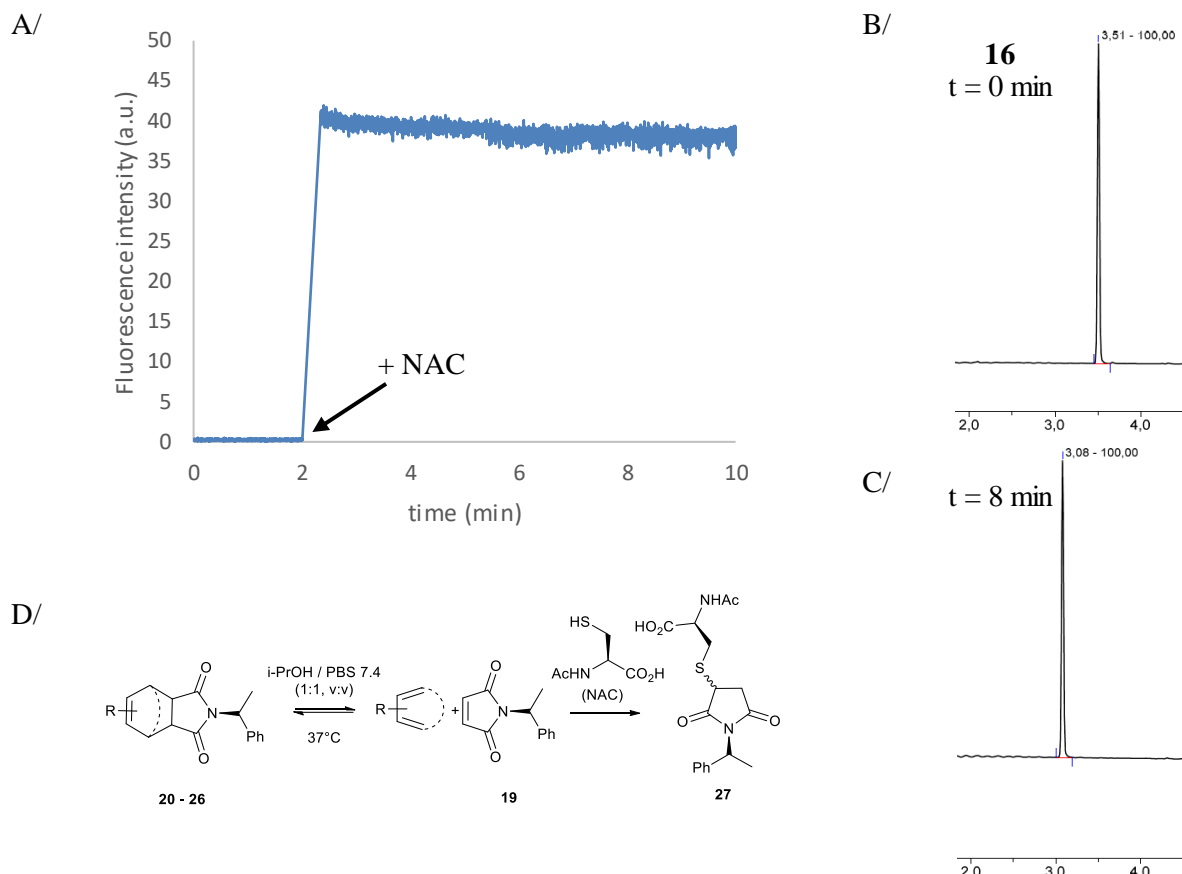


Figure S49. (A) Time-dependent fluorescence increase of probe **16** (1 mM) in the presence of NAC (10 mM, 10 equiv.) at $\lambda_{\text{em}} = 560$ nm and $\lambda_{\text{ex}} = 330$ nm. (B) RP-HPLC of isolated probe **16** ($\lambda = 330$ nm, sB). (C) RP-HPLC of the reactional mixture after 8 minutes of reaction ($\lambda = 330$ nm, sB). (D) rD-A study in the presence of NAC as fast maleimide-trapping agent.

500 µL of a stock solution of the conjugate **20-26** (2 mg of corresponding conjugate in 1 mL of iPrOH), were added to a 1 mL Eppendorf containing NAC (10 equiv.) in PBS pH 7.4 (500 µL). Then, the mixture was heated to 37 °C in a water-bath. Unless otherwise stated, aliquots for LC-MS analyses were prepared after 24 h as follows: to the reactional mixture (100 µL) were added iPrOH (50 µL) and H₂O (50 µL). Thioether **27** was only detected if maleimide **19** was formed from a retro-Diels-Alder process, and subsequently trapped by *N*-acetylcysteine through a thio Michael addition. All aliquots were stored at -25 °C pending LC-MS analyses (System C).

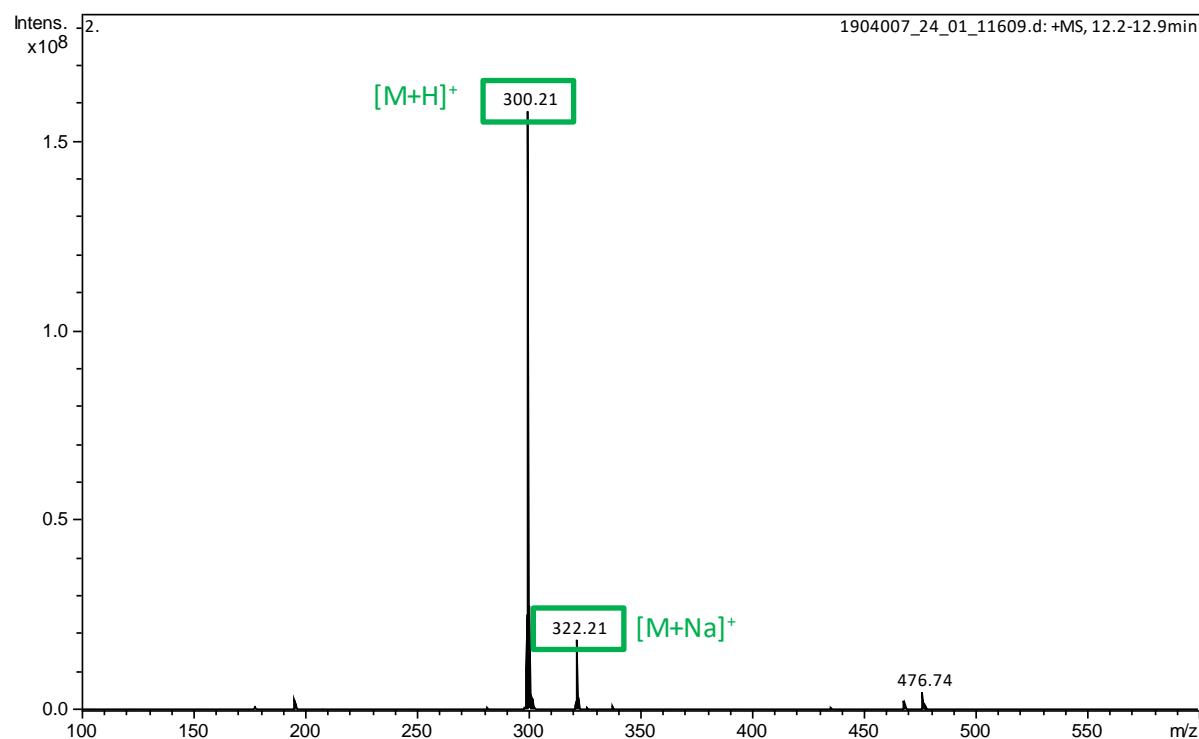
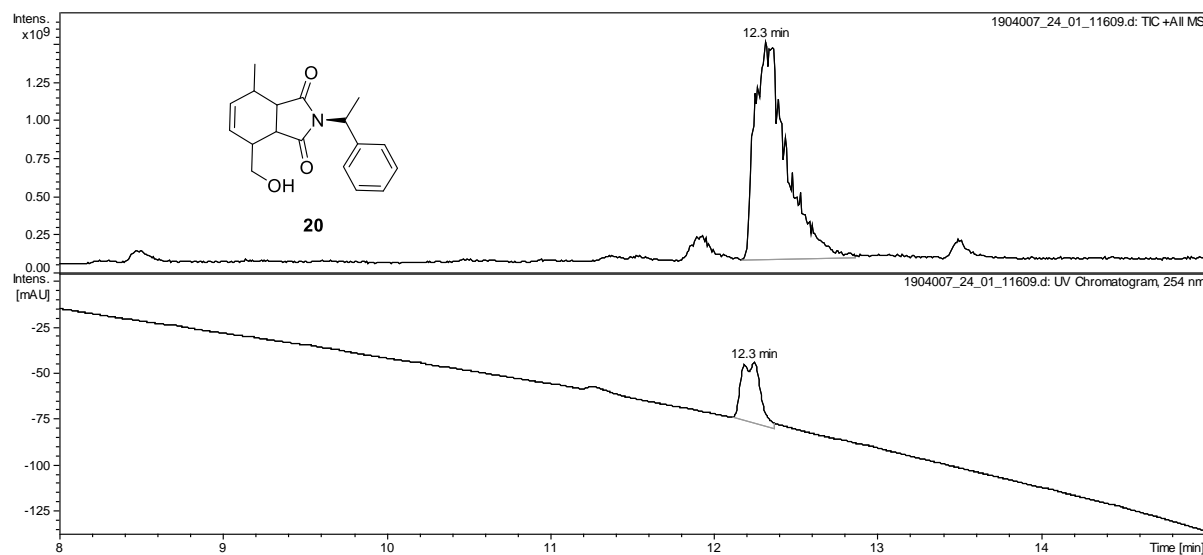
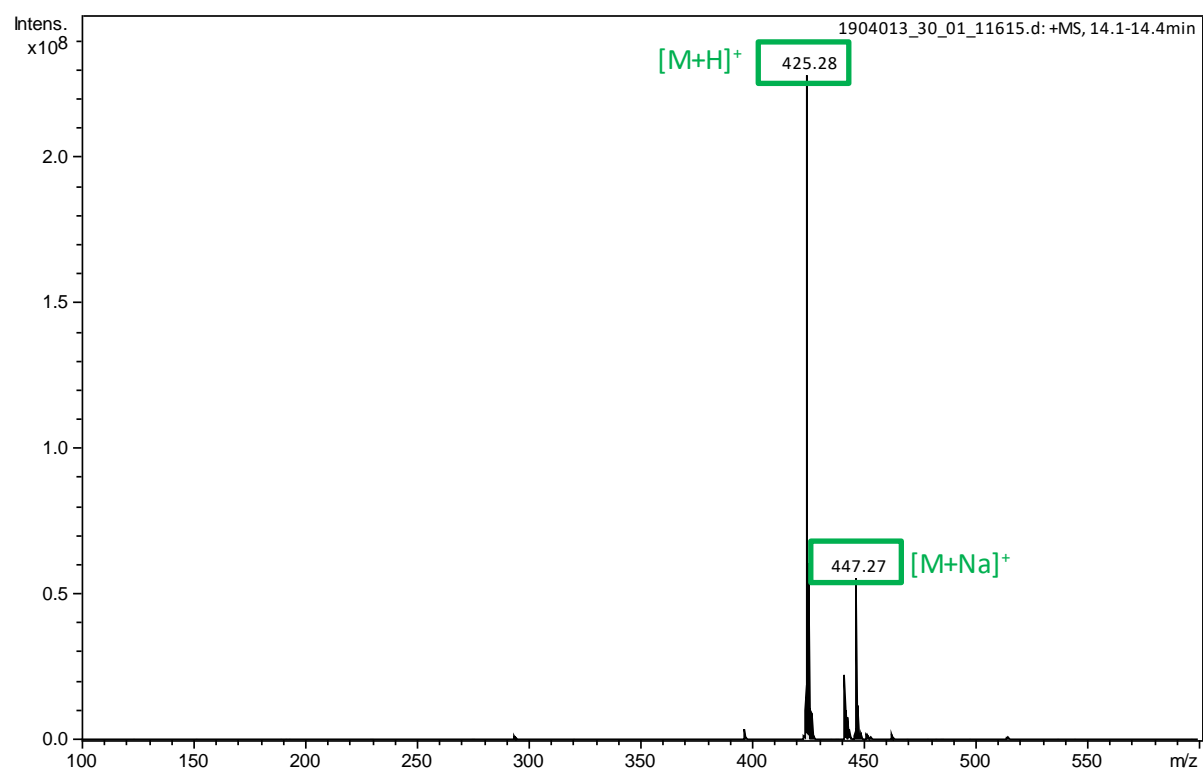
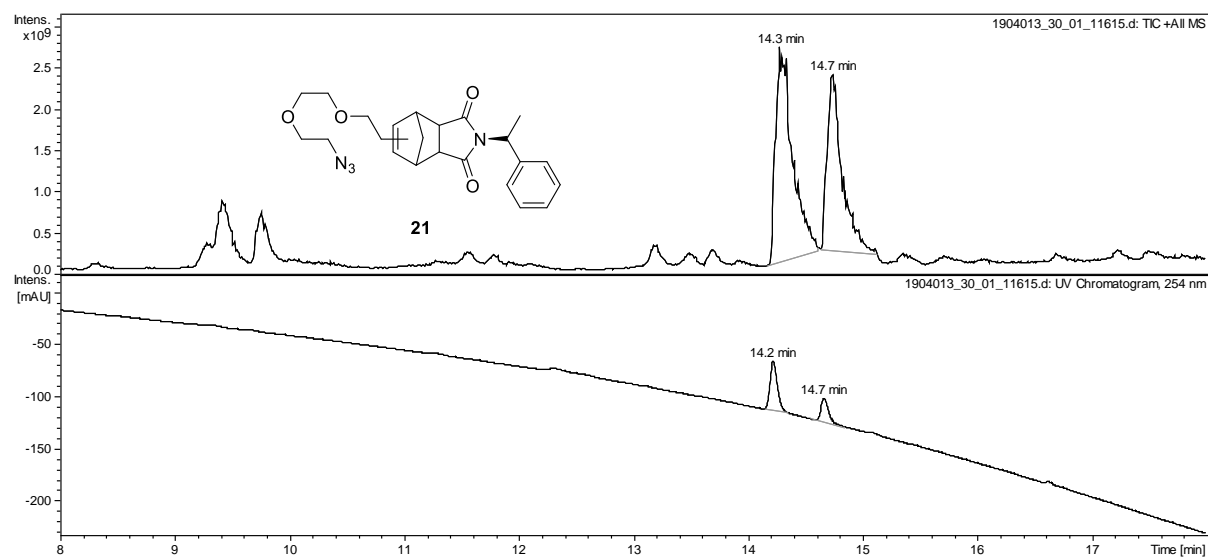


Figure S50. TIC, UV (254 nm) chromatograms and MS (ESI+) mass spectrum of r-D-A with **20**.



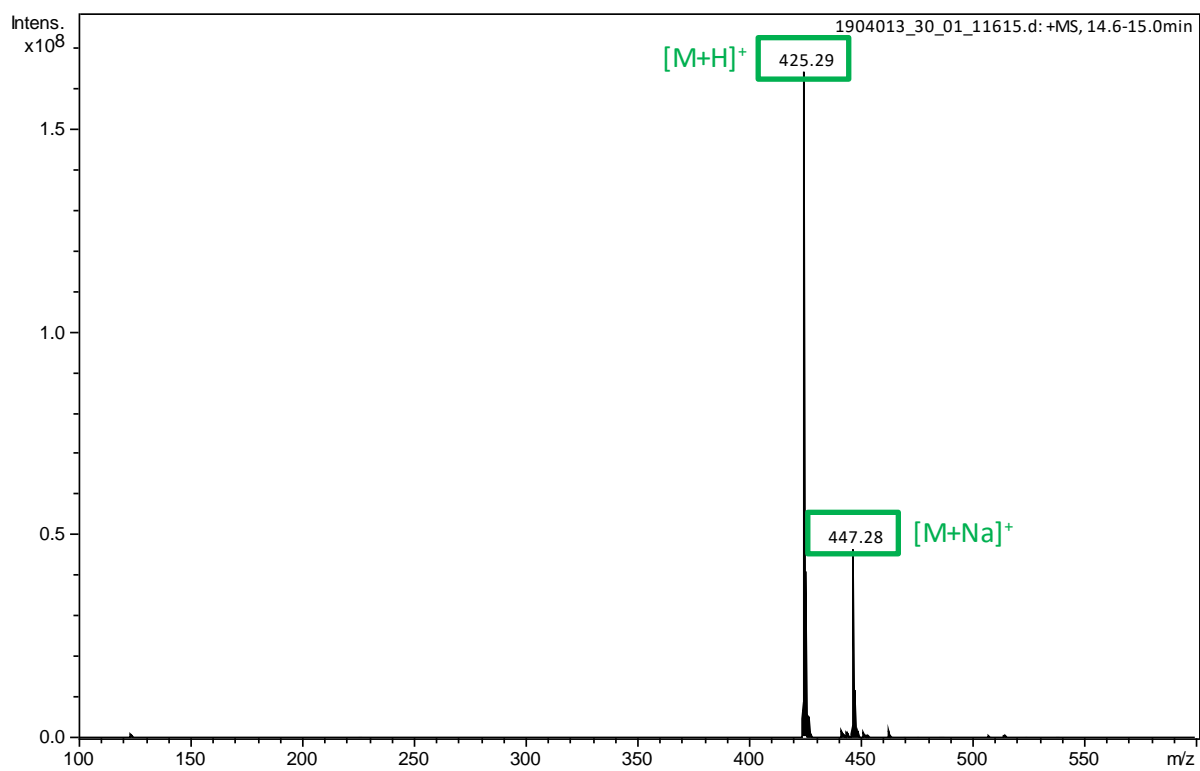


Figure S51. TIC, UV (254 nm) chromatograms and MS (ESI+) mass spectra of r-D-A with **21**.

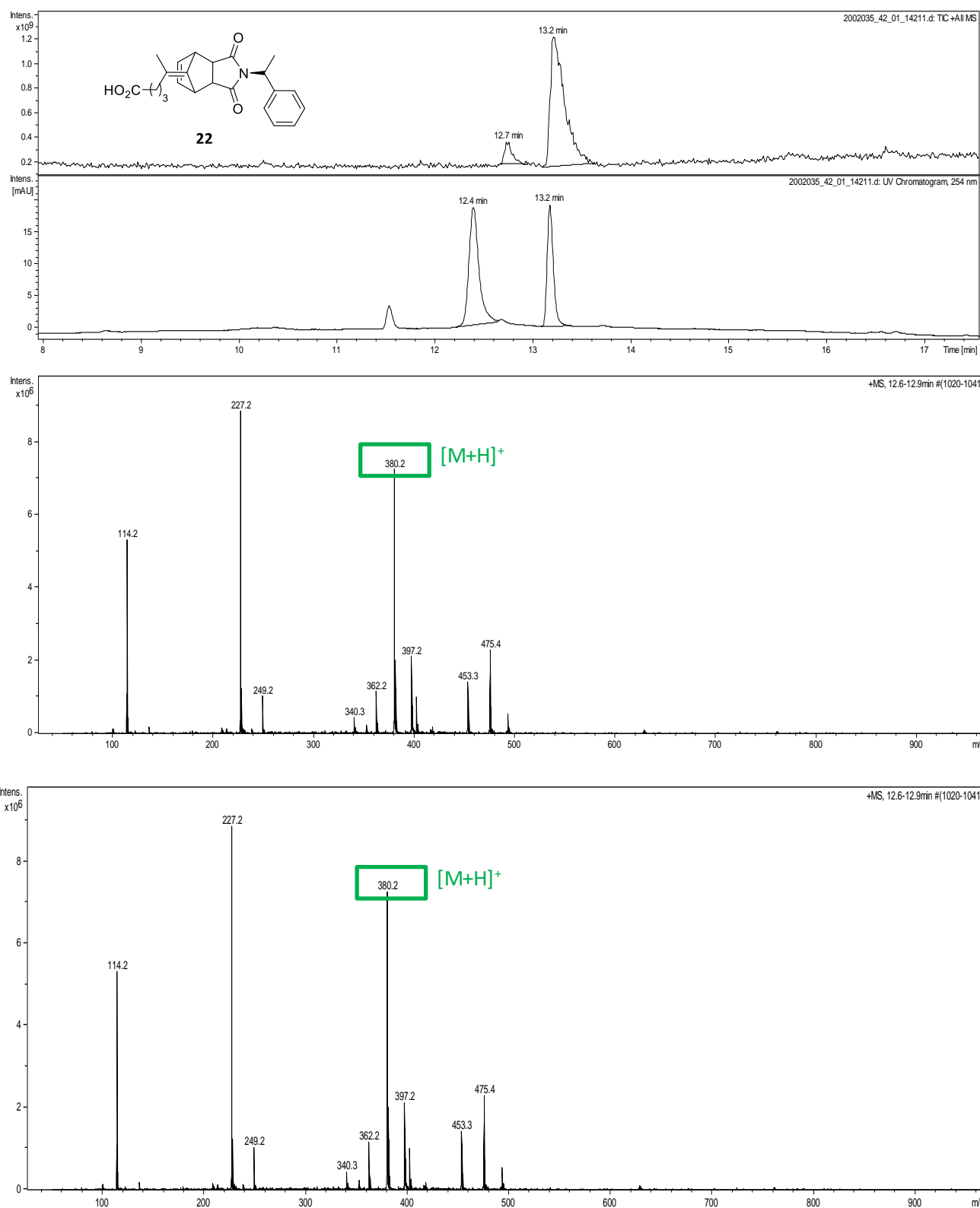
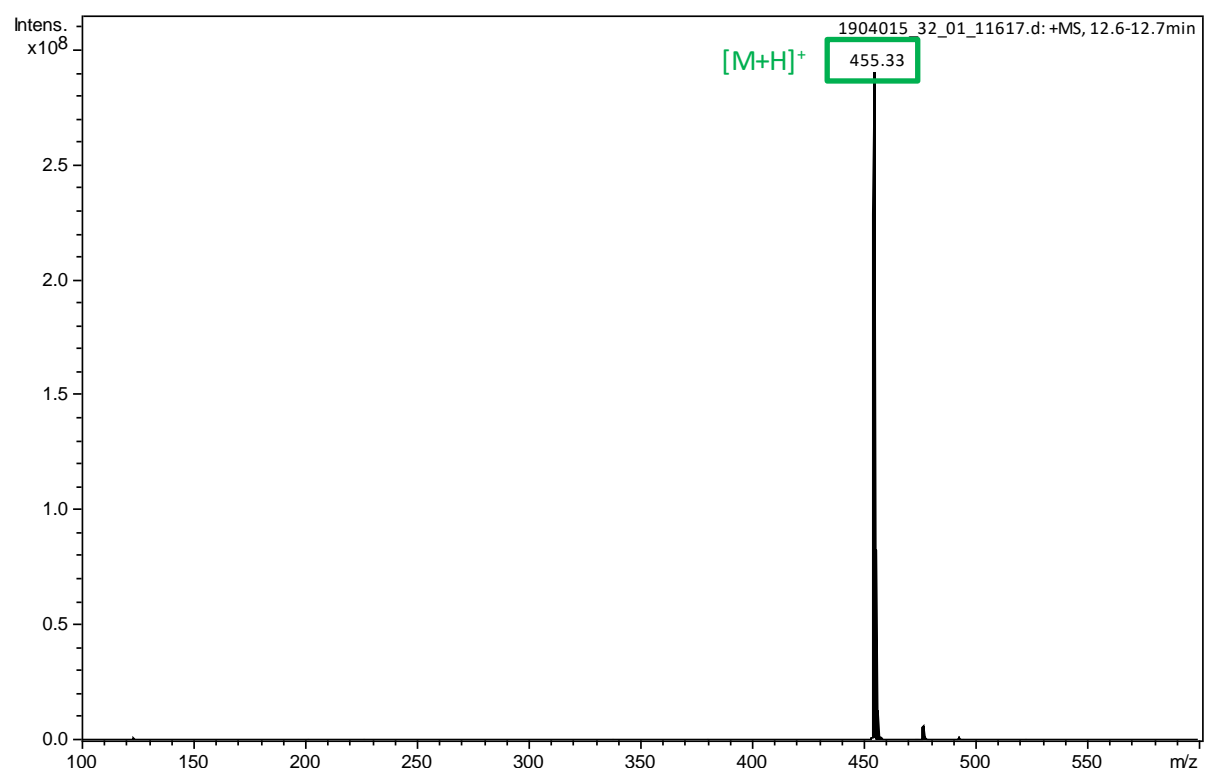
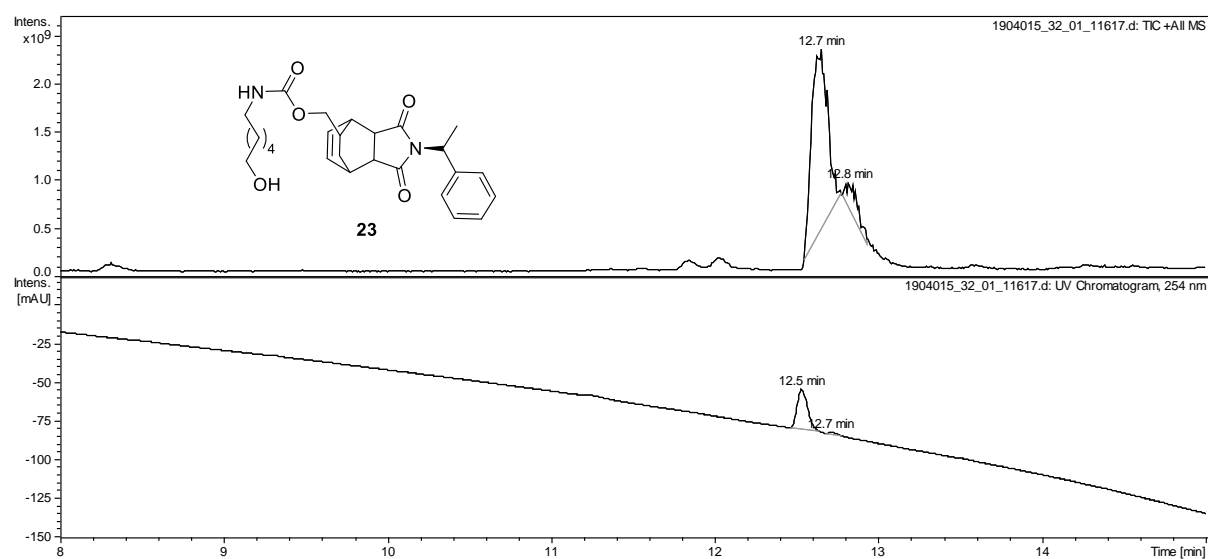


Figure S52. TIC, UV (254 nm) chromatograms and MS (ESI+) mass spectra of r-D-A with **22**.



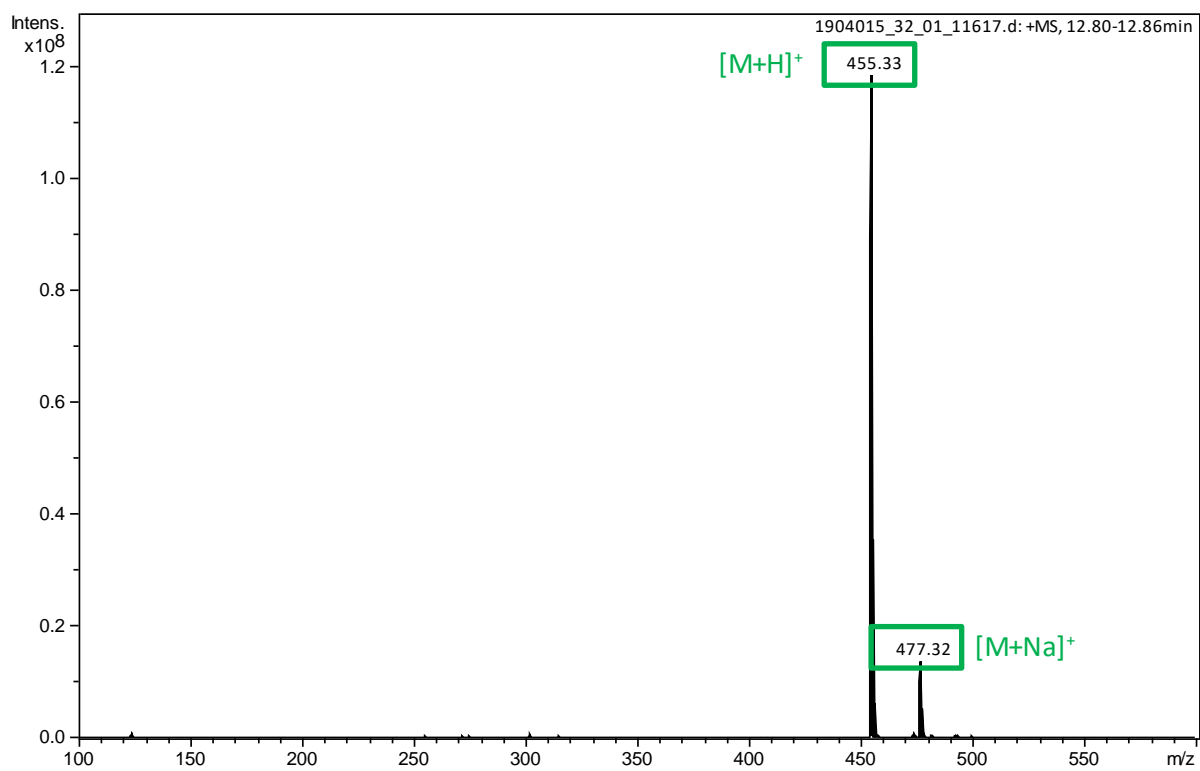


Figure S53. TIC, UV (254 nm) chromatograms and MS (ESI+) mass spectra of r-D-A with **23**.

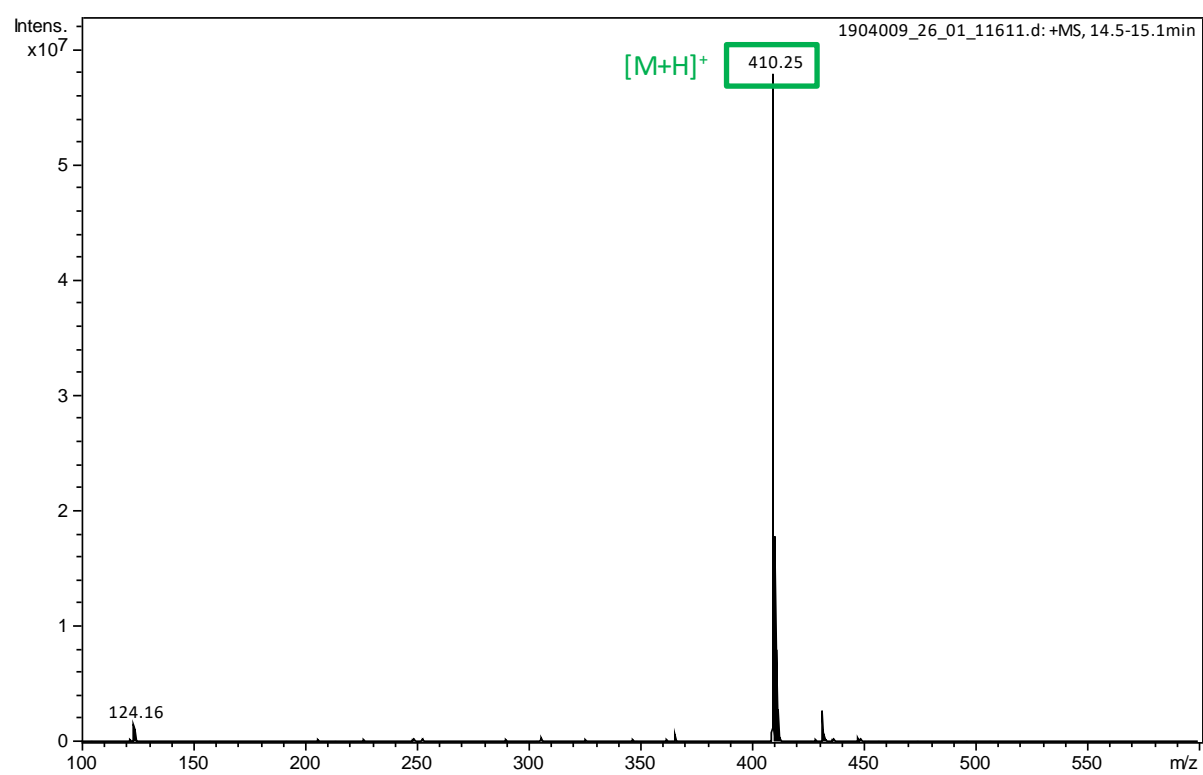
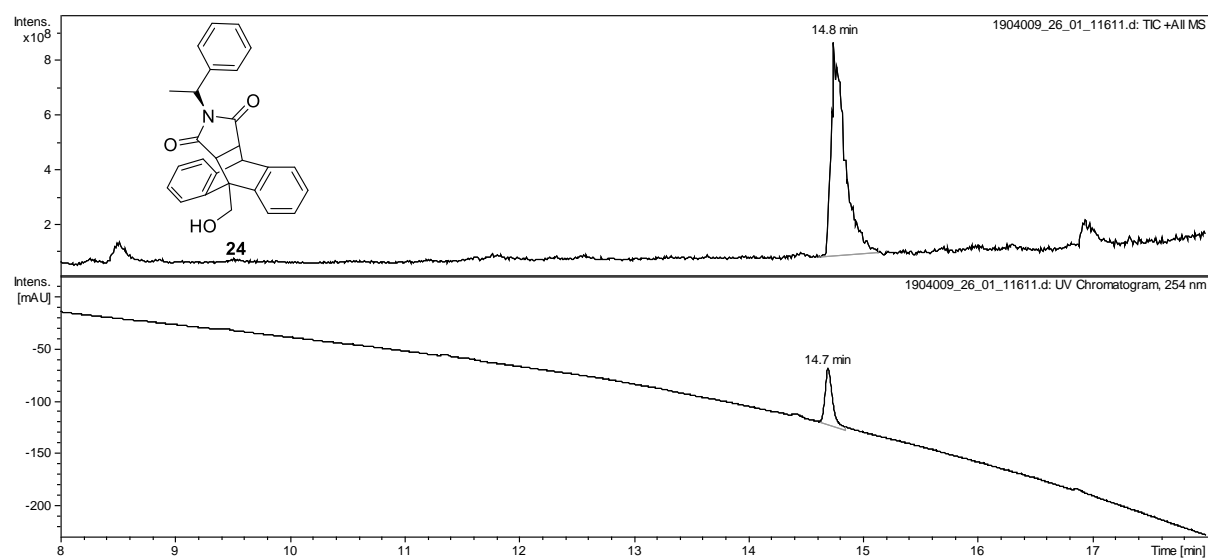
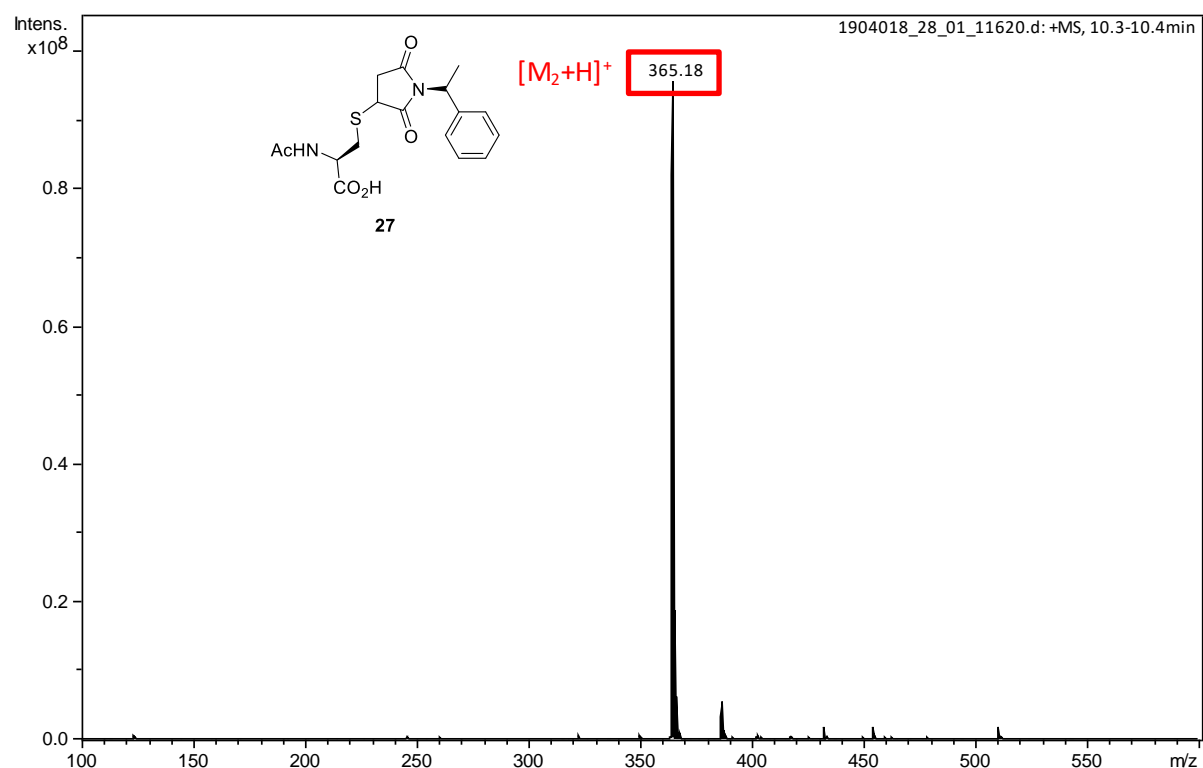
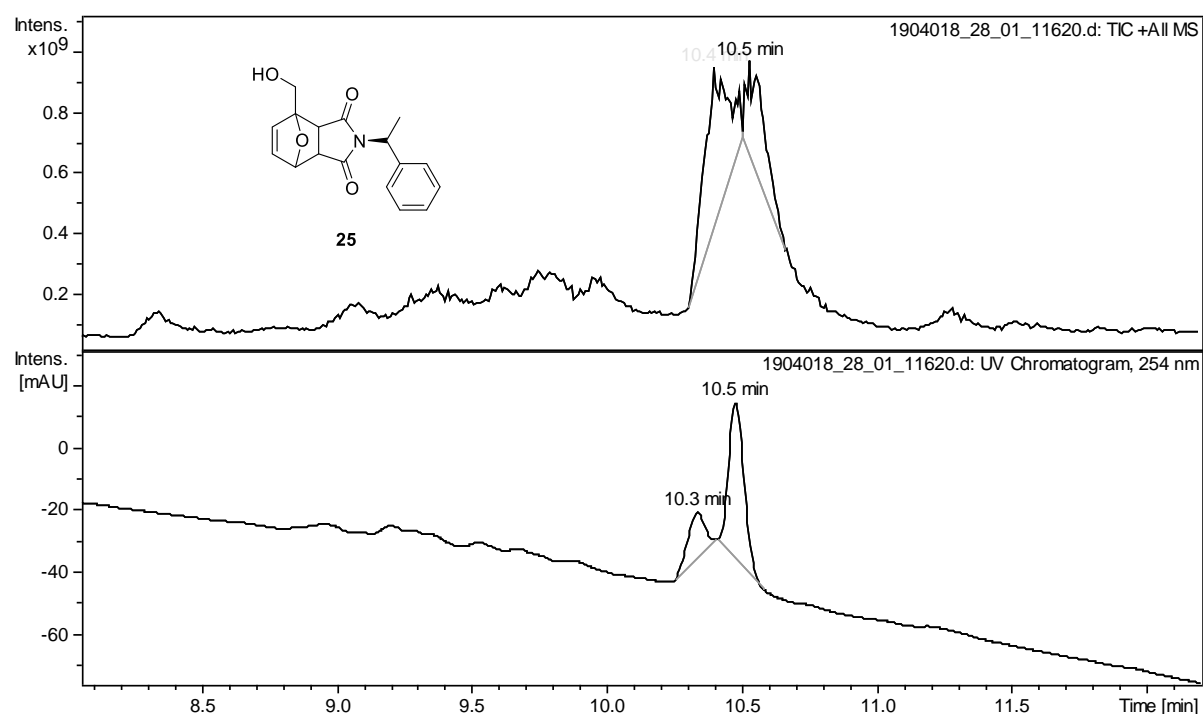
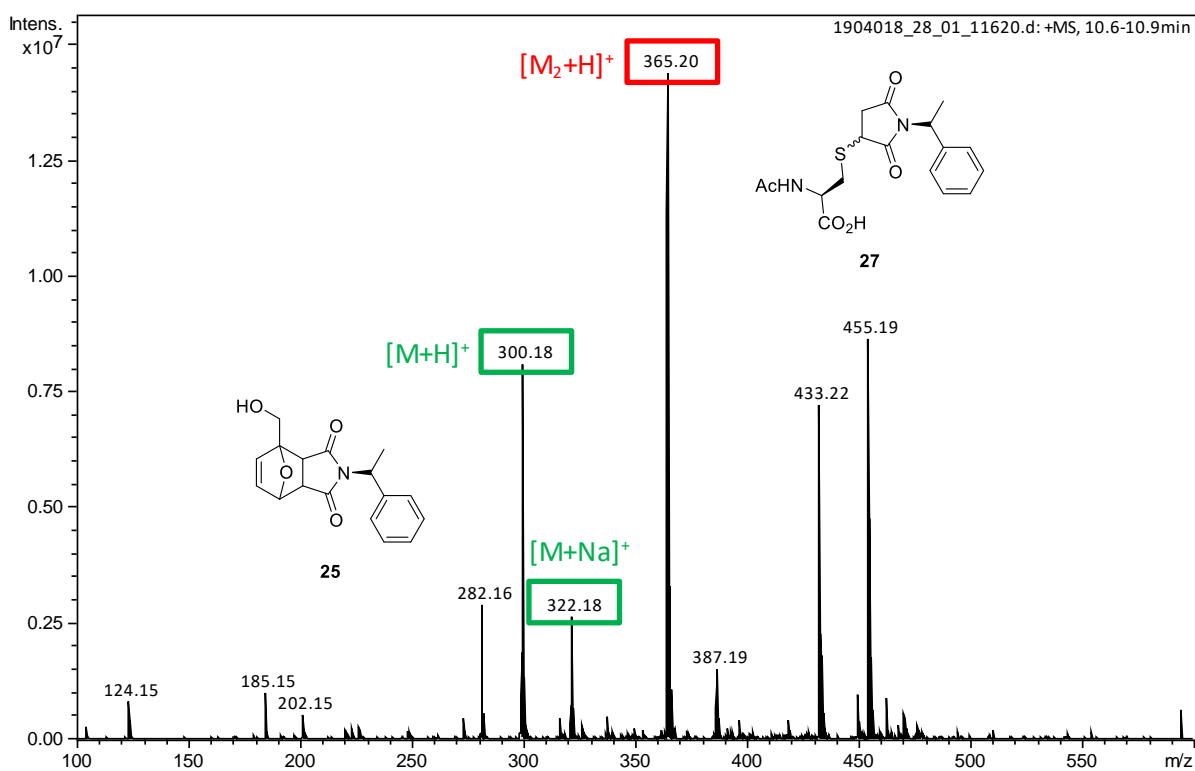
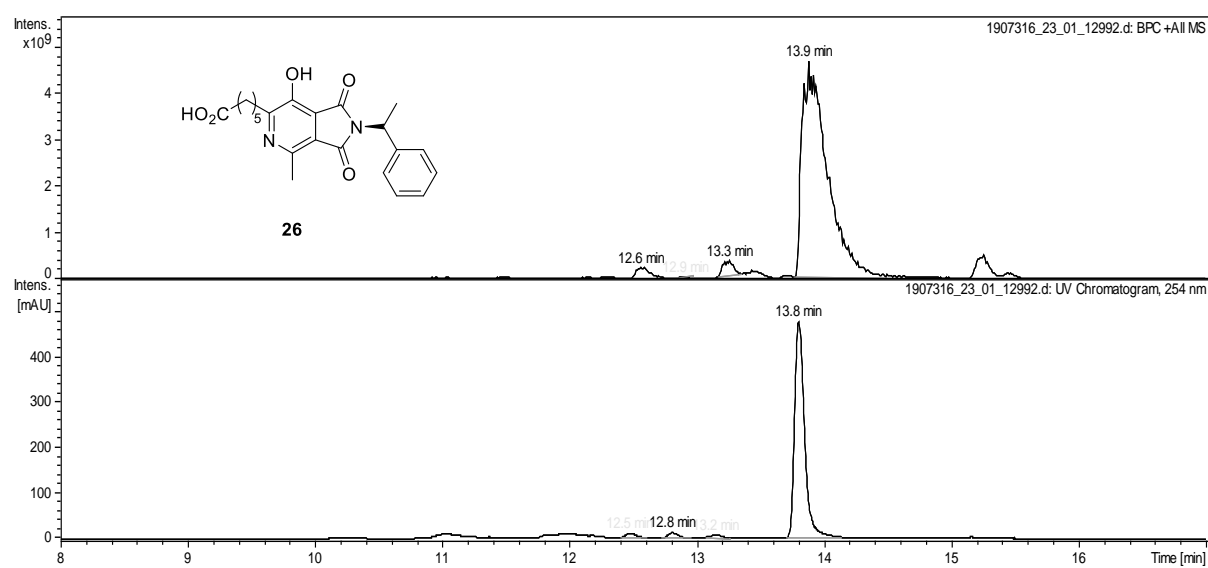


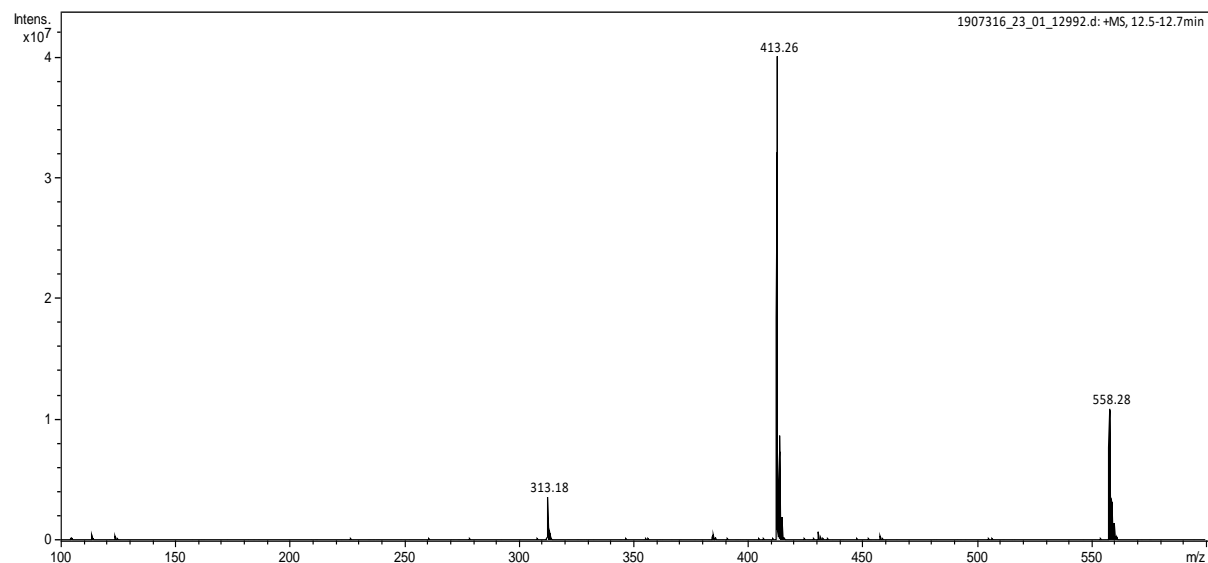
Figure S54. TIC, UV (254 nm) chromatograms and MS (ESI+) mass spectrum of r-D-A with **24**.

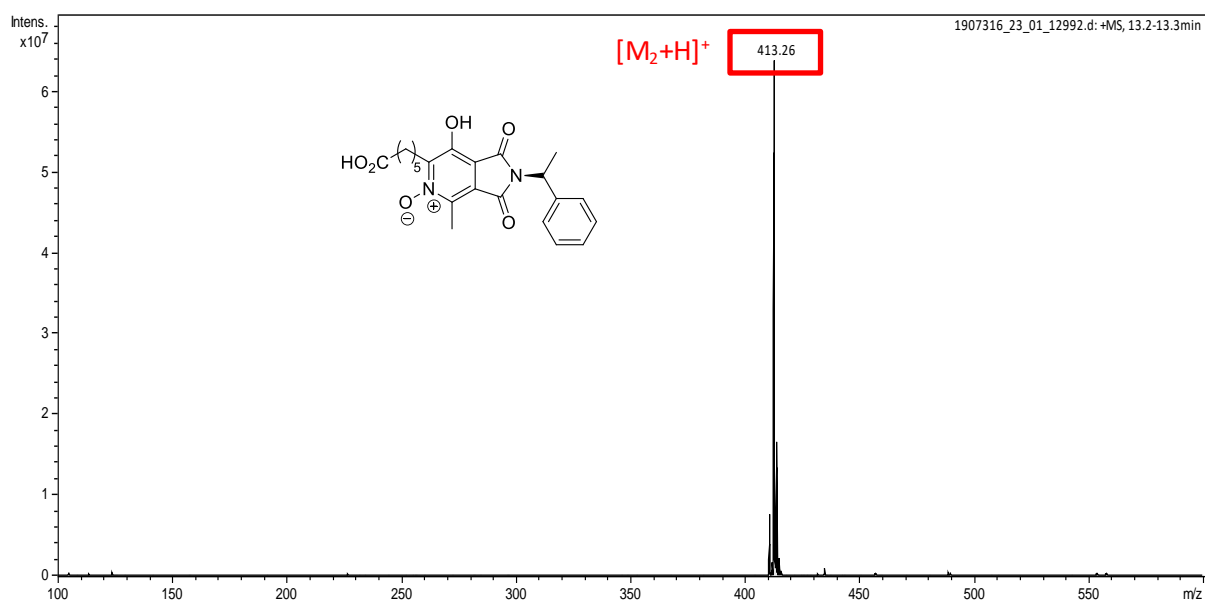
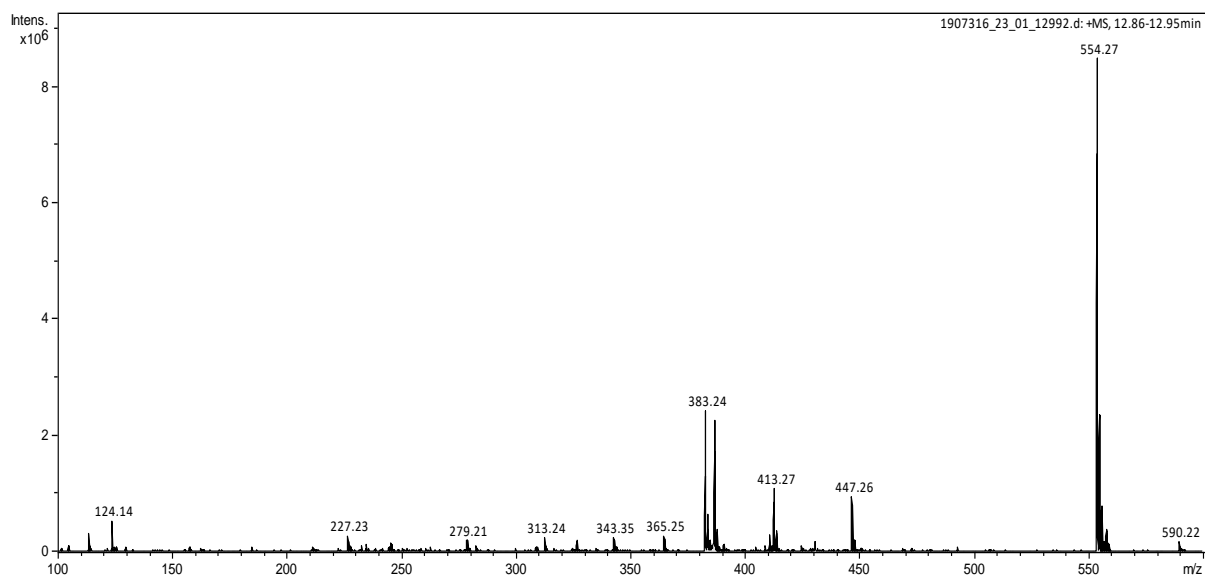






Retention time (min)	% area 254 nm (%)
12.5	2.0
12.8	2.4
13.2	1.9
13.8	93.6





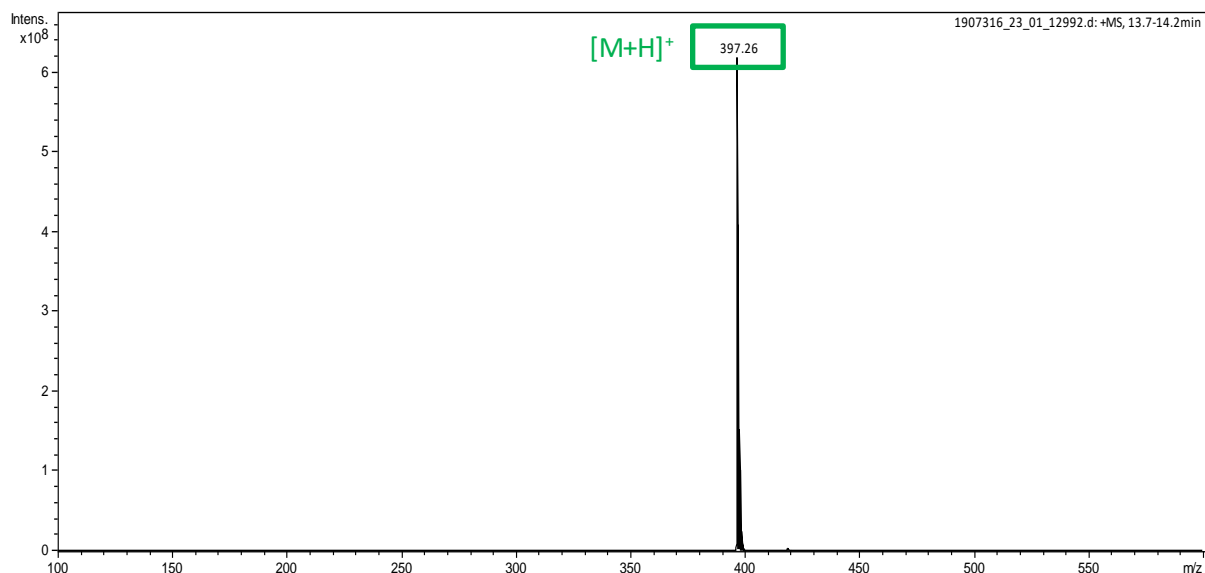


Figure S56. TIC, UV (254 nm) chromatograms and MS (ESI+) mass spectra of r-D-A with **26**.

c) Study of conjugates 20-26 stability in human blood plasma (HBP)

50 µL of a stock solution of the conjugate **20-26** (1 mg of corresponding conjugate in a solution of 100 µL of DMSO/iPrOH, 1:1, v:v) were added to an 2 mL Eppendorf containing HBP (500 µL). Then, the mixture was heated to 37 °C in a water-bath. After 24 h, the mixture was diluted with EtOH (500 µL) which led to the formation of a precipitate. The mixture was centrifuged for 30 min at 11 000 rotations/min. Then, the supernatant was withdrawn with a syringe and filtered through an HPLC filter (porosity: 0.45 µm). All aliquots were stored at -25°C pending LC-MS analyses (System C).

Blanks 1 and 2 from HBP were prepared following the same procedure without Diels-Alder product.

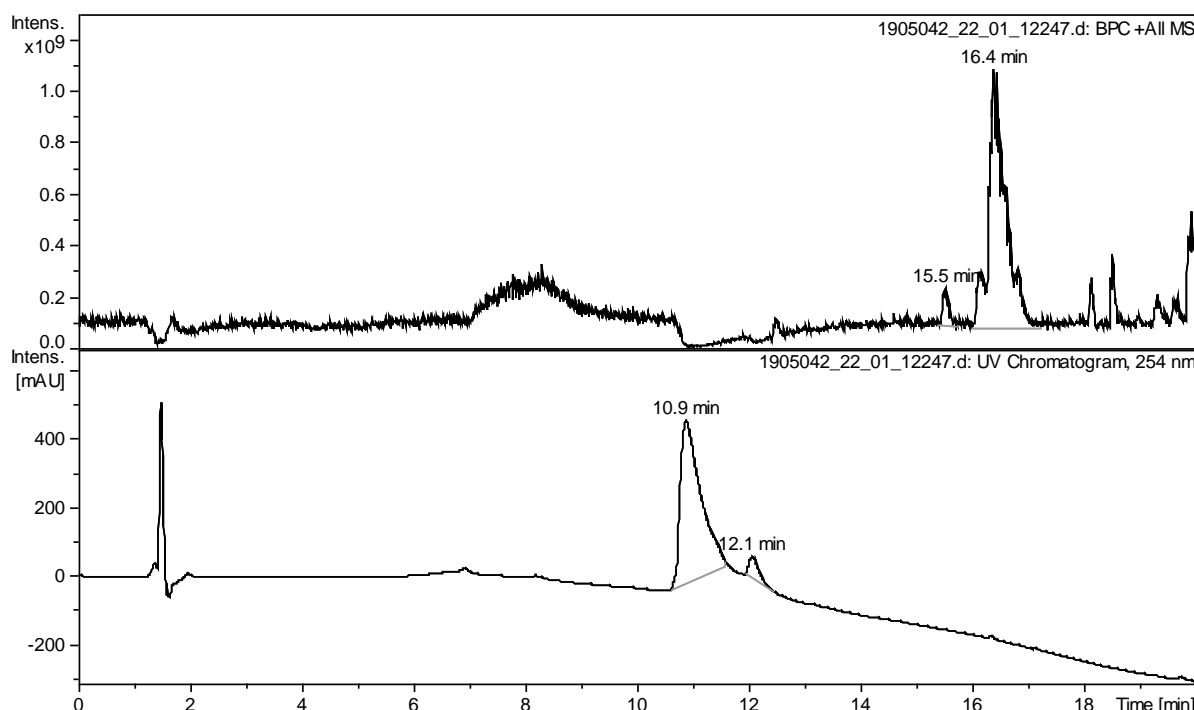


Figure S57. TIC, UV (254 nm) chromatograms of human blood plasma (Blank 1).

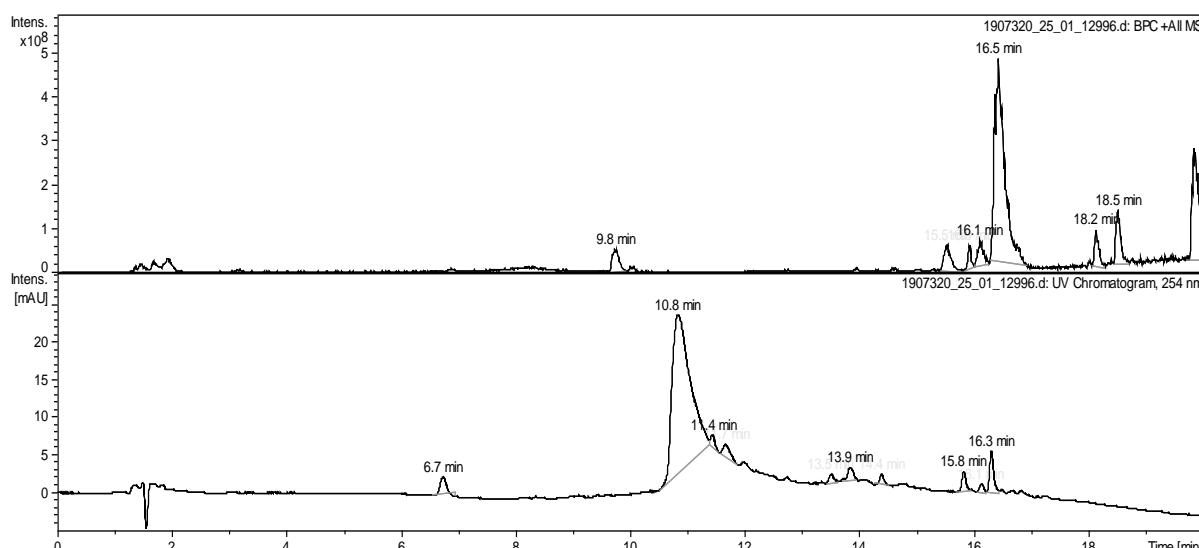
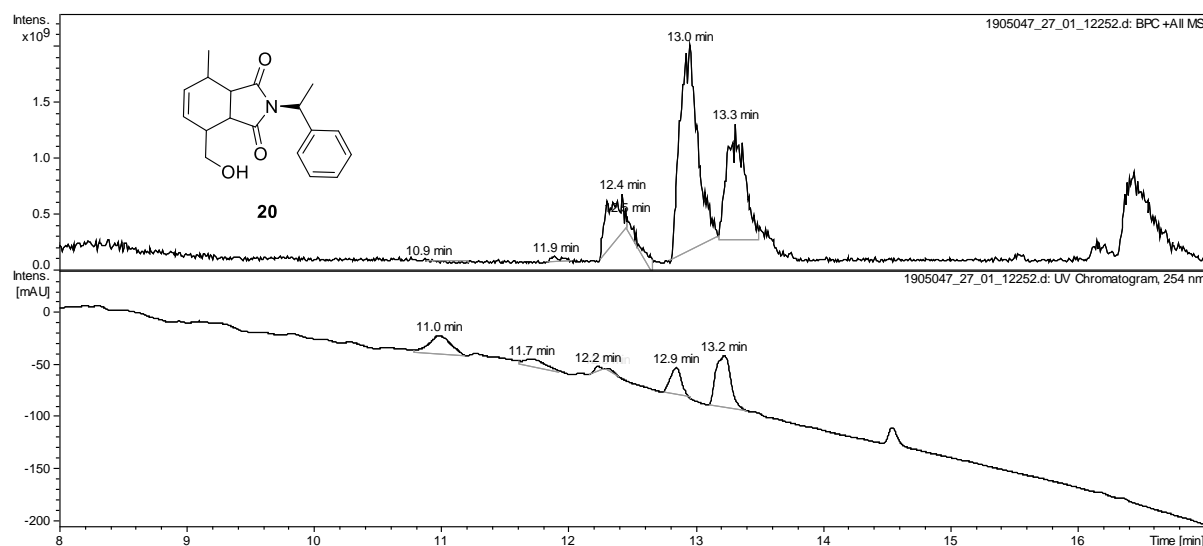
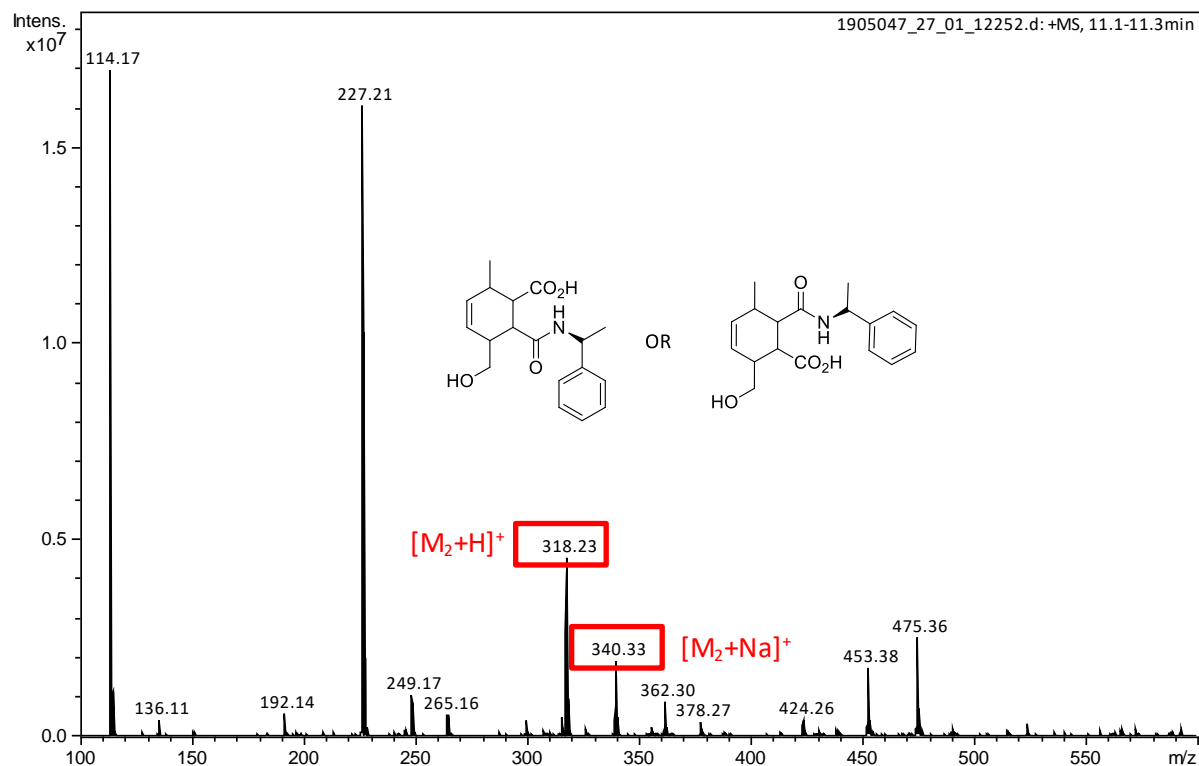
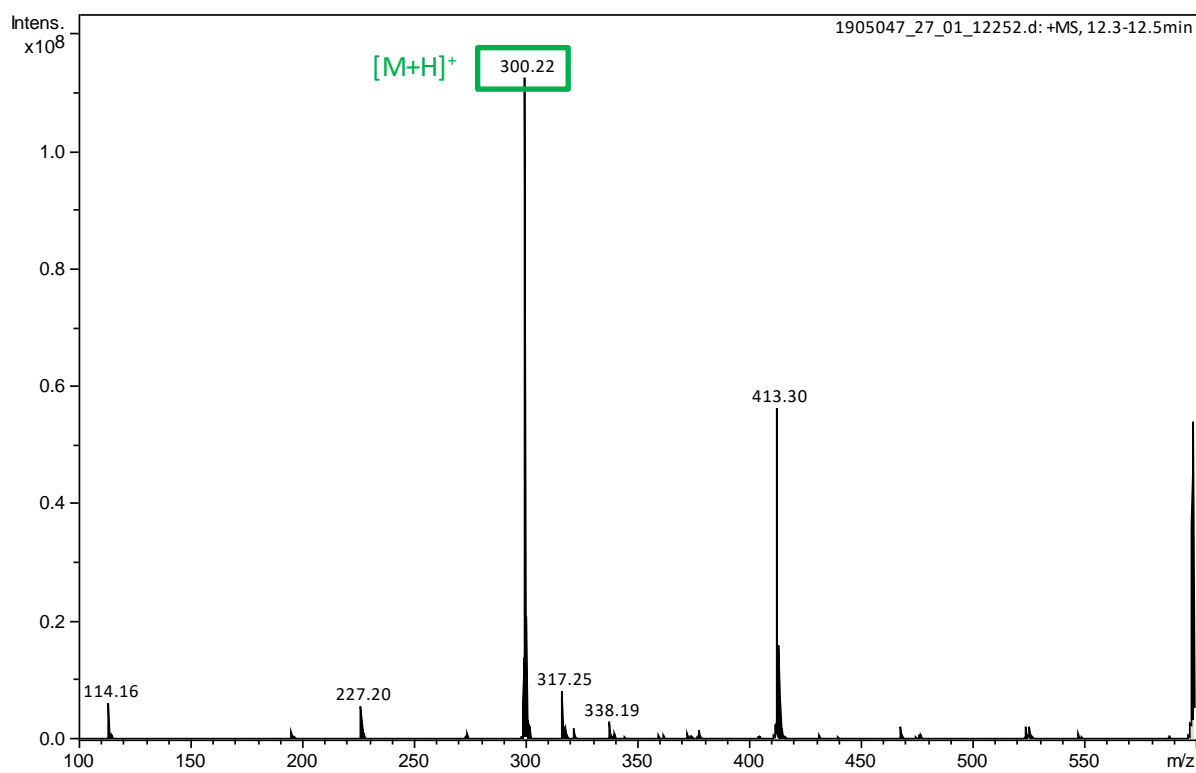
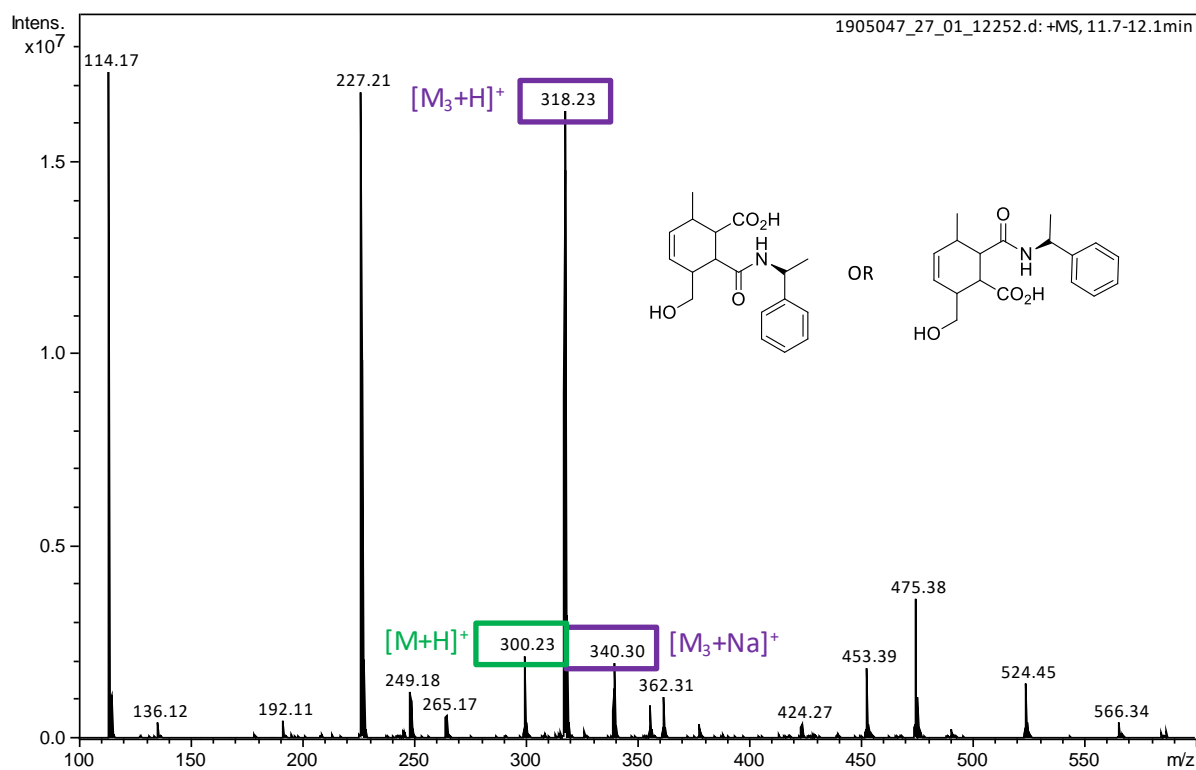


Figure S58. TIC, UV (254 nm) chromatograms of human blood plasma (Blank 2).



Retention time (min)	% area 254 nm (%)
11.0	24.3
11.7	10.7
12.2	1.7
12.3	0.8
12.9	17
13.2	45.5





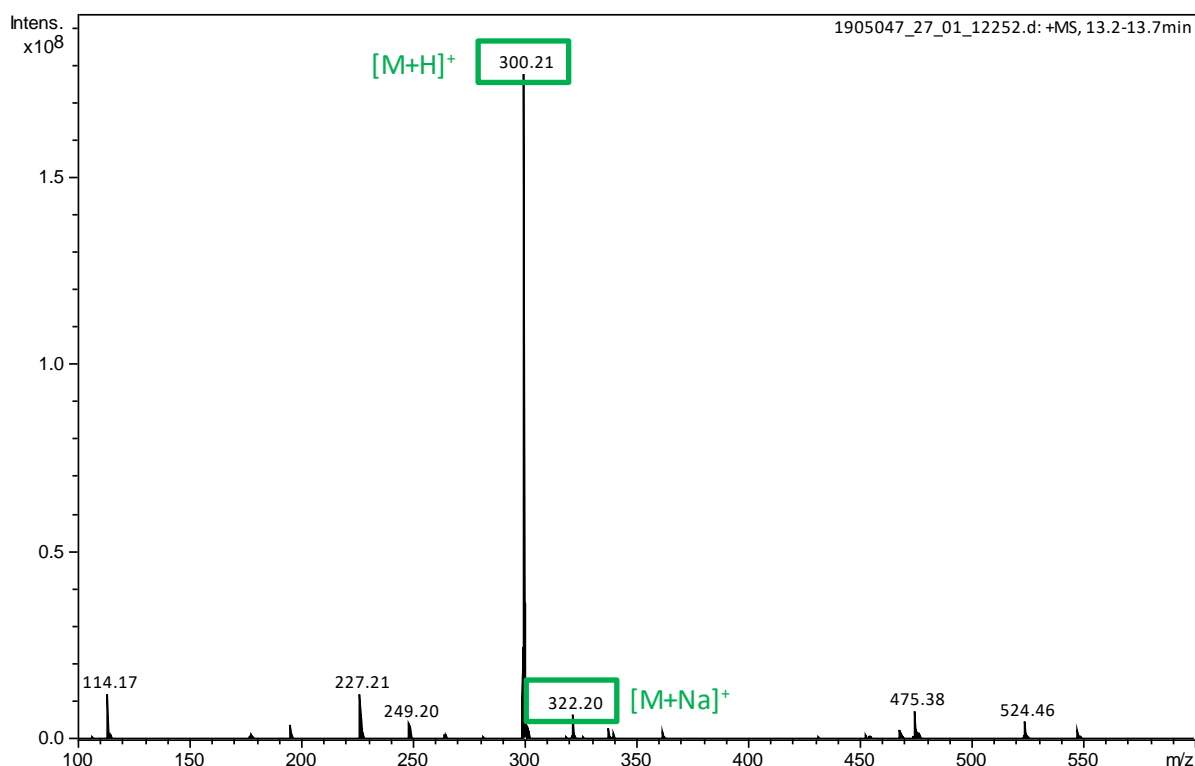
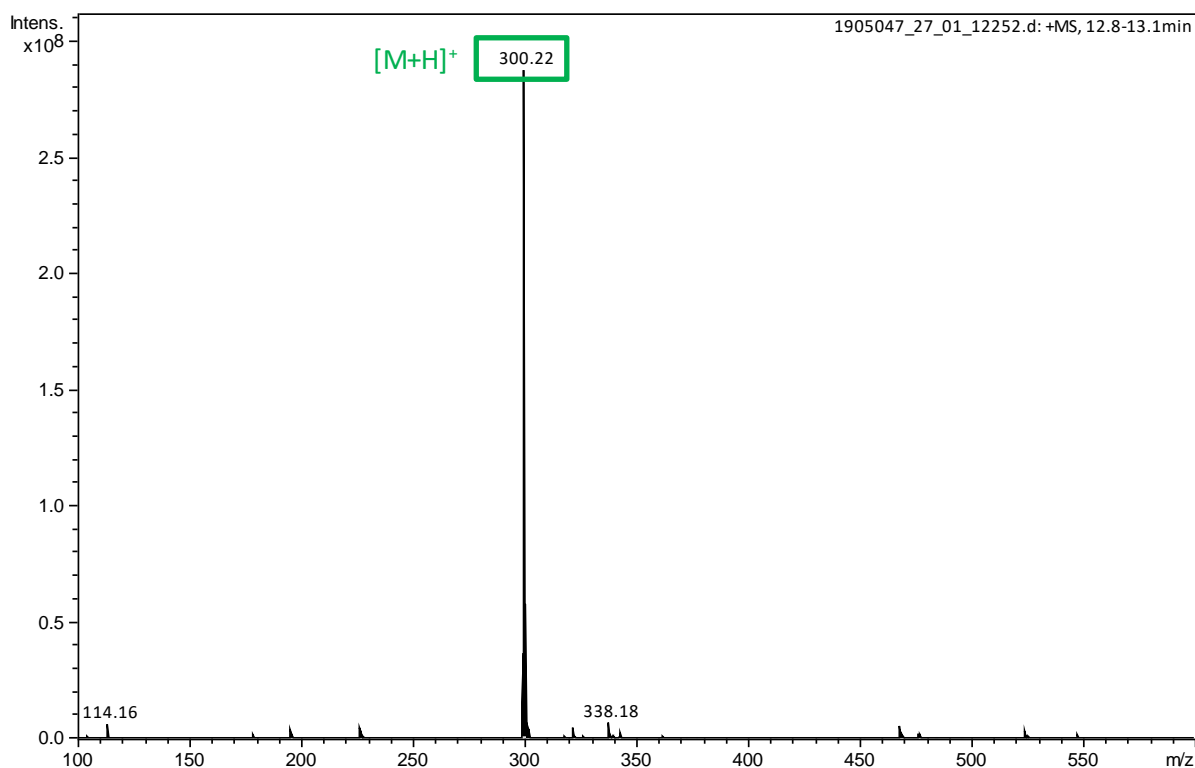
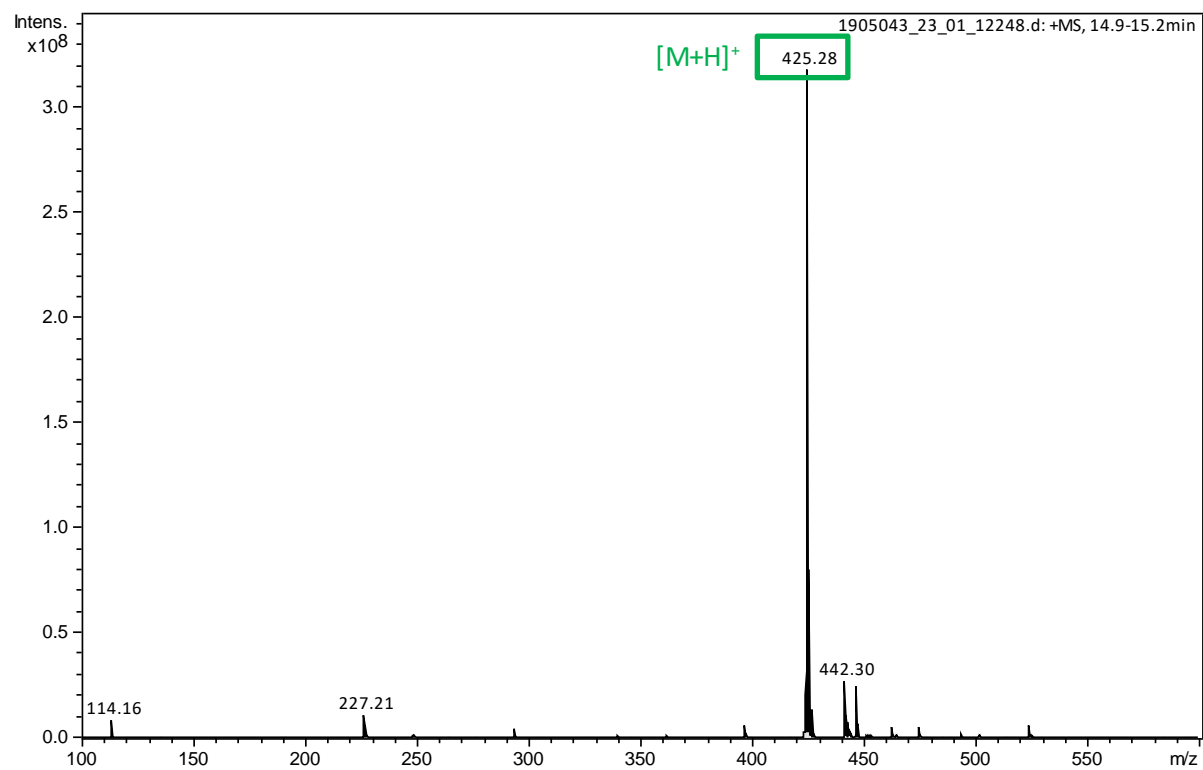
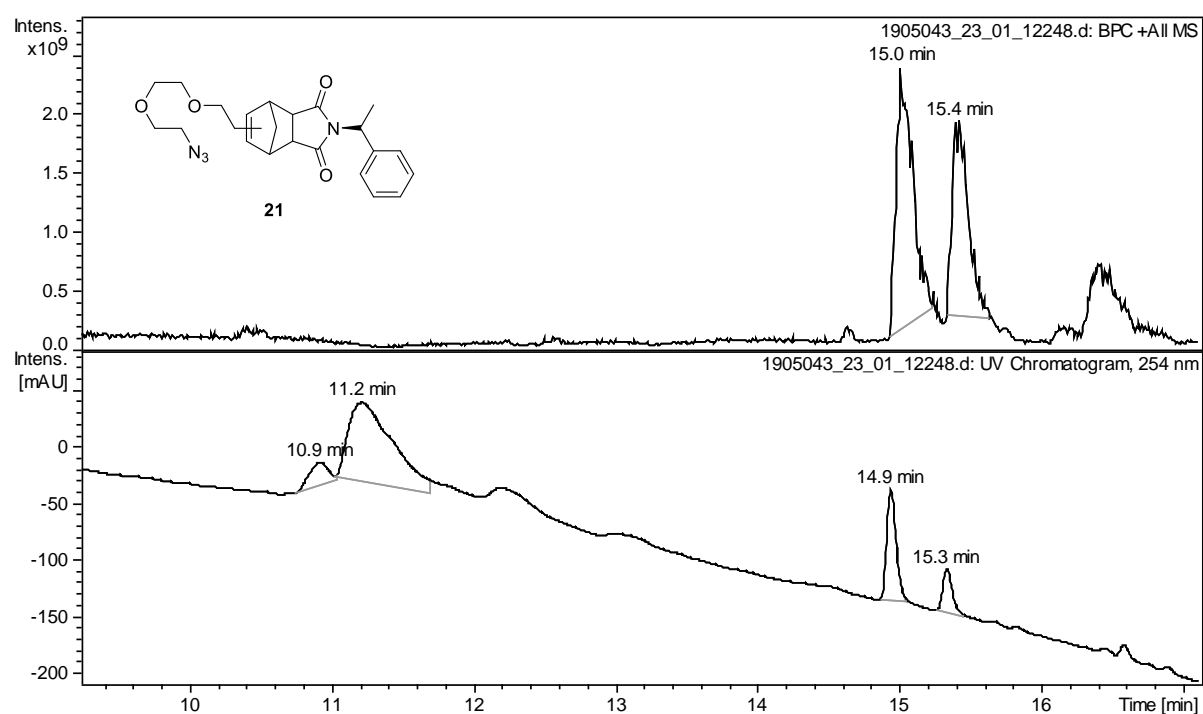


Figure S59. TIC, UV (254 nm) chromatograms and MS (ESI+) mass spectra of **20** after 24 h in human blood plasma.



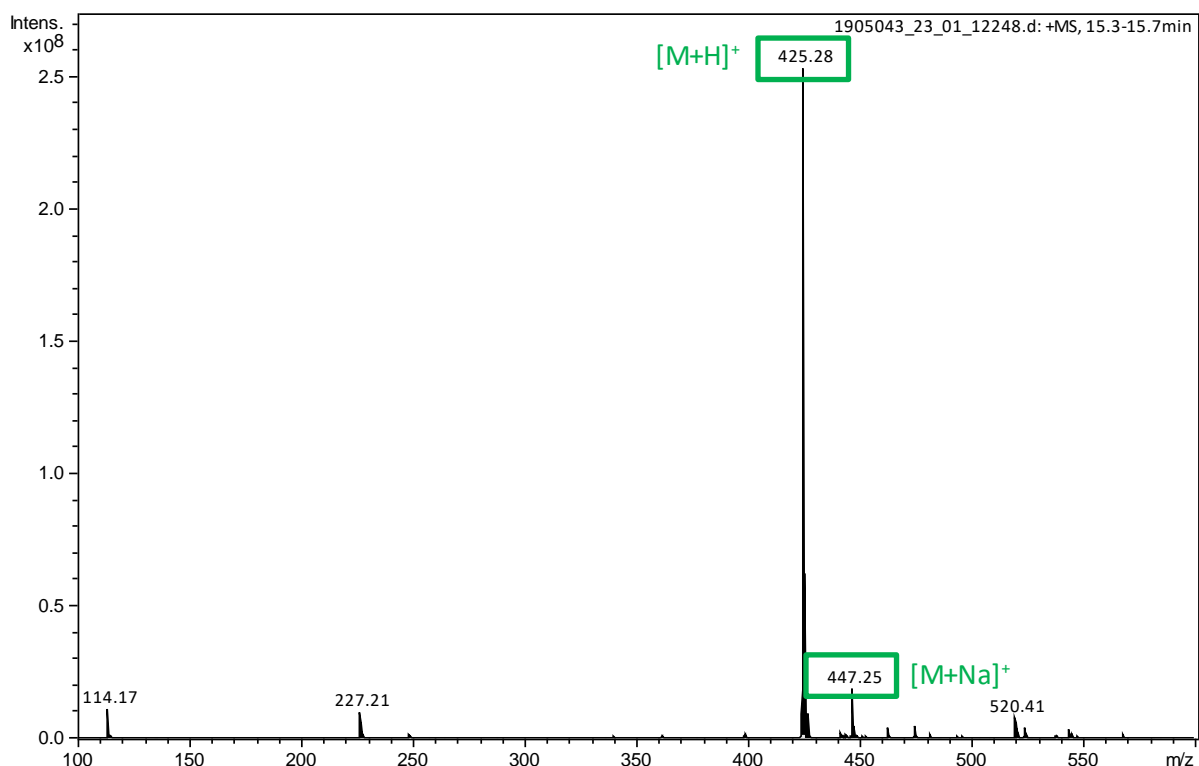


Figure S60. TIC, UV (254 nm) chromatograms and MS (ESI+) mass spectra of **21** after 24 h in human blood plasma.

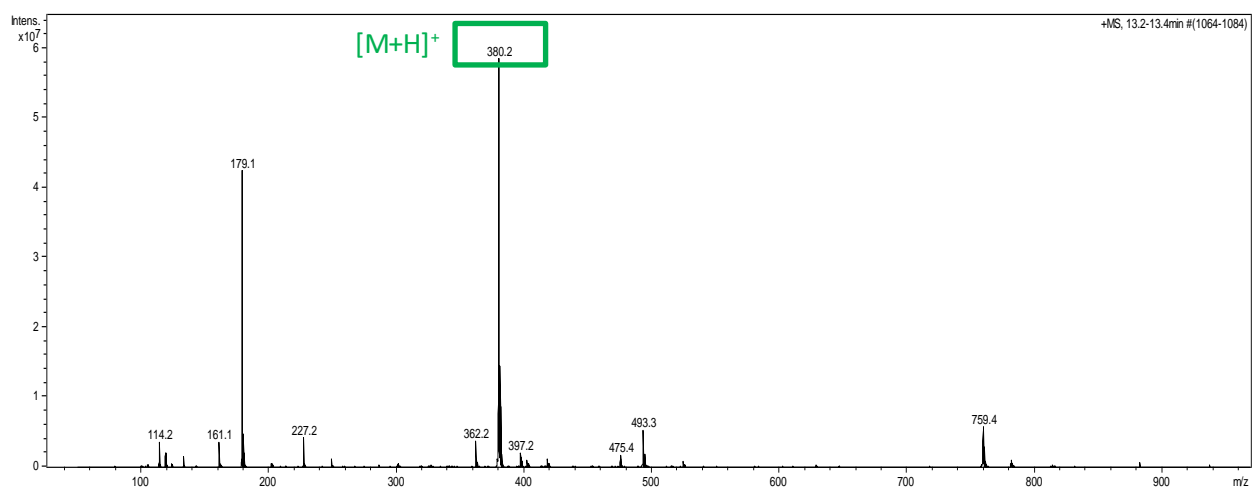
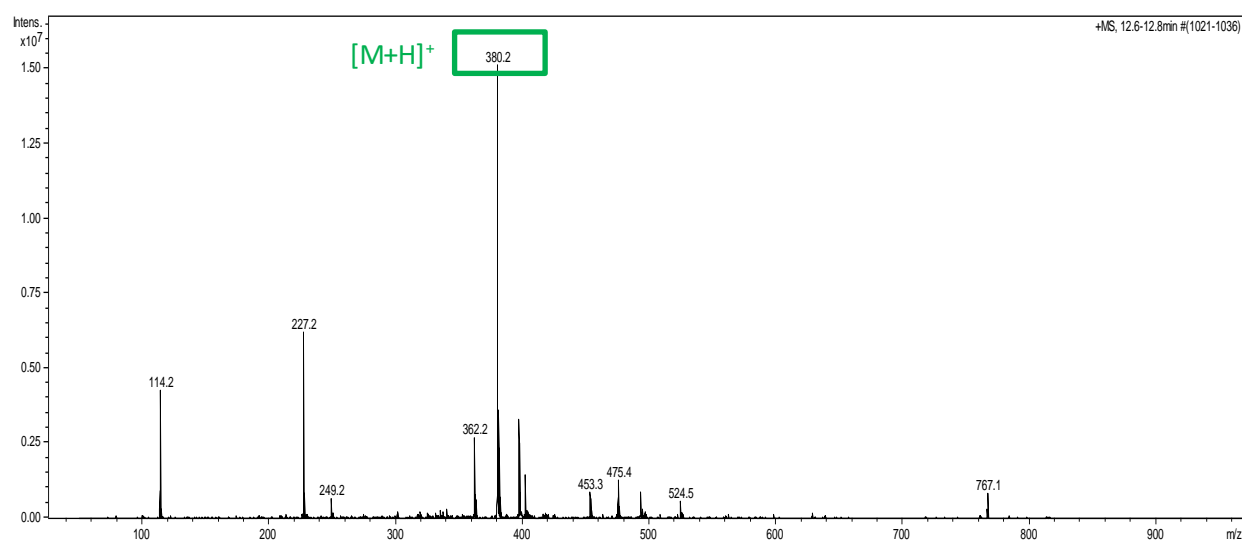
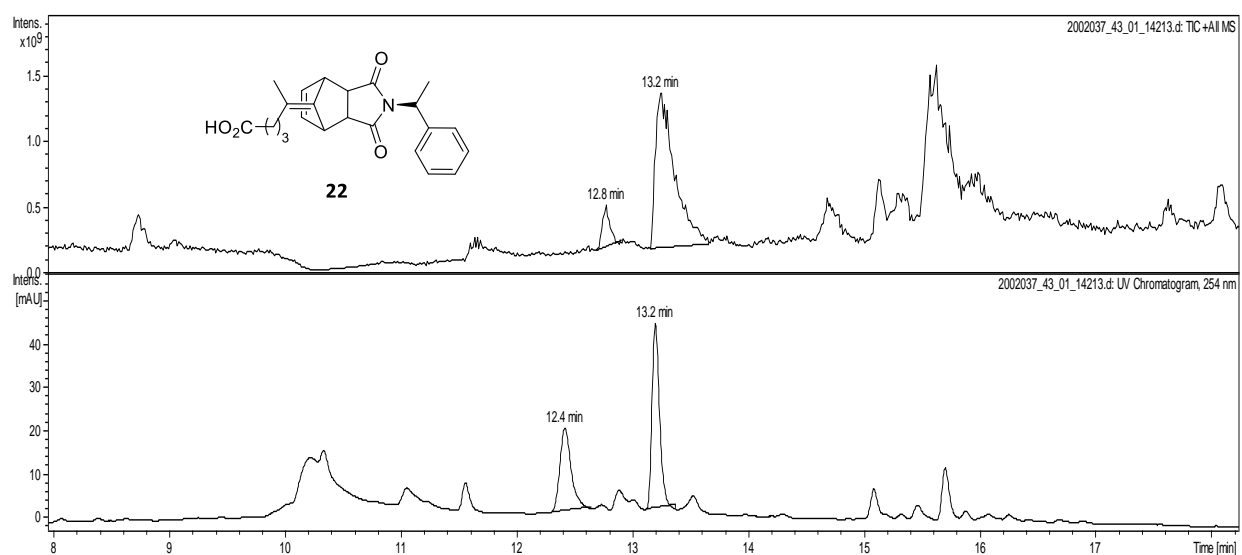
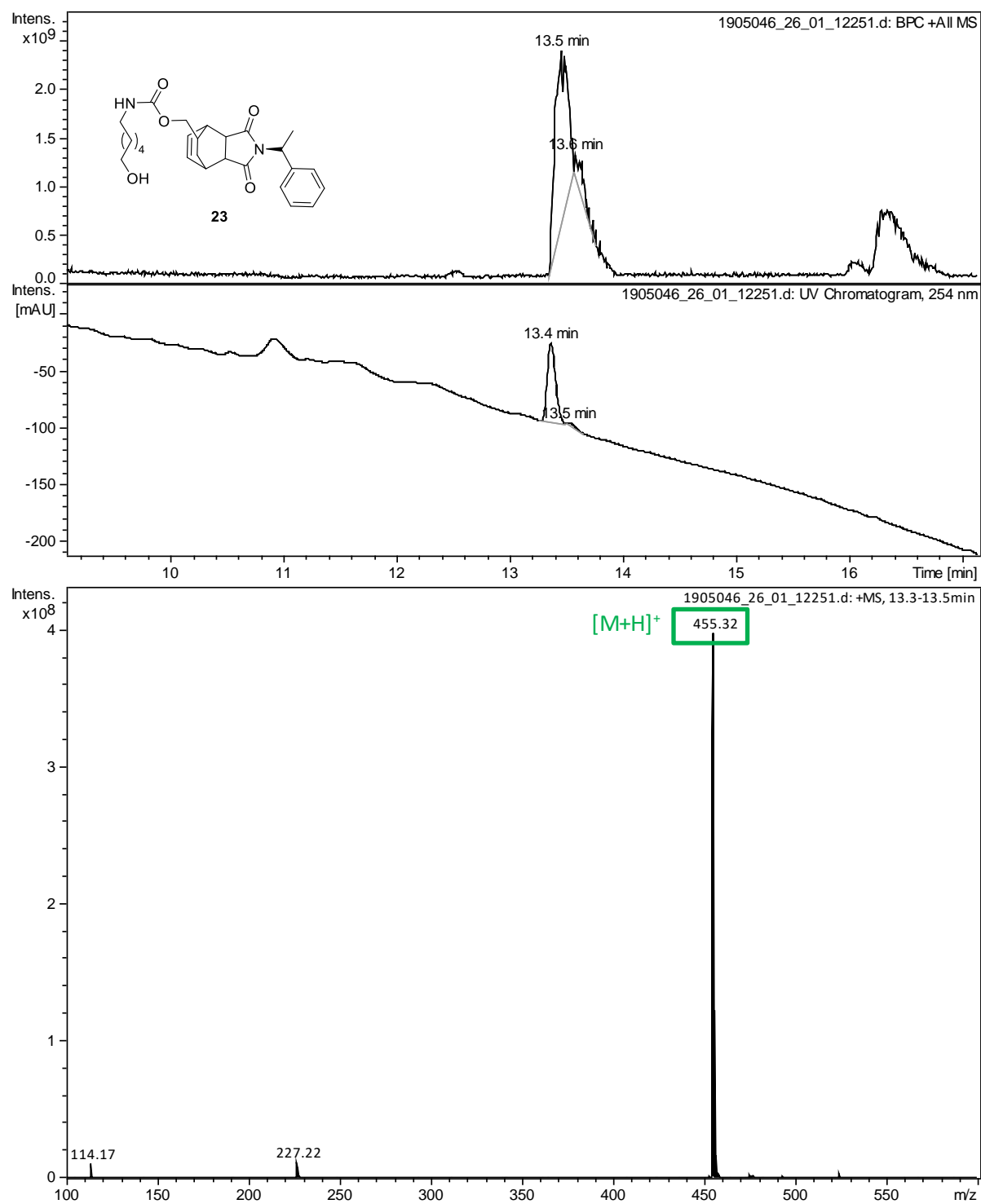


Figure S61. TIC, UV (254 nm) chromatograms and MS (ESI+) mass spectra of **22** after 24 h in human blood plasma.



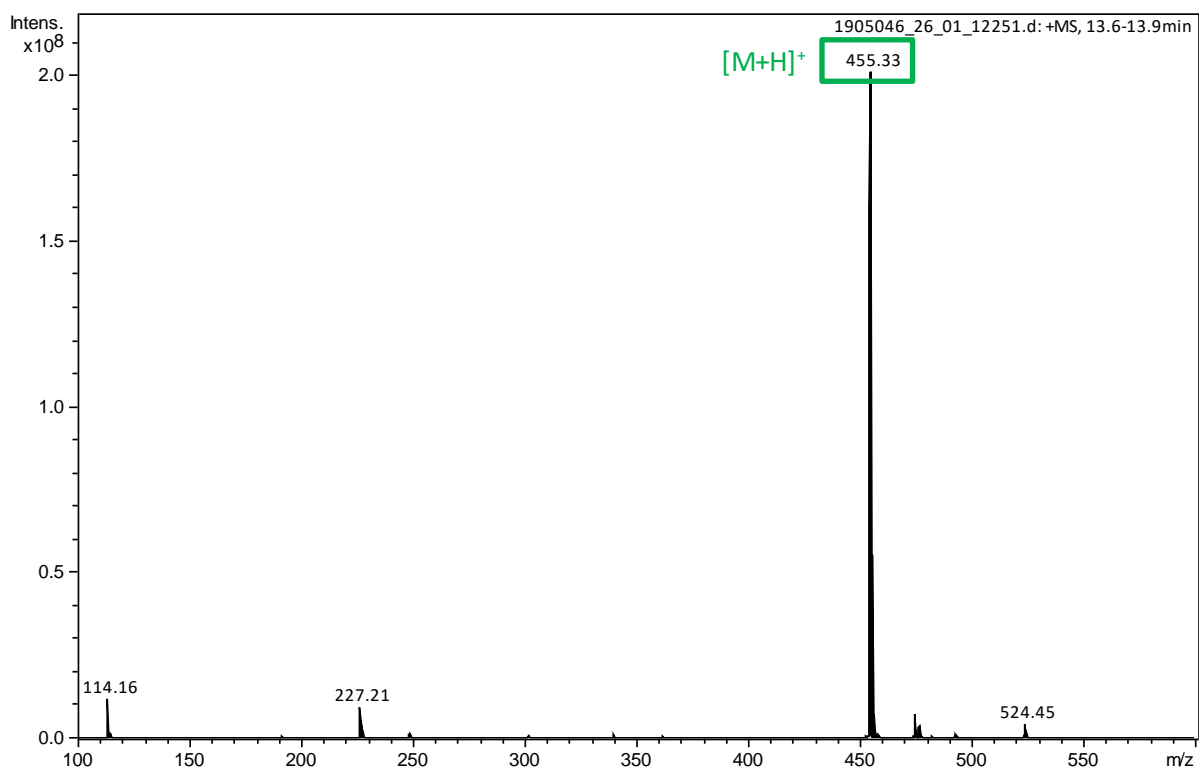


Figure S62. TIC, UV (254 nm) chromatograms and MS (ESI+) mass spectra of **23** after 24 h in human blood plasma.

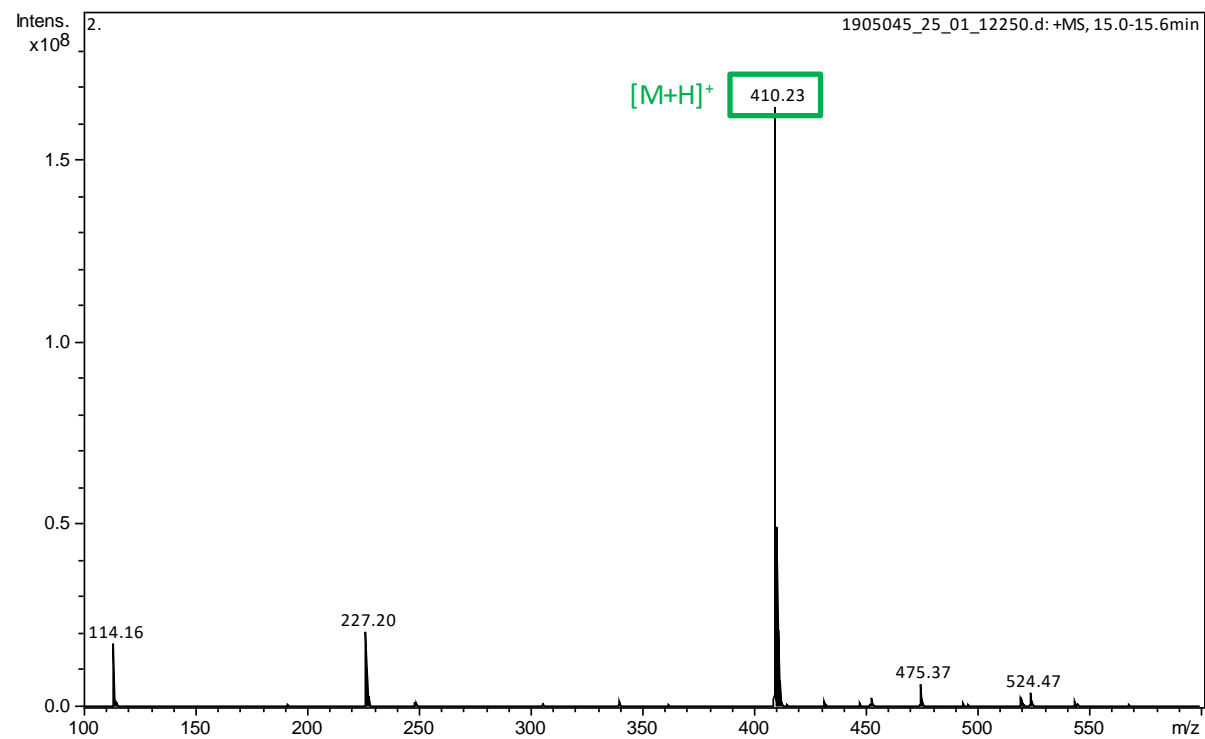
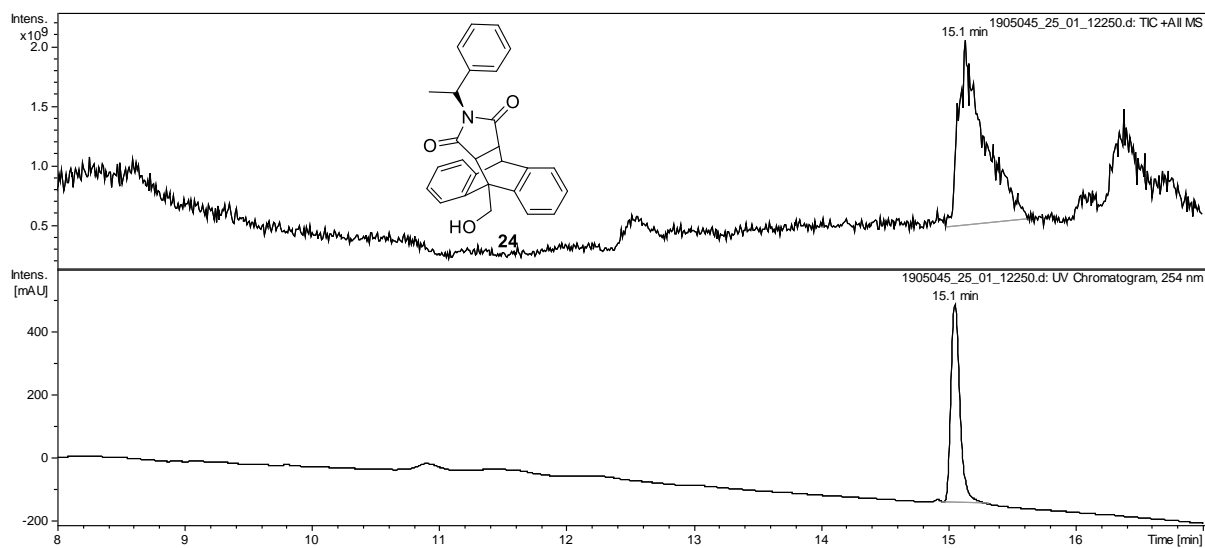


Figure S63. TIC, UV (254 nm) chromatograms and MS (ESI+) mass spectra of **24** after 24 h in human blood plasma.

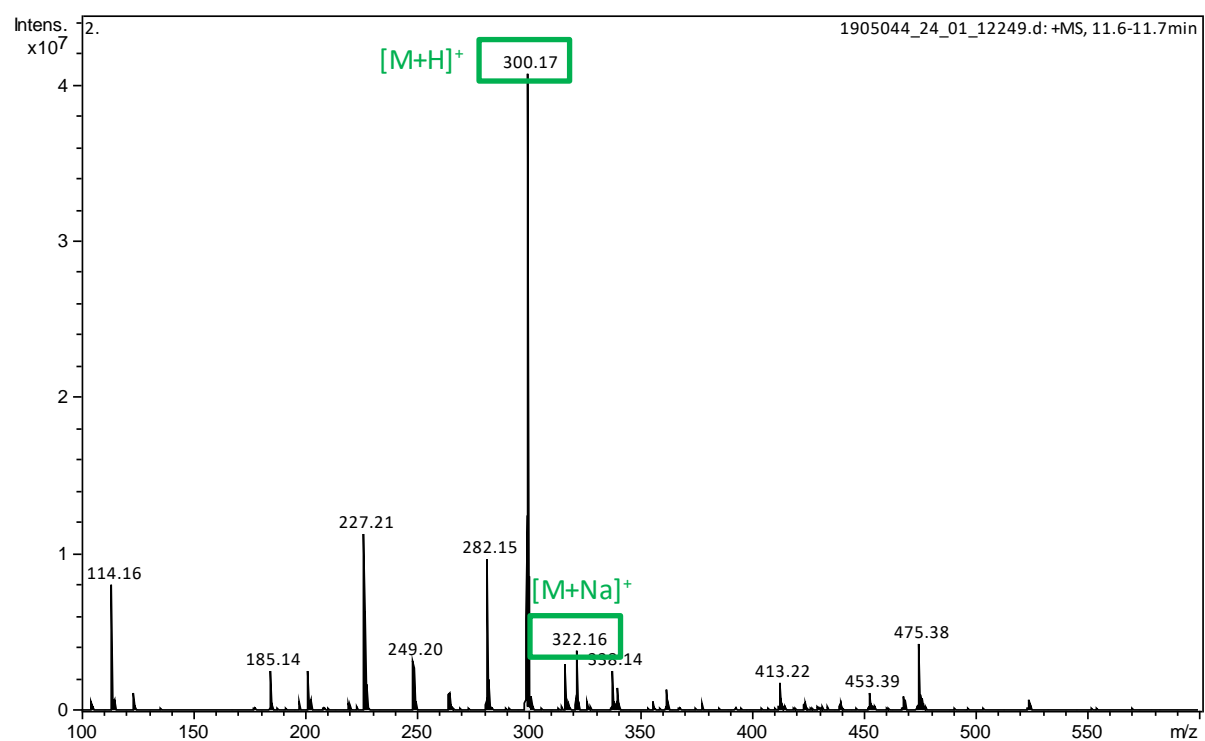
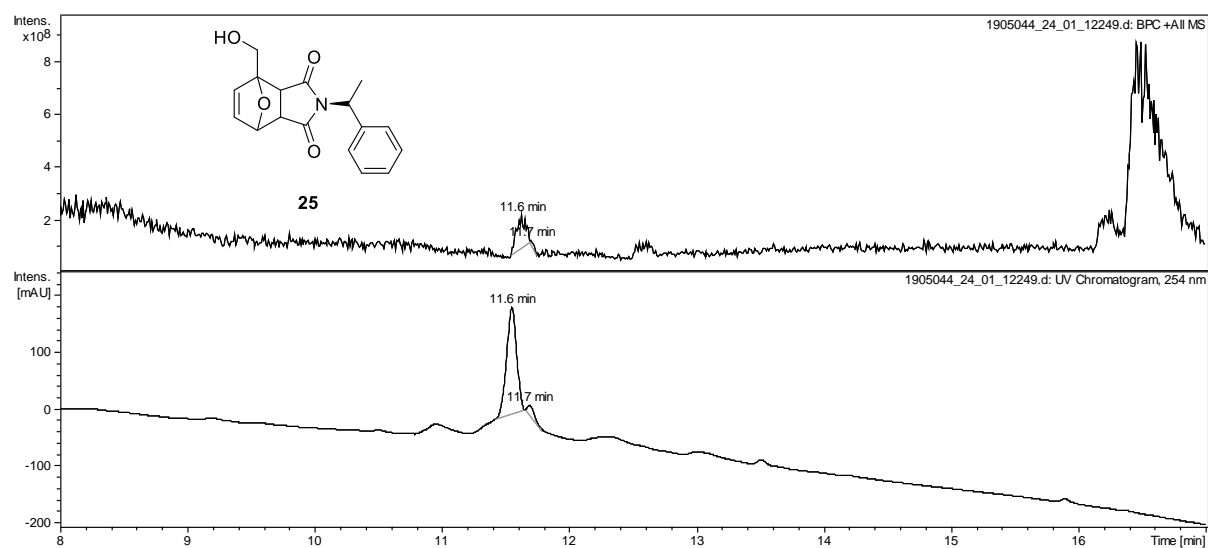
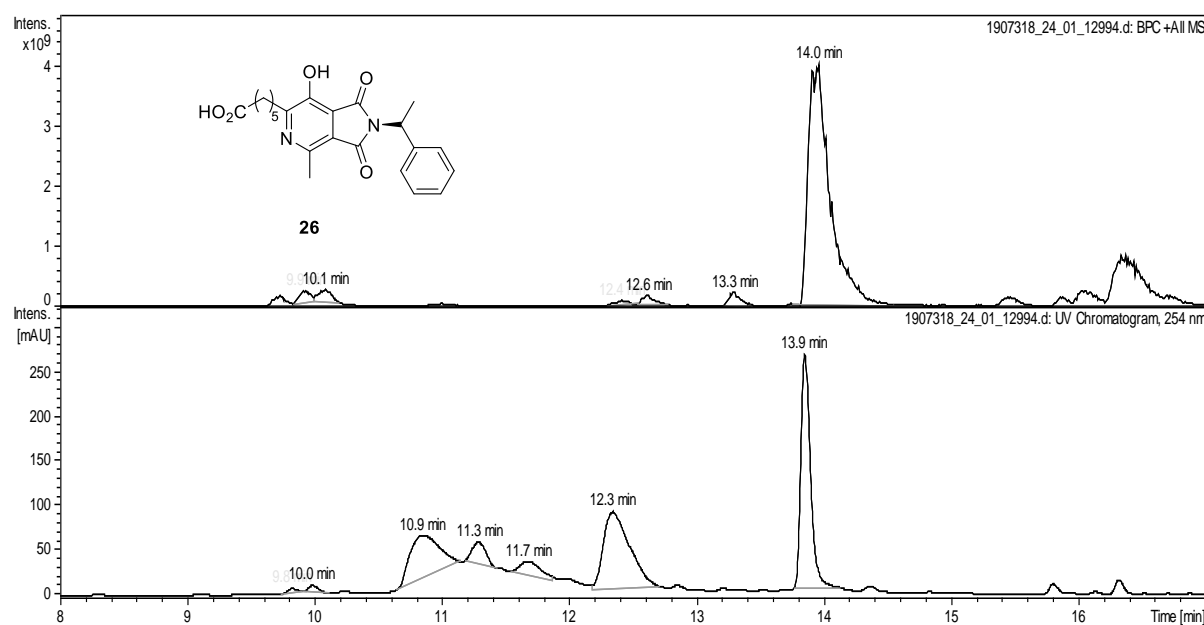
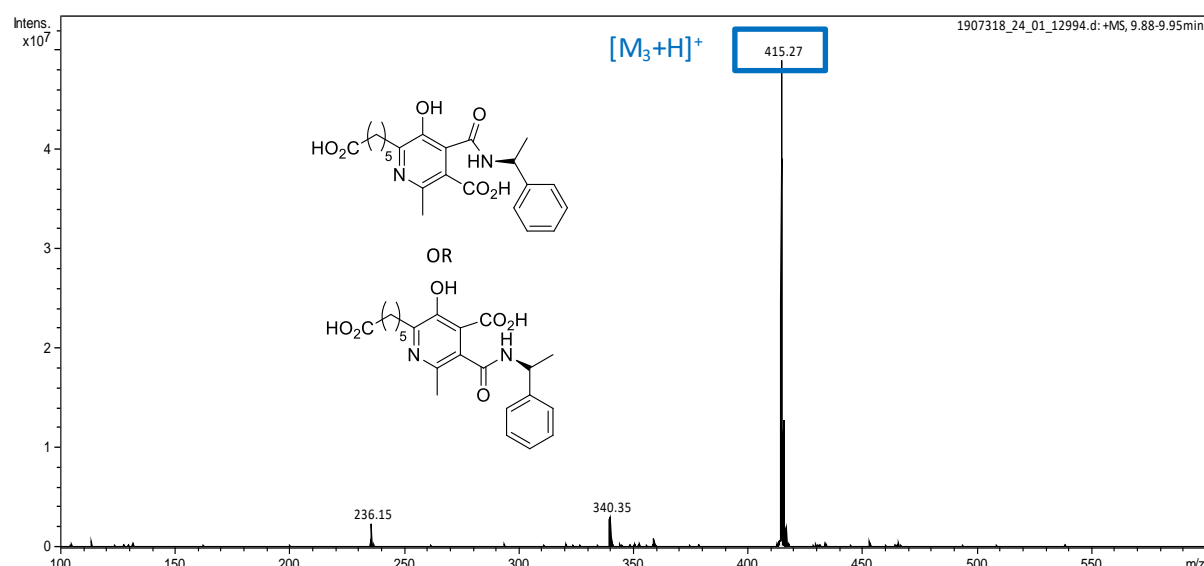
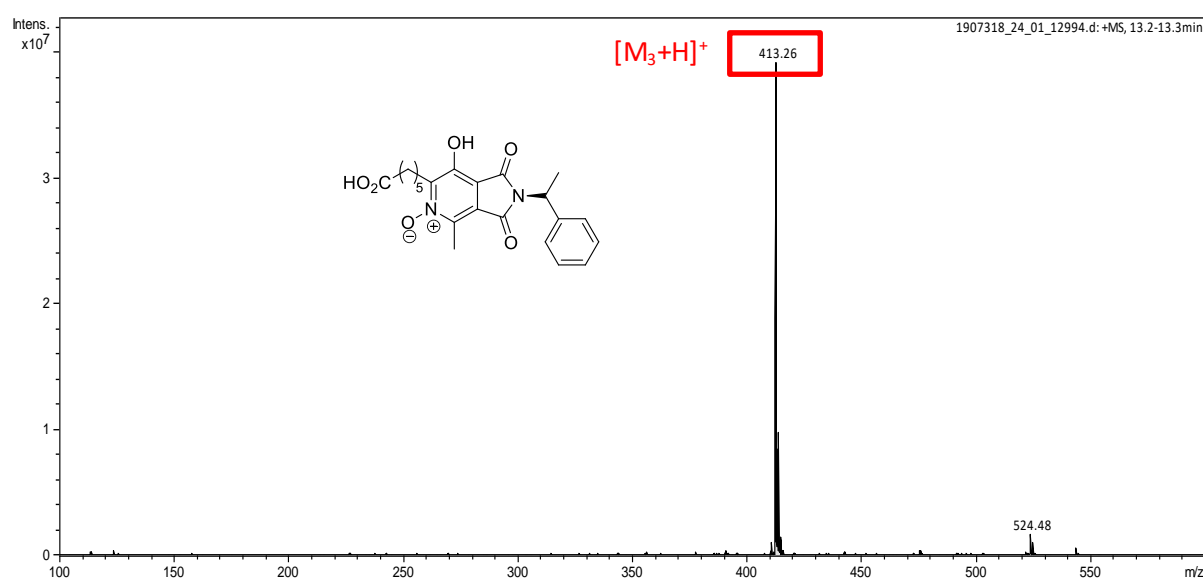
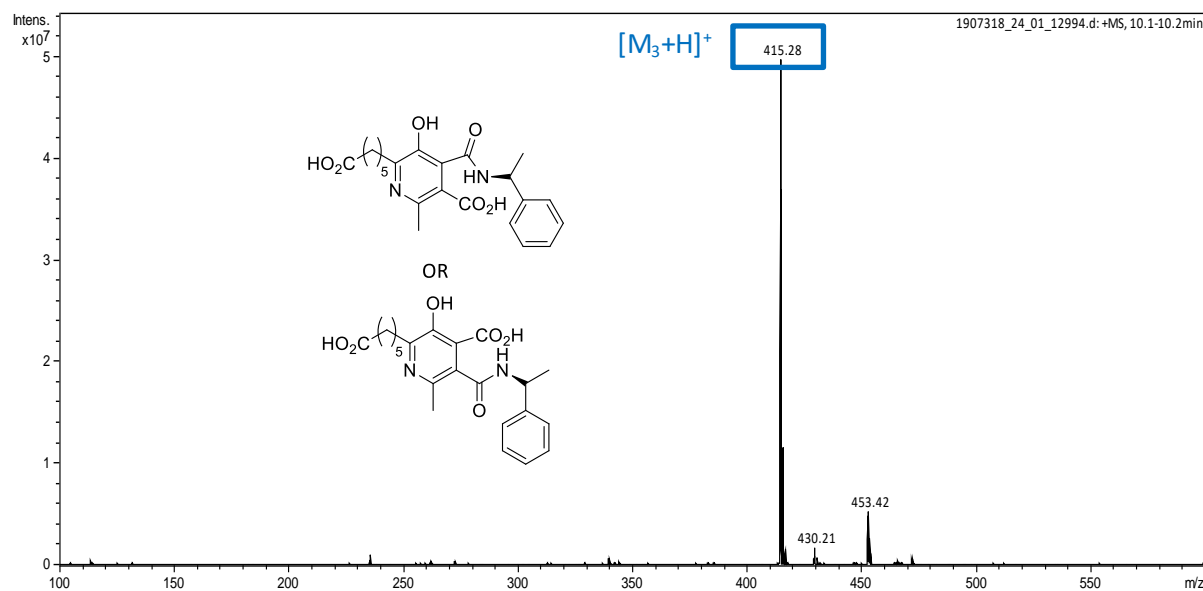


Figure S64. TIC, UV (254 nm) chromatograms and MS (ESI+) mass spectrum of **25** after 24 h in human blood plasma.



Retention time (min)	% area 254 nm (%)
9.8	2.7
10.1	1.6
13.3	traces
13.9	95.7





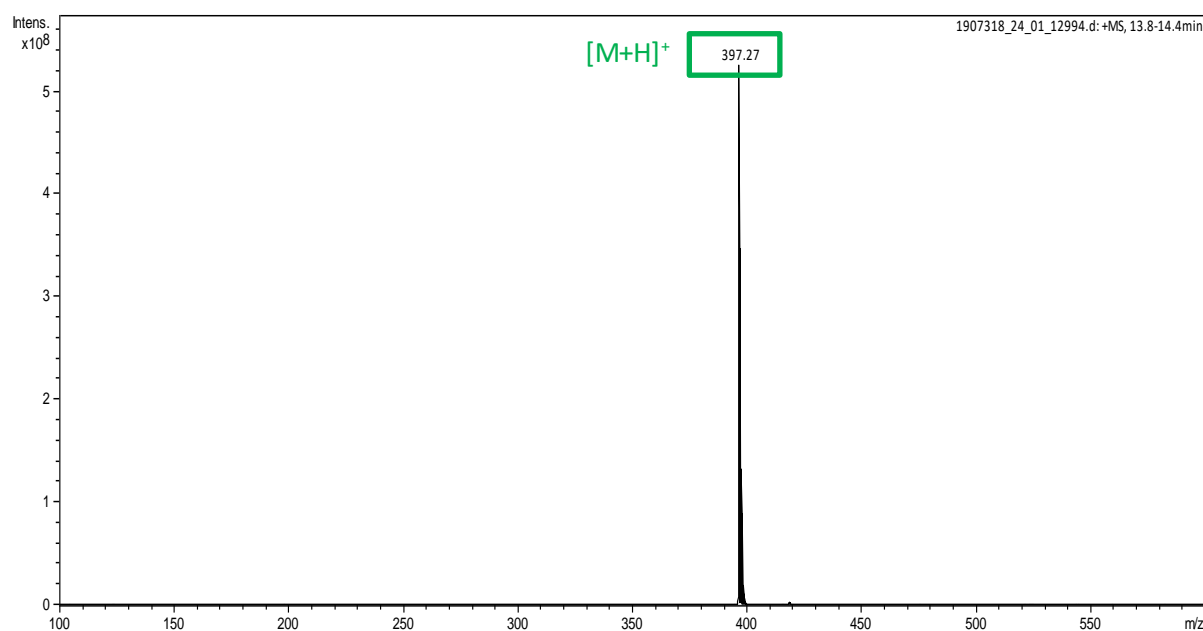


Figure S65. TIC, UV (254 nm) chromatograms and MS (ESI+) mass spectra of **26** after 24 h in human blood plasma.